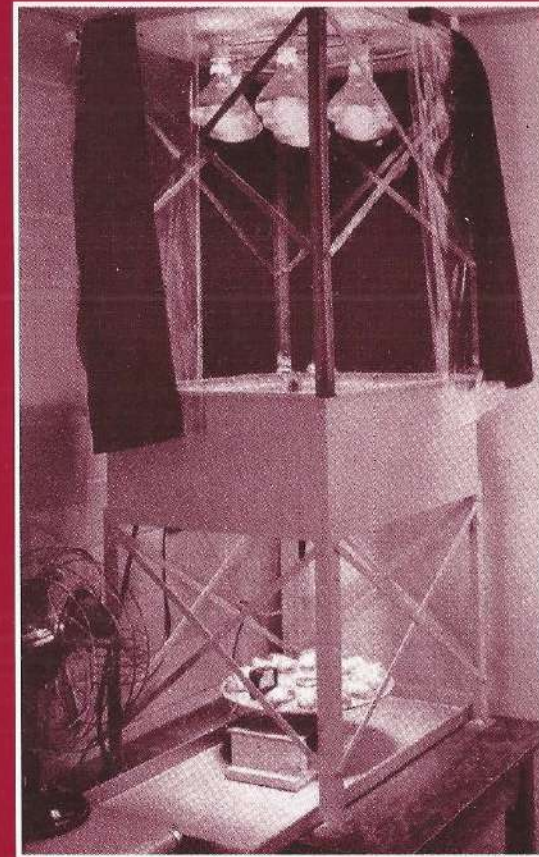


Photosensitizer-monoclonal antibody conjugates for selective photodynamic therapy of cancer



Maarten Vrouwenraets

**Photosensitizer-monoclonal antibody conjugates
for selective photodynamic therapy of cancer**

VRIJE UNIVERSITEIT

**Photosensitizer-monoclonal antibody conjugates
for selective photodynamic therapy of cancer**

ACADEMISCH PROEFSCHRIFT

ter verkrijging van de graad van doctor aan
de Vrije Universiteit Amsterdam,
op gezag van de rector magnificus
prof.dr. T. Sminia,
in het openbaar te verdedigen
ten overstaan van de promotiecommissie
van de faculteit der Geneeskunde
op vrijdag 21 maart 2003 om 13.45 uur
in de aula van de universiteit,
De Boelelaan 1105

The research described in this thesis was performed at the Department of
Otolaryngology/Head and Neck Surgery, *Vrije Universiteit* Medical Center,
Amsterdam, the Netherlands.

Cover photo: Radiation apparatus used by Lipson and Baldes. Copied from:
The photodynamic properties of a particular haematoporphyrin derivative.
Archives of Dermatology, 82: 508-516, 1960.

Printed by Drukkerij C. Regenboog, Groningen

door

Martinus Bernardus Vrouwenraets

geboren te Rheden

promotoren: prof.dr. A.A.M.S. van Dongen
prof.dr. G.B. Snow
copromotor: dr. G.W.M. Visser

Ter herinnering aan mijn moeder

Voor mijn vader

CONTENTS

Chapter 1	General introduction: Basic principles, applications in oncology and improved selectivity of photodynamic therapy <i>Anticancer Research, in press</i> Aim and outline of the thesis	9 39
Chapter 2	Development of <i>meta</i> -tetrahydroxyphenylchlorin-monoclonal antibody conjugates for photoimmunotherapy <i>Cancer Research, 59: 1505-1513, 1999</i>	51
Chapter 3	Targeting of a hydrophilic photosensitizer by use of internalizing monoclonal antibodies: a new possibility for use in photodynamic therapy <i>International Journal of Cancer, 88: 108-114, 2000</i>	79
Chapter 4	Targeting of aluminum (III) phthalocyanine tetrasulfonate by use of internalizing monoclonal antibodies: improved efficacy in photodynamic therapy <i>Cancer Research, 61: 1970-1975, 2001</i>	97
Chapter 5	Comparison of aluminium (III) phthalocyanine tetrasulfonate- and <i>meta</i> -tetrahydroxyphenylchlorin-monoclonal antibody conjugates for their efficacy in photodynamic therapy <i>in vitro</i> <i>International Journal of Cancer, 98: 793-798, 2002</i>	117
Chapter 6	Summary and conclusions	135
	Samenvatting en conclusies	143
	List of abbreviations	151
	Dankwoord	153
	Curriculum vitae	155

Chapter 1

GENERAL INTRODUCTION:

**Basic principles, applications in oncology
and improved selectivity of photodynamic therapy**

AND

AIM AND OUTLINE OF THE THESIS

Maarten B. Vrouenraets, Gerard W.M. Visser,
Gordon B. Snow and Guus A.M.S. van Dongen

Part of this chapter will be published in Anticancer Research

CONTENTS

GENERAL INTRODUCTION

I. Basic principles

- a. Photodynamic therapy
- b. Photochemistry
- c. Targets for PDT
- d. Photosensitizers
- e. Potential applications of photodynamic therapy

II. Clinical results

- a. Head and neck cancer
- b. Lung cancer
- c. Disseminated intraperitoneal tumors
- d. Locoregional breast cancer recurrences
- e. Brain tumors
- f. Mesothelioma
- g. Bladder cancer
- h. Basal cell carcinoma

III. Advanced delivery of photosensitizers

- a. Liposomes
- b. Ligand-based targeting
- c. Photosensitizing adenovirus
- d. Water-soluble polymer carriers
- e. pH-Responsive polymeric micelles
- f. Photosensitizer-monoclonal antibody conjugates

AIM AND OUTLINE OF THE THESIS

GENERAL INTRODUCTION

I. Basic principles

a. Photodynamic therapy

Photodynamic therapy uses light as the modus operandi in oncology. Cytotoxicity is achieved *via* a photosensitizer which is the light absorbing agent. After injection, the sensitizer shows a certain selectivity for tumor tissue by a mechanism that is not fully understood. Due to the higher sensitizer concentration in the tumor compared to the surrounding normal tissue, the tumor can be visualized by sensitizer fluorescence. Subsequently, irradiation of the tumor area with laser light in the red or near-infrared region (600-800 nm, depending on the sensitizer used) leads to excitation of the sensitizer, followed by generation of singlet oxygen, a cytotoxic form of oxygen. As the laser light can be applied locally, it is possible to target the tumor with some precision.

Already in 1900 the phenomenon of a photodynamic effect had been observed. Raab, a medical student in the group of Von Tappeiner in Munich, found that acridine (Fig. 1A) killed *paramecia* (a freshwater ciliate protozoan), but only in the presence of daylight (1). A few years later Jodlbauer and Von Tappeiner demonstrated that oxygen was crucial for this effect (2). They were also the first who investigated treatment of cancer in this way, by using fluorescein derivatives, including eosin (Fig. 1B), in patients with basal cell carcinoma (3). The sensitizer was applied at or near the skin by brushing or local injection, while an arc lamp or sunlight was used as light source.

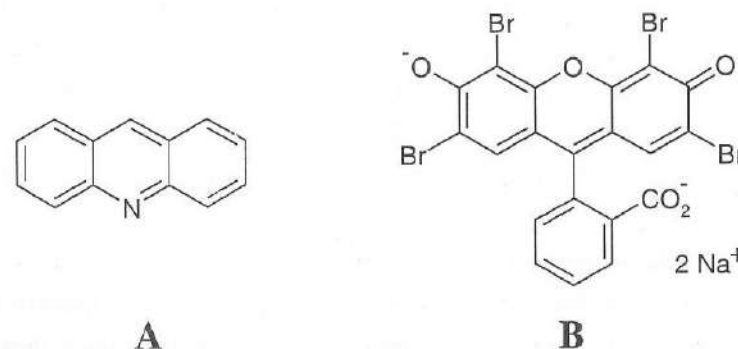


Figure 1. Chemical structure of acridine (A) and eosin (B).

Despite these early promising results, in subsequent years progress was rather slow. In 1924, Policard observed porphyrin fluorescence in experimental tumors, and concluded that porphyrins showed preferential tumor uptake (4). About 20 years later Auler and Banzer succeeded in tumor cell killing with a sensitizer containing the porphyrin moiety (5). A landmark in the history of PDT was the development of a photosensitizer called "haematoporphyrin derivative" (HpD) in 1960 (6). The promising initial results obtained with this compound (*vide infra*), together with the improved laser technology and light delivery and measuring techniques, led to a growing interest in PDT in the following years.

b. Photochemistry

In PDT, singlet oxygen is the key agent of cellular damage. This excited oxygen is a very reactive molecule and therefore rapidly reacts with many types of biomolecules. Especially molecules in membranes, like unsaturated lipids, cholesterol and the α -amino-acids tryptophan, histidine and methionine, are extremely vulnerable to reaction with singlet oxygen. Singlet oxygen has a short lifetime ($< 0.04 \mu\text{sec}$) and a radius of action ($< 0.02 \mu\text{m}$) (7), which is short in comparison with the diameter of a tumor cell ($\pm 10 \mu\text{m}$).

The initial step in singlet oxygen formation is light-induced excitation of the sensitizer, which results in an elevated electron energy state. In this excited state several processes can occur. It can directly return to the ground state, under emission of light which is referred to as fluorescence. The excited sensitizer can also directly react with a substrate, leading to radical intermediates. This Type I photo-oxygenation process plays a minor role in photodynamic damage. To generate a photodynamic effect, the excited sensitizer should shift to the triplet state by "intersystem crossing", a process in which the excited electron undergoes electron spin conversion to a lower excited state. For photosensitizers to be effective, a long-lived triplet state is necessary. Therefore, not all light-absorbing compounds are equally effective. In this triplet state the sensitizer can react with oxygen, leading to singlet oxygen. This so-called Type II photo-oxygenation process is schematically presented in Figure 2.

In PDT, light is used with a wavelength which is maximally absorbed by the sensitizer. This maximum absorption wavelength of the sensitizer is an important parameter in PDT, since light of a longer wavelength penetrates deeper into the tissue, thereby making treatment of larger tumors possible.

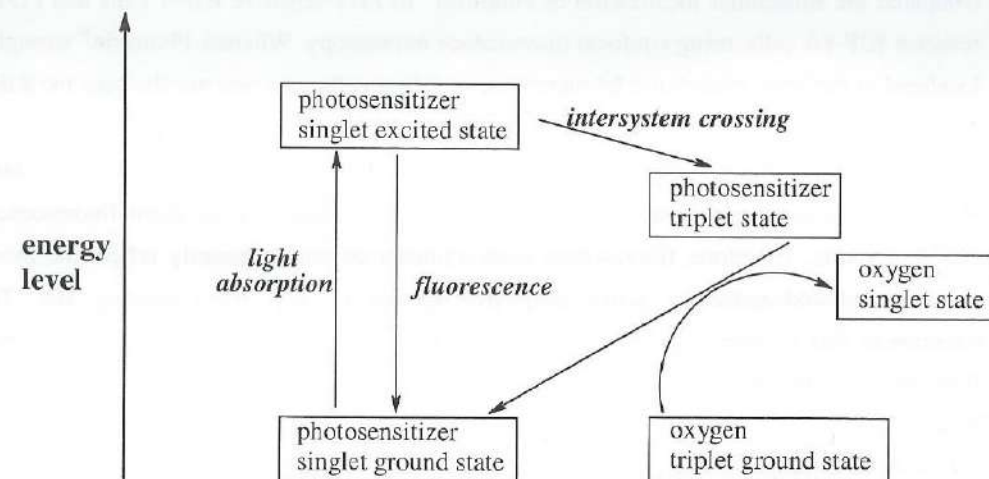


Figure 2. Schematic presentation of the type II photo-oxygenation process.

c. Targets for PDT

The potential cellular and subcellular targets for photodynamic effects have been intensively studied. Besides direct cell killing as a result of phototoxic cell damage, indirect effects also seem to play an important role in the destruction of tumor tissue.

c1. Direct effects

Direct cytotoxicity results from incorporation of the sensitizers into cellular membranes and might depend on the type of sensitizer used.

Membrane damage leads to swelling, bleb formation, shedding of vesicles containing cytosolic enzymes and inhibition of membrane enzymes. Intracellular porphyrin localization has been reported to occur first within the plasma membrane (8). After several hours of incubation, redistribution within the cell occurs extending its localization to the nuclear membrane and other organelles, especially mitochondria and lysosomes. The specific pattern of localization possibly depends on the cell type and/or sensitizer. Shulok *et al.* (9) studied the localization of HpD in human bladder tumor cell line MGH-U1 using fluorescence microscopy. They showed that HpD did not localize in a specific subcellular site, but rapidly

(within 1-2 hours) translocated to lipophilic membranous structures. Wilson *et al.* (10) compared the subcellular localization of Photofrin® in PDT-sensitive RIF-1 cells and PDT-resistant RIF-8A cells, using confocal fluorescence microscopy. Whereas Photofrin® strongly localized in the inner mitochondrial membrane of RIF-1 cells, this was not the case for RIF-8A cells, suggesting the importance of mitochondrial damage for phototoxicity.

Care should be taken, however, when interpreting Photofrin® localization data because this sensitizer consists of numerous porphyrin species with different fluorescence quantum yields. Therefore, fluorescence measurements do not necessarily reflect the most important photodynamically active porphyrin species at any given binding site. To circumvent this problem, Woodburn *et al.* (11) synthesized a range of pure, monomeric Photofrin®-related porphyrins, varying in hydrophobicity and charge. The subcellular localization was studied in C₆ glioma and V79 Chinese hamster lung fibroblast cells using confocal laser scanning microscopy. Generally, porphyrins with dominantly cationic side chains localized in mitochondria, whereas those with a more anionic character appeared to localize in lysosomes. In a subsequent study (12) to assess the phototoxicity of these compounds in C₆ cells, a significant correlation was found between subcellular localization and degree of phototoxicity. The most phototoxic compounds (with cationic side chains) localized in mitochondria.

Also the mitochondria themselves are sensitive targets. Chiu *et al.* (13) showed that photodynamic treatment of mouse L5178Y-R cells with silicon phthalocyanine tetrasulfonate (SiPcS₄) caused release of cytochrome *c* into the cytosol, which is a critical step in the mitochondrial pathway of apoptosis. This release was not the result of immediate damage to the mitochondrial membrane, as it occurred 15 min after illumination.

Fabris *et al.* (14) determined the intracellular localization and phototoxicity of zinc phthalocyanine (ZnPc) as a function of the incubation time in the rat embryo fibroblast cell line 4R. After 2 h incubation, fluorescence microscopy showed that ZnPc was located in the Golgi apparatus and to a lesser extent in the plasma membrane. After 24 h, ZnPc was still present in the Golgi apparatus, but a mitochondrial localization could be clearly observed as well. Necrosis, due to loss of plasma membrane integrity and depletion of intracellular ATP, was the prevailing mode of cell death after 2 h incubation. In contrast, illumination performed after 24 h incubation caused only partial inhibition of plasma membrane activities, and cell death occurred largely by apoptosis.

The main subcellular target of *m*THPC-mediated PDT has not yet been determined. A diffuse cytoplasmic distribution of *m*THPC was observed in V79 Chinese hamster lung

fibroblasts (15), murine myeloid leukemia M1 cells (16) and HT29 human colon adenocarcinoma cells (17) using confocal microscopy. The endoplasmatic reticulum, mitochondria, Golgi apparatus and nuclear membrane were stained by *m*THPC, whereas no *m*THPC fluorescence was observed in the nucleus. Yow *et al.* (18) showed, in two nasopharyngeal carcinoma cell lines (HK1 and CNE2), that *m*THPC-mediated PDT ruptured the mitochondria, indicating that mitochondria are an important subcellular target.

A number of studies have addressed the possible involvement of DNA damage in PDT phototoxicity, but have come to contradictory conclusions. Ramakrishnan *et al.* (19) observed that, in L5178 mouse lymphoma cells treated with chloroaluminium phthalocyanine, phototoxicity was correlated with the formation of DNA-protein crosslinks, and also with the number of DNA strand breaks observed. In contrast, Dougherty *et al.* (20) concluded that PDT has generally a low potential for causing DNA damage, since most sensitizers do not accumulate to a large extent in cell nuclei. The results probably depend strongly on the model system (cell line/sensitizer) used, as was shown by Kessel (21) for two purpurin (a chlorin derivative) photosensitizers in murine leukemia L1210 cells. For etiopurpurin, toxicity was related to the degree of inhibition of DNA synthesis, while for the tin complex of etiopurpurin a correlation with the level of membrane damage was found.

c2. Indirect effects

The vasculature seems to be the most critical target for indirect photodamage. As a result of PDT-induced damage to the vascular endothelium, hypoxia, anoxia and deprivation of nutrients in the tumor might arise. The underlying mechanism of action, however, might depend on the sensitizer used: PDT with Photofrin® or mono-L-aspartyl chlorin₆₆ leads to vessel constriction and thrombus formation (22,23), while the use of phthalocyanines causes vascular leakage (24).

Another indirect effect is the induction of a strong inflammatory reaction (25). After photodynamic treatment, destroyed tumor cells are phagocytosed by macrophages. These antigen presenting cells can process tumor-specific antigens and present them on their membrane surface, thereby inducing T lymphocyte mediated cellular immunity.

d. Photosensitizers

d1. Hematoporphyrin derivative (HpD)

HpD is the product mixture formed upon solubilizing hematoporphyrin (Fig. 3A) in aqueous media. HpD is prepared by treatment of hematoporphyrin in acetic acid with 5% sulfuric acid as a catalyst ("HpD Stage I"), followed by treatment with an alkaline solution and neutralization. The resulting solution, ready for injection, is called HpD Stage II. It consists of a mixture of mono-, di- and oligomers, all containing the porphyrin moiety.

In 1961, the applicability of HpD Stage II as a diagnostic agent was demonstrated (26). Tumor tissue could be visualized after illumination with UV light, due to the selective tumor uptake of the sensitizer. In the 1970's, its therapeutic potency became clear (27, 28). Because the oligomeric fraction of HpD Stage II appeared to be largely responsible for phototoxicity, purification methods were developed to remove part of the mono- and dimers (29). This resulted in the commercial product Photofrin[®], which has been registered for the palliative treatment of totally and partially obstructing cancers of the esophagus (30), as well as for lung cancer (31).

Nowadays, Photofrin[®] is still the only world-wide registered photosensitizer for treatment of cancer, despite the following limitations: first, even after purification it consists of about 60 compounds and therefore it is difficult to reproduce its composition. Second, the compound has a suitable absorption maximum at 630 nm, however, its molar absorption coefficient at this wavelength is low ($1170 \text{ M}^{-1}\text{cm}^{-1}$). Therefore, high sensitizer and light doses have to be delivered to the tumor. Third, the uptake in tumor tissue is not very selective. A typical example is a study of Orenstein *et al.* (32), who obtained low tumor to normal tissue ratios in C26 colon carcinoma bearing mice, resulting in severe normal tissue damage. Finally, cutaneous photosensitivity, caused by uptake of the sensitizer in the skin, is rather long-lasting with Photofrin[®]-based PDT. For that reason, patients treated with Photofrin[®] have to avoid sunlight for about 4-6 weeks.

Because the characteristics of Photofrin[®] are far from optimal, several new sensitizers were developed. Most effort was put into the development of pure porphyrin derivatives, because this porphyrin moiety is an efficient generator of singlet oxygen.

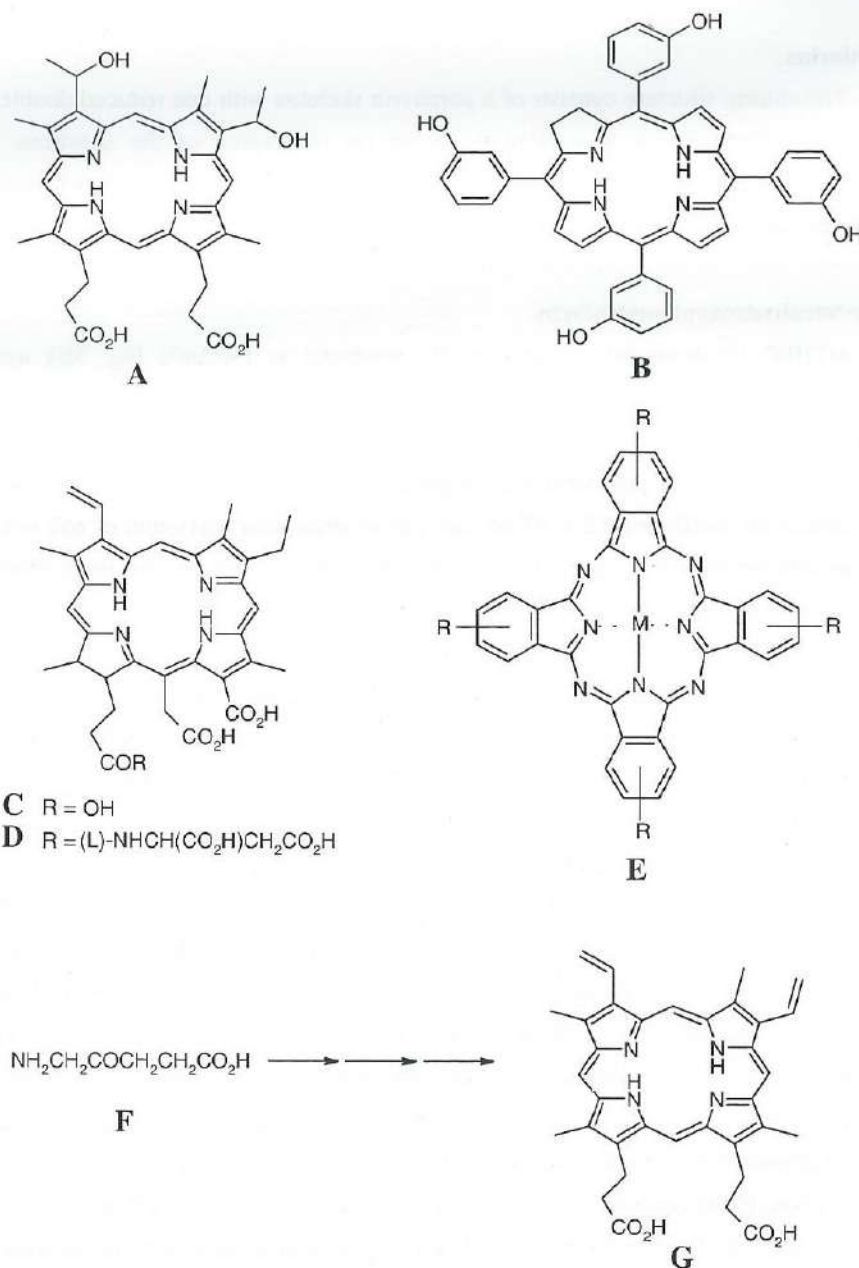


Figure 3. Chemical structures of haematoporphyrin (A), *m*THPC (B), chlorin *e*₆ (C), mono-L-aspartylchlorin *e*₆ (D), phthalocyanine (E), ALA (F) and protoporphyrin IX (G).

d2. Chlorins

The chlorin structure consists of a porphyrin skeleton with one reduced double bond, resulting in absorbance at a wavelength in the far red region of the spectrum. *Meta*-tetrahydroxyphenylchlorin and mono-L-aspartylchlorin e_6 are the two most frequently applied chlorin-type sensitizers.

• *Meta*-tetrahydroxyphenylchlorin

*m*THPC (or temoporfin, commercially produced as Foscan®; Fig. 3B) was first described by Bonnett *et al.* in 1989 (33), in their study on a series of *meso*-tetrahydroxyphenyl porphyrin derivatives. They relatively easily synthesized *m*THPC with a high yield and purity. Its photochemical properties are favorable: it has a strong absorption (molar extinction coefficient $2.2 \times 10^4 \text{ M}^{-1}\text{cm}^{-1}$) at an absorption maximum of 652 nm. In an extensive comparative *in vivo* study (34), *m*THPC appeared to be the most phototoxic compound of this series, with the lowest normal tissue toxicity.

Nevertheless, *m*THPC also shows lack of selectivity. In a phase I clinical trial, Ronn *et al.* (35) obtained in 17 patients with prostate ($n = 6$), bronchial ($n = 1$), nasopharyngeal ($n = 3$), and laryngeal ($n = 3$) cancer, and mesothelioma ($n = 1$), laryngeal papilloma ($n = 2$), or basal cell nevus syndrome ($n = 1$), moderate tumor to adjacent tissue ratios of 1.3-2.9. In relation to this, Hettiaratchy *et al.* (36) reported on the incidence of phototoxicity in a group of 14 healthy volunteers after a single dose of 0.100-0.129 mg/kg. Six men developed severe superficial burns on the left forearm and more superficial burns on other body areas. Wound healing was much slower than with conventional thermal injury. In a reaction to these observations, Scotia (manufacturer of *m*THPC) reported that in a group of 957 healthy volunteers and patients, only 22 (2.3%) showed phototoxicity (37). The company attributed the high incidence of the adverse reactions described by Hettiaratchy *et al.* to problems during the administration of the drug, resulting in its leaking out. This can lead to delayed and prolonged photosensitivity reactions in the affected tissues. While the U.S. Food and Drug Administration (FDA) rejected *m*THPC in 2000, the European Medicines Evaluation Agency (EMA) approved the sensitizer in 2001 for the palliative treatment of patients with advanced head and neck squamous cell carcinoma failing prior therapies and unsuitable for radiotherapy, surgery or systemic chemotherapy.

• Mono-L-aspartylchlorin e_6

Because the natural compound chlorophyll a , which has a chlorin-type structure, is sensitive to auto-oxidation and therefore unsuitable for PDT, several derivatives of this compound have been developed. Under vigorous basic conditions chlorin e_6 is formed (Fig. 3C). This compound has only moderate *in vivo* activity, as Kostenich *et al.* (38) showed in C3H mice bearing sarcoma M-1 xenografts. They obtained a cure rate of only 30%, using a high sensitizer and light dose (10 mg/kg and 180 J/cm^2 24 h p.i., resp.). Therefore chlorin e_6 was further modified, resulting in a large family of derivatives. The most prominent member of this group is mono-L-aspartylchlorin e_6 (NPe6 or MACE, Fig. 3D), which has an absorbance peak at 654 nm and a molar extinction coefficient $4.0 \times 10^4 \text{ M}^{-1}\text{cm}^{-1}$.

d3. Phthalocyanines

Since the 1930's, the group of phthalocyanines, especially the Cu-complexes, has been used as commercial pigments, *e.g.* in ball-point inks. For PDT, they are very interesting because of their high extinction coefficients (up to $2 \times 10^5 \text{ M}^{-1}\text{cm}^{-1}$) in the red region. Furthermore, the synthesis of phthalocyanines is quite straightforward. The phthalocyanine structure (Fig. 3E) is somewhat different from the porphyrin structure. These structural differences result in a long-wavelength absorbance in the 650-700 nm region. Phthalocyanines can be chelated with a variety of metal ions. Most phototoxic appeared to be the zinc^{II}- and aluminium^{III}-complexes (39,40), because both ions lengthen the triplet state lifetime of the sensitizer.

Because the phthalocyanine moiety is very hydrophobic, sulfonated derivatives were developed in an attempt to increase hydrophilicity. Unfortunately, upon sulfonation mixtures of compounds were obtained, which could not be fully separated. Paquette *et al.* (41) studied, in Chinese hamster lung fibroblast cell line V-79, the cellular uptake and phototoxicity of sulfonated phthalocyanines. Uptake and toxicity appeared to be related to the degree of sulfonation, as both increased in the series $\text{AlPcS}_4 \rightarrow \text{AlPcS}_3 \rightarrow \text{AlPcS}_2$. Due to its hydrophilicity, AlPcS_4 is taken up by the cells less efficient than the amphiphilic AlPcS_2 . In BALB/c mice bearing EMT-6 mammary tumors, AlPcS_2 was 10 times more phototoxic than AlPcS_4 (42). The effect of varying hydrophobicity on efficacy has also been demonstrated by Pandey *et al.* (43) with derivatives of the sensitizer pheophorbide-a (a degradation product of chlorophyll a). In SMT-F bearing DBA/2 mice, phototoxicity increased with a decrease in polarity of the sensitizer.

d4. δ -Aminolaevulinic acid (ALA)

ALA (Fig. 3F) is a remarkable sensitizer, as it is actually a precursor. This compound is a naturally-occurring amino-acid, and an early intermediate in the biosynthesis of heme. The enzymes involved in this biosynthesis convert ALA to the phototoxic compound protoporphyrin IX (PpIX) (Fig. 3G). The last step in the formation of photochemically inactive heme is the incorporation of iron into PpIX, under the action of the enzyme ferrochelatase. By adding exogenous ALA, PpIX may accumulate because of the limited capacity of ferrochelatase. Because the activity of this enzyme is lower in some tumors (44), PpIX accumulates with a certain selectivity. A second enzyme active in the PpIX and heme biosynthesis pathway that contributes to tumor selectivity is porphobilinogen deaminase, which catalyzes the formation of uroporphyrinogen from porphobilinogen. Because the activity of this enzyme is higher in some tumors (45), PpIX accumulates with some selectivity. The tumor concentration of PpIX formed endogenously from exogenous ALA reaches its maximum around 1-6 h after systemic administration of ALA (46). Tumor selectivity appears to be higher than for Photofrin[®]. As an example, in a study of Lofgren *et al.* (47) with papillomavirus-infected rabbits, the highest PpIX concentration ratio between papilloma and normal skin was 6:1 (4 h p.i.).

Excitation of PpIX occurs at 635 nm, offering no advantage over HpD in the depth of tissue penetration. Another disadvantage of ALA is its hydrophilic nature, which hampers penetration through cell membranes. This problem may be alleviated by the use of lipophilic ALA derivatives (often esters) which can penetrate cells more easily (48).

e. Potential applications of photodynamic therapy

Nowadays, PDT is under investigation for a variety of applications in oncology. The most favorable treatment sites are those which are easily accessible for illumination and have limited thickness of tumor, such as in superficial skin lesions or early-stage carcinomas of the aerodigestive tract, bronchus, or genitourinary tract. PDT is theoretically an ideal therapeutic strategy for widespread intraperitoneal disease, for which no curative treatment options exist.

Furthermore, PDT may have a role as an adjuvant local modality, especially in locations where the risk of local failure is high. At the time of surgery, maximal exposure of the tissues at risk allows optimal light delivery. Therefore, PDT is a suitable therapy to be delivered at the time of surgical resection. In these cases, PDT offers an advantage over radiotherapy as it causes less damage to underlying normal tissue. Possible sites for this

approach include malignancies in the peritoneal and pleural cavity, as well as malignant gliomas.

Palliatively, PDT could be applied for treatment of obstructing cancers, such as esophageal and lung cancer. Results with clinical PDT applied in the aforementioned areas will be described in the following paragraphs.

Another application of PDT is its use as a method for bone marrow purging. High-dose chemotherapy and autologous bone marrow transplantation are used as a treatment for acute leukemia and non-Hodgkin's lymphoma. Relapse rates tend to be higher in autologous marrow graft than allogenic bone marrow transplantation, partly because autologous grafts carry the possibility of tumor cell contamination. Reduction of this contamination by PDT would be a great improvement. As the sensitizer can be removed before re-infusion of the treated cells into the patient, systemic photosensitization can not take place. Brasseur *et al.* (49) reported on the use of the sensitizer TH9402, a dibrominated rhodamine derivative, for *ex vivo* purging, using human breast cancer (MCF-7 and T-47D) and multiple myeloma (RPMI 8226 and NCI-H929) cell lines. An eradication rate of more than 5 logs was obtained, whereas significant toxicity towards normal hematopoietic stem cells was absent. This was explained by a probably more rapid and more efficient sensitizer uptake by malignant cells. Daziano *et al.* (50) showed the potency of ALPc for selective elimination of TF-1 cells (an acute myeloid leukemia cell line) when mixed with normal peripheral blood leukocytes.

II. Clinical results

a. Head and neck cancer

The current standard methods for treatment of head and neck squamous cell carcinoma (HNSCC) are surgery and radiotherapy, which are both associated with significant morbidity. Surgery can result in functional and aesthetical impairment, while radiotherapy can cause adverse effects such as loss of taste, laryngeal dysfunction and osteoradionecrosis. Therefore the possibilities for PDT in this area, as a more patient-friendly approach, have been intensively studied. In addition, the good accessibility of these tumors for illumination make them excellent targets for PDT.

Initially, PDT for HNSCC was mainly used palliatively. One of the first studies was performed by Keller *et al.* (51) in 1985, who treated 11 patients with tumors of the oral cavity, larynx and neck with the sensitizer HpD (dose 1.5-2 mg/kg, light dose 25-60 J/cm² at 630 nm 48-72 h p.i.). Limited palliation (a partial response = PR) was achieved in 7 out of 8 far-advanced patients, while all 3 patients with less extensive lesions showed a complete response (CR). After several other promising reports on HpD-mediated PDT in HNSCC patients (52,53), interest in this treatment modality grew rapidly. However, in the early '90's, limitations on the use of HpD became apparent. Monnier *et al.* (54) showed, in a study involving 41 patients (2 mg/kg, 60-150 J/cm² at 630 nm 72 h p.i.) with early SCC of the pharynx, esophagus and tracheobronchial tree, that PDT was only effective for cancers staged *in situ* or microinvasive (21/23 CR). Also the tumor selectivity was found to be poor, leading to complications like stenosis, fistulae, and severe sunburn in 6 patients. The authors concluded that more selective sensitizers were required. A year later, Gluckman (55) concluded, from a study with 41 patients (2 mg/kg, 50-100 J/cm² at 630 nm 72 h p.i.), that HpD-mediated PDT could be useful for "condemned mucosa" (*i.e.*, biopsy-proven multicentric, premalignant and overt malignancy, (7/8 CR, lasting 5-53 months)) and early focal cancers (11/13 CR, 4 CR's recurred between 8 and 12 months after treatment), but not for palliation of advanced cancers. In these patients, the palliation obtained was not more effective than standard therapeutic regimens.

The development of *m*THPC renewed interest in PDT for HNSCC because of its improved photochemical properties. In a *m*THPC PDT study (0.15 mg/kg, 75-100 J/cm² at 514 nm for esophageal tumors, and 8-12 J/cm² at 652 nm for other tumors, 96 h p.i.) involving 36 carcinomas *in situ* or microinvasive SCC's of the upper aerodigestive tract, and 4 larger tumors, Grosjean *et al.* (56) reported that 83% of the early stage tumors showed no

recurrence (mean follow-up 15.3 months). Of the 4 T1 and T2 tumors, only 1 achieved a complete response. In another study, Savary *et al.* (57) treated early stage second primary SCC of the esophagus, bronchi and mouth (0.15 mg/kg). For treatment of the bronchi and mouth, 652 nm light was used (7-16 J/cm²), whereas the esophagus was treated with 514 nm (75-100 J/cm²). Of the 33 lesions treated in this trial (all carcinoma *in situ* or microinvasive carcinoma) 28 showed no recurrence (85%; mean follow-up 14 months).

Fan *et al.* (58) studied the use of the sensitizer ALA for the treatment of premalignant lesions (n = 12) or SCC (n = 6) of the oral cavity (60 mg/kg, 100-200 J/cm² at 628 nm 2.5-4 h p.i.). PDT for dysplasia of the mouth produced consistent epithelial necrosis with excellent healing, while repeat biopsy was normal (n = 5) or less dysplastic (n = 7) in all 12 patients. Response in patients with SCC was less satisfactory, as only 3 of the 6 patients became free of tumor. Apparently, the PDT effect was too superficial, since the depth of necrosis was measured to range from 0.1 to 1.3 mm.

On the basis of the experiences gained over the last 15 years, PDT has been recognized as a potentially viable treatment modality for HNSCC. Its considerable therapeutical potential has recently been reported by Biel (59), in a review on a selection of studies on PDT of early HNSCC. Out of 217 patients, 194 (89%) showed a CR, and 23 patients (11%) showed a PR. Furthermore, PDT can be applied without significant morbidity, even when applied repeatedly, while postoperative pain is moderate and can be effectively managed. A disadvantage is the necessity for the patient to remain out of bright sunlight for at least 4 weeks, as a result of skin photosensitization, due to the lack of tumor selectivity of the sensitizer.

b. Lung cancer

The majority of lung cancer patients (85%) are diagnosed with locally advanced tumors and/or metastasis. Surgical resection provides the best chance for cure, but, unfortunately, this is only feasible in about 15% of the cases (60). Obviously there is a need for other treatment modalities to improve local control. Because tumors in the main airways are within the reach of bronchoscopic instruments, PDT in this area could be an attractive option. The illumination procedure (performed under local anaesthesia) is relatively simple, as a laser fiber can be introduced *via* a flexible bronchoscope. In 1982, Hayata *et al.* (61) were the first to investigate a possible benefit from PDT in a group of 13 lung cancer patients mainly with advanced-staged tumors (2 stage-I patients, 8 stage-III, and 3 stage-IV). With

HpD (2.5-4.0 mg/kg, 100 J/cm² at 630 nm 48 h p.i.), local effects were obtained in all patients, without significant improvement in survival.

For advanced-stage lung tumors, PDT is nowadays used in two settings. In one setting, PDT is performed prior to surgery to increase the number of operable patients, or to reduce the extent of resection. Konaka *et al.* (62) reported that, in a group of 25 lung cancer patients who underwent preoperative PDT with Photofrin[®] (2.0 mg/kg, 50 J/cm² at 630 nm 48 h p.i.), this approach was successful for 22 patients: of 5 patients presenting initially with inoperable disease, 4 were converted to operable status, and in 18 out of 20 patients the extent of resection was reduced. In the other setting, PDT is used as a palliative treatment for patients with airway obstruction. A recent prospective controlled randomized trial in 31 patients with partial or complete airway obstruction (63) showed that PDT (2.0 mg Photofrin[®]/kg, illumination at 630 nm 40-50 h p.i., total fluence not reported) and Nd-YAG laser resection showed similar effectiveness: all patients in both groups experienced symptomatic relief after treatment. A more prolonged survival in the PDT group was observed, which was explained by differences in tumor stage between the groups. A disadvantage of PDT was the higher incidence of adverse effects as dyspnoea and photosensitization. A second study in 100 patients (64) also showed the suitability of PDT for palliation, as the mean endoluminal obstruction fell from 86% to 18% after treatment (2 mg Photofrin[®]/kg, 50 J/cm² at 630 nm 24-72 h p.i.). For patients with end stage tumors and therefore a relatively short life expectancy, however, the avoidance of sunlight for a long time due to skin photosensitivity after PDT is a major problem.

For patients with early-stage lung carcinoma, PDT has curative potential. In a group of 54 patients with 59 carcinomas, 50 (85%) showed a CR after PDT with Photofrin[®] (2 mg/kg, 150-360 J/cm² at 630 nm 48 h p.i.) (65). The median duration of CR was 14 months, while the estimated longitudinal tumor extent was the only independent prognostic factor for CR. Nakamura *et al.* (66) concluded that curative PDT with Photofrin[®] of early hilar lung carcinoma is possible when the tumor size is < 8 mm, and the lesion does not extend to the peripheral bronchus. However, Van Boxem *et al.* (67) recently compared the degree of healing and damage of the bronchial wall after PDT with Photofrin[®] (2 mg/kg, 400 J/cm² at 630 nm 48 h p.i.), Nd-YAG laser resection and electrocautery for early-stage intraluminal cancer. Although the numbers of patients were small, differences between the treatment groups were striking. Electrocautery caused only little damage (scarring in 1 out of 17 patients), whereas after PDT (4 out of 6) and Nd-YAG laser treatment (5 out of 6) severe

scarring was observed. The authors concluded that electrocautery is the most appropriate at first line.

c. Disseminated intraperitoneal tumors

Disseminated intraperitoneal tumor is a pattern of disease spread in gastrointestinal malignancies, ovarian cancer and sarcomas that often occurs in the absence of lymphatic or hematogenous metastases. There is no curative therapy available, because chemotherapy has limited effect, radiotherapy would imply excessive toxicity, and surgical resection fails because all peritoneal surfaces are contaminated with tumor. To improve therapeutic outcome, the combination of surgical debulking with intraperitoneal PDT (IPPDT) could be an effective approach. IPPDT presents a great challenge for two reasons. Since the tissue geometry in the peritoneal cavity is extremely complex, it is difficult to deliver a uniform light dose to the peritoneal surface. In addition, there is the problem of effectively treating numerous tumors of variable size, with different blood supplies.

This most probably explains why only a few clinical studies, all performed with Photofrin[®], have been described with IPPDT. In 1993, DeLaney *et al.* (68) reported the results of a phase I study, in which 39 patients received intraoperative IPPDT after debulking surgery. Initially, 630 nm light at 2.8-3.0 J/cm² was used 48 h p.i. (sensitizer dose 2.5 mg/kg), which led to small bowel edema and perforation. Light dose escalation up to 3.75 J/cm² was achieved by using less penetrating 514 nm green light. Because only a small number of patients remained free of disease for a significant duration, no real assessment of efficacy could be made.

Bauer *et al.* (69) described the preliminary results of a phase II trial with 11 patients using PDT for the treatment of intraperitoneal carcinomatosis and sarcomatosis. More recently, they reported the results of 42 patients (70). Two days after injection of 2.5 mg/kg Photofrin[®], surgical tumor debulking (to a thickness of 5 mm or less) and PDT were performed. Illumination was performed with 630 nm light (5-10 J/cm²), except for the small bowel and colon, which were treated with 532 nm green light (2.5 J/cm²). Toxicity was acceptable and there were no bowel perforations. The median survival was 21 months, with a trend toward longest survival in ovarian cancer and shortest in gastrointestinal cancers. However, the relative contribution of surgical resection versus PDT is unknown.

d. Locoregional breast cancer recurrences

Chest wall recurrences are a frequent problem (up to 20%) in patients treated by mastectomy for breast cancer. Conventional management includes surgical excision, radiotherapy, or both. As extensive resection often requires plastic surgical resection, and the CR rate of radiotherapy is limited to 65%, PDT might be a suitable alternative treatment. Using Photofrin® (1-2 mg/kg, 25-100 J/cm² at 630 nm 48 h p.i.), Taber *et al.* (71) treated 11 lesions in 7 patients. They observed a total response rate of 91% (73% CR (8/11), 18% PR (2/11)).

Wyss *et al.* (72) treated 89 lesions in a group of 7 patients with *m*THPC-mediated PDT. The patients received 0.10 mg/kg and a light dose of 5 J/cm² at 652 nm 48 h p.i. (n = 3) or 0.15 mg/kg and 10 J/cm² 96 h p.i. (n = 4). All the lesions showed complete response. PDT therefore is an effective treatment for chest wall recurrence in patients for whom other treatments have failed.

e. Brain tumors

The life expectancy of patients with high grade malignant gliomas is about 15 months despite surgery, radiotherapy and chemotherapy. Because radical resection is not possible due to infiltrating growth into normal brain parenchyma, PDT has been investigated extensively as an adjuvant treatment. In 1996, Kostron *et al.* (73) reported the results of PDT in patients presenting with primary (n = 12) or recurrent (n = 12) glioblastoma. All patients received various formulations of HpD, 24-72 h prior to surgery. After maximal resection, PDT was performed with light doses between 15 and 260 J/cm² at 630 nm. An improvement in survival was observed for primary (median survival 19 months: range 0.5-27 months vs 15 months without PDT) as well as recurrent glioma patients (median survival 9 months: range 3-18 months vs 3 months without PDT). However, the authors concluded that the results were disappointing, as all responses were only temporarily. This was attributed to the fact that, even after debulking the tumor, large volumes remained due to infiltration into normal brain.

To improve tumor resection before PDT, the same group refined their approach (74). A phase-II study was performed with 22 patients with primary and recurrent glioblastoma to assess the feasibility and effectiveness of the combination of intraoperative photodynamic diagnosis and fluorescence-guided resection, mediated by *m*THPC (0.15 mg/kg). In addition, PDT was performed (light dose 20 J/cm² at 652 nm 96 h p.i.). After excitation with 370-440 nm light, tumor areas with *m*THPC fluorescence (652 nm) could be seen by the naked eye and by video-assisted diagnosis. On the basis of 138 tissue samples, a sensitivity of 88% and

a specificity of 96% was achieved, demonstrating a high degree of correlation between the presence of *m*THPC fluorescence and the presence of malignant glioma. The clinical outcome of this study has not been reported yet.

f. Mesothelioma

The incidence of malignant mesothelioma has increased during the last decades, due to asbestos exposure. Asbestos was excessively used in the 1960s, and to a lesser extent in the 1970s. The need for innovative treatment is urgent, because treatment with surgery, radiotherapy, or chemotherapy has not resulted in successful local control. Current therapies yield median survival rates of only 9-14 months. Therefore the intraoperative use of PDT (IPDT) could be an attractive option to achieve local control of disease.

With HpD, results of IPDT were disappointing. Pass *et al.* (75) treated 31 patients in a phase I study. PDT was performed 48 h after sensitization (2 mg/kg) with a total light dose of 15-35 J/cm² at 630 nm. Unfortunately, no increased survival was observed (mean 12 months).

Baas *et al.* (76) studied the use of *m*THPC for IPDT of mesothelioma. In 1997, a study was performed in 5 patients (0.1 mg/kg *m*THPC, 10 J/cm² at 652 nm 96 h p.i.), in which the monitoring of light delivery to the thoracic cavity was optimized. Recently (77), a phase I/II dose escalation study was described with 28 patients, which showed that the maximum tolerable dose was 0.1 mg/kg (4 days before undergoing surgery and IPDT (10 J/cm² at 652 nm)). The median survival time was 10 months. Local tumor control was achieved in 13 of the 26 patients (9 months after treatment). However, the authors concluded that the combination of extensive surgical resection and IPDT was too toxic to consider this as an attractive treatment option, and stated that more limited surgical resections should be performed. Another disadvantage is that it has recently been shown that >50% of the mesothelioma patients develop distant metastases. Therefore these patients need an effective systemic therapy, besides local control of disease.

g. Bladder cancer

Superficial bladder cancer is generally managed by transurethral resection. Unfortunately, more than 70% of the patients have 1 or more recurrences after initial therapy. Adjuvant intravesical chemotherapy or immunotherapy (using bacillus Calmette-Guerin (BCG)) is therefore indicated in patients at high risk for recurrence, *i.e.* patients with stage T1, rapidly recurring or high grade stage Ta, and carcinoma *in situ* (CIS). Although intravesical chemotherapy has demonstrated reduction in short-term tumor recurrence rates, it

has not altered disease progression. BCG, a non-specific immune stimulant, is currently the most effective agent. However, patients in whom standard regimens have failed are candidates for an alternative treatment. Therefore PDT has been evaluated for recurrent superficial papillary transitional cell carcinoma (TCC) and refractory CIS, as well as prophylaxis of recurrent superficial TCC.

Nseyo *et al.* (78) studied the role of whole bladder PDT in the management of refractory/recurrent CIS, as an alternative to cystectomy. A group of 36 patients (in all of them at least 1 course of BCG had failed) was treated (2 mg/kg Photofrin[®], 15 J/cm² at 630 nm 40-50 h p.i.). After 3 months, 58% of the patients had a CR, but at a mean follow-up of 12 months (range 9 to 48), 10 of the 21 CRs had recurrence. So PDT spared 31% of the patients radical cystectomy.

Waidelich *et al.* (79) used ALA for treatment of 24 patients with CIS (n = 5) and papillary tumors (n = 19). They all had recurrences (mean 6), despite multiple transurethral resections, intravesical chemotherapy and BCG treatment. Forty mg/kg ALA was administered orally 4-6 hours before illumination (40 J/cm² at 514 nm, and 20 J/cm² at 635 nm). At a medium follow-up of 36 months (range 12-51), 3 of the 5 patients with CIS and 4 of the 19 with papillary tumors were free of recurrence. The low tumor volume and intraepithelial nature of CIS make that condition susceptible to PDT.

However, complications relating to bladder function appear to be important limiting factors of PDT in urology. The lack of tumor selectivity can lead to deeper bladder wall destruction such as muscle fibrosis and permanently reduced bladder capacity, incontinence, and upper tract deterioration. According to Grönlund-Pakkanen *et al.* (80), it is currently too complicated to treat bladder cancer with PDT, and further studies to avoid irreversible functional impairment should be performed.

h. Basal cell carcinoma

Basal cell carcinoma (BCC) of the skin is a local disease that rarely metastasizes. The first-line treatment is surgery. Multiple lesions, especially on the face, however, can lead to cosmetic problems. Because PDT causes very limited scarring of normal tissue, this could be an attractive alternative treatment for multiple BCCs.

Photofrin[®] and ALA-mediated PDT have achieved response rates up to 95% (81,82). Both treatments have drawbacks, like prolonged skin photosensitivity (in the case of Photofrin[®]), limited penetration depth and long treatment times (10-40 min per lesion). To determine whether the use of *m*THPC enabled the treatment of multiple tumors in a short

period of time, Baas *et al.* (83) performed a phase I/II study. *m*THPC (0.1 mg/kg) was administered to 5 patients, each with 12-200 BCCs (estimated thickness < 3 mm). Best results were obtained (86% CR) when illumination was performed 2 days p.i. with 15 J/cm² at 652 nm. Illumination time was only 150 s per lesion, and the skin healed without scarring. As *m*THPC has the potential to treat also thicker BCCs (> 5 mm), *m*THPC-mediated PDT for BCC could become a convenient and effective method.

III. Advanced delivery of photosensitizers

As described in the previous paragraph, PDT has been applied for the treatment of a variety of tumor types. Promising results were obtained especially in head and neck cancer, locoregional breast cancer recurrences, and basal cell carcinoma. However, most of these studies revealed a lack of tumor selectivity of the photosensitizers. Especially for PDT of large surface areas, as in the treatment of disseminated intraperitoneal tumors or mesothelioma, this can result in severe normal tissue damage. Also the treatment of organs like the bladder is hampered by moderate tumor:non-tumor ratio's. Therefore improvement of the tumor selectivity of photosensitizers is a major issue in PDT. This section describes the strategies used to achieve this.

a. Liposomes

It has been shown (84) that liposomes are removed from the circulation within a few minutes by the macrophages of the reticuloendothelial system (RES), resulting in extensive accumulation in the liver and spleen. This has limited the prospect of using liposomes for transporting drugs to sites different from those of the RES. Despite this, the use of liposomes, which incorporate the sensitizers in the phospholipid bilayer, to deliver highly or moderately hydrophobic photosensitizers to tumors has been studied. A variety of lipids was used for liposome preparation.

A study of Soncin *et al.* (85) clearly demonstrated the problems associated with liposomal delivery of sensitizers. The sensitizer Ge(IV)-octabutoxy-phthalocyanine (GePc), a hydrophobic phthalocyanine derivative, was incorporated in unilamellar liposomes consisting of dipalmitoylphosphatidyl-choline (DPPC) and i.v. administered to BALB/C mice bearing MS-2 fibrosarcoma. The maximum tumor uptake was about 25% of that observed with GePc delivered in the standard ethoxy castor oil (Cremophor) formulation. This decreased uptake was attributed to the more rapid blood clearance of the liposomes.

Also HpD has been incorporated in liposomes consisting of DPPC (86). This time the i.p. route of administration was chosen for mice bearing MS-2 fibrosarcoma. Liposomal sensitizer accumulated in the tumor at a slower rate than the free compound, but the maximum tumor concentration was twice as high. Skin uptake was lower, while liver uptake was as high as for the free compound. The phototoxicity of this liposomal formulation was not determined.

Also with the hydrophobic Zn-phthalocyanine, administered i.v. in various liposomal formulations to tumor bearing nude mice, favorable tumor to non-tumor ratios (4 to 10) were obtained (87). Because the *in vivo* behavior of the free sensitizer, delivered in Cremophor, was not determined, it is not possible to verify whether liposomes improved tumor targeting.

b. Ligand-based targeting

b1. Insulin

Akhlyna and co-workers extensively studied the use of insulin as a ligand for selective photosensitizer delivery. Thereto insulin-BSA-chlorin₆₆ conjugates (molecular weights 5.8, 80, and 0.6 kDa, resp.) with a molar ratio of 13:1:16 were prepared. After binding to its receptor, the conjugates were internalized by receptor-mediated endocytosis and taken up by endosomes. In *in vitro* cultured human hepatoma PLC/PRF/5 cells, conjugates exhibited significantly higher photosensitizing activity than the free compound (88,89). Because an excess of free insulin was shown to completely inhibit phototoxicity, cellular uptake was receptor-specific.

More recently, they adopted a strategy to target the conjugate to the cell nucleus, thereby hypothesizing that this would increase the toxicity of the conjugate (90). Thereto a 2.7 kDa-variant of the nuclear localization signal (NLS) of the simian virus SV40 large tumor antigen was covalently linked to the BSA moiety of an insulin-BSA-chlorin₆₆ conjugate. The results in PLC/PRF/5 cells showed that an insulin-BSA-NLS-chlorin₆₆ conjugate with a molar ratio of 3:1:4:5 was about 7 times more effective than a NLS-lacking conjugate, and about 15 times more efficient than the free chlorin₆₆. Confocal laser scanning microscopy data confirmed that nuclear sensitizer levels were higher for the NLS-containing conjugates.

In the same cell line they showed (91) that co-incubation of the NLS-containing conjugates with adenoviruses enhanced the nuclear sensitizer levels by about 2-fold. This effect is based on the capability of viruses to lyse endosomes. Because a limiting step in the transportation to the nucleus is the release of the conjugates from the endosomes, the use of viruses can increase the nuclear targeting efficiency.

In these studies insulin was used as a model ligand. This approach could be applicable to a variety of ligands and cancer-cell types, for example insulin-like growth factors and nerve growth factor for targeting of neuroblastomas, and melanocyte-stimulating hormone for melanoma. However, whether the insulin-based conjugates are capable of selective targeting of these tumors *in vivo* remains to be seen. Until now, biodistribution and/or *in vivo* efficacy

studies have not been reported. A problem could be, in this respect, that albumins are readily taken up by the liver (and therefore are often used for liver targeting of drugs) (92).

b2. Epidermal growth factor

Because several tumor types, including HNSCC and carcinomas of the esophagus, bladder and lung, express the epidermal growth factor receptor (EGFR) to a high extent, its natural ligand EGF is an attractive candidate as a targeting vehicle. On binding to its receptor, EGF is internalized through receptor-mediated endocytosis, enabling the intracellular accumulation of sensitizers. Gijsens *et al.* covalently conjugated EGF to the sensitizer Sn(IV)-chlorin_{e6} using HSA or dextran as a carrier (93). A carrier was used to increase the molar ratio between EGF and the sensitizer. Furthermore, a carrier can substantially increase the short plasma half-life of EGF (1.5 min). For the HSA-conjugates, loss of affinity of EGF for its receptor was moderate, in contrast to the dextran-conjugates, in which EGF had lost most of its affinity.

In vitro, a conjugate with a EGF:HSA:Sn(IV)-chlorin_{e6} molar ratio of 3:1:3 showed an IC₅₀ value of 63 nM (27 kJ/m²; MDA-MB-468 breast adenocarcinoma cells), while free Sn(IV)-chlorin_{e6} in a concentration up to 1 μM did not show any antiproliferative effect. An excess of free EGF completely abolished phototoxicity, indicating a ligand/receptor trafficking pattern.

b3. Adenoviral proteins

Viruses require α_v integrins for internalization. Expression of integrins is frequently changed in lung cancer, especially in small cell lung cancer. While the α_v subunits are not predominantly present in healthy lung tissue, their expression in lung cancer cell lines is upregulated (94). Allen *et al.* (95) used this increased expression for selective sensitizer targeting. The sensitizer AIPc₄ was covalently coupled to several adenovirus type 2 capsid proteins, including the hexon, the penton base, and the fiber, *via* 1 or 2 caproic acid spacer chains. With 1 spacer, conjugates with a sensitizer:capsid protein molar ratio from 15:1 up to 33:1 were obtained, while these values were 28:1 to 54:1 for 2 spacers.

In vitro phototoxicity experiments with the adenocarcinoma lung cancer cell line A549 revealed that phototoxicity with these conjugates was low. The LD₅₀, the light dose required to induce 50% cell kill (determined with the MTT assay), with a 1 μM concentration of conjugated sensitizer, was > 18 J/cm² for all conjugates. Results of *in vivo* efficacy studies, performed in BALB/C mice bearing mouse mammary EMT-6 tumors, were disappointing.

The phototoxicity of the sensitizer-capsid conjugates was as high as (hexon-conjugates), or lower (the penton base- and fiber conjugates) than the control (in this case the free sensitizer was modified with 2 spacer chains).

c. Photosensitizing adenovirus

A recently developed approach to increase tumor selectivity is the genetic targeting of the photosensitizer ALA (96). This approach is based on adenoviral transduction of a mutant of ALA synthase (ALA-S), the rate-limiting enzyme in heme synthesis. This mutant lacks the regulatory elements, leading to the formation of large amounts of ALA-S. In this way the virus was able to increase the PpIX (protoporphyrin IX) production in H1299 non-small cell lung carcinoma cells, and also to photosensitize these cells. The next step in this development will feature the production of new viruses with tumor-specific promoters, which will restrict the overexpression of ALA-S to tumor cells. A major limitation of this concept is that it is only applicable for ALA, which is not a very effective sensitizer. Moreover, selective targeting of tumor cells by adenovirus, and obtaining an efficient transduction efficiency, is a challenge on its own.

d. Water-soluble polymer carriers

The covalent binding of photosensitizers to water-soluble polymers can result in nonspecific accumulation of these conjugates in the tumor. In general, macromolecules show a prolonged retention in solid tumors compared to low molecular weight compounds. This is caused by the slower diffusion of macromolecules out of the tumor, because of the size dependency of the diffusion rate.

Shiah *et al.* studied the use of *N*-(2-hydroxypropyl)methacrylamide co-polymers for targeting of the sensitizer mesochlorin_{e6}. Free and conjugated sensitizer were *i.v.* injected in OVCAR-3 xenografts bearing nude mice. The co-polymer-bound drug was cleared more slowly from the blood than the free drug (half-lives 1.2 h and 23 min., resp.), while 18 h *p.i.* tumor uptake was about 5 times higher (97). PDT with co-polymer-bound sensitizer (1.5 mg/kg mesochlorin_{e6} equivalent, 220 J/cm² at 650 nm, 12 and 18 h *p.i.*) in the same animal model resulted in significant suppression of tumor growth, although no complete tumor regressions were found (98).

In order to prolong the serum half-life and therefore to improve tumor localization properties, *m*THPC was covalently bound with all four of its hydroxy groups to polyethylene glycol (PEG)-5000. Westermann *et al.* (99) radiolabeled *m*THPC and *m*THPC-PEG with ¹²⁵I

to allow more precise *in vivo* analyses. Comparison of tumor uptake in nude mice bearing colon carcinoma xenograft LS174T, showed 72 h after i.v. injection a %ID/g of 7.7% for *m*THPC-PEG and 4.0% for free *m*THPC. The tumor:non-tumor ratios were more than 2 times higher for ^{125}I -*m*THPC-PEG than for free ^{125}I -*m*THPC. The lower tumor uptake of free *m*THPC was attributed to its shorter serum half-life. Preliminary PDT experiments in the same animal model showed that a 2-fold higher light dose was needed for *m*THPC-PEG to result in equal phototoxicity.

This lower efficacy of pegylated *m*THPC was not found by Ris *et al.* (100). They showed that, in nude mice bearing human SCC or adenocarcinoma xenografts and using the same light dose for both types, the pegylated form led to more extensive tumor necrosis in SCC xenografts, while efficacy in adenocarcinoma xenografts was equal.

Reuther *et al.* observed (101) in RAG-2 mice bearing oral SCC XF 354 xenografts, that pegylated *m*THPC was less effective than free *m*THPC. They explained this observation by the lower ability of pegylated *m*THPC to generate singlet oxygen. Singlet oxygen formation appeared to be about 30% of that of free *m*THPC, probably due to the inactivation of singlet oxygen by PEG. These data strongly suggest that pegylation of *m*THPC will not improve the efficacy of PDT significantly, which was also demonstrated in a rat liver tumor model by Rovers *et al.* (102). They showed that, in contrast to *m*THPC, *m*THPC-PEG accumulated in normal liver as a function of time.

The potential use of unsubstituted aluminium chloride phthalocyanine (AlClPc) has not been fully exploited due to its strong hydrophobic character, which renders it difficult to formulate for *in vivo* administration. Therefore, Brasseur *et al.* (103) produced 2 water-soluble derivatives by axial coordination of PEG-2000 or polyvinylalcohol (PVA, MW 13000-23000) to the central aluminium ion. The pharmacokinetics were studied in EMT-6 bearing BALB/C mice, and the results revealed that the AlPc-PVA derivative showed a prolonged plasma half-life (6.8 h) compared to AlClPc (2.6 h) and AlPc-PEG (23 min), lower retention by liver and spleen, and higher tumor:skin and tumor:muscle ratios (12 and 27, resp., 24 h p.i.). The remarkable short half-life of AlPc-PEG was explained by the fact that small PEG polymers (MW 2000) freely translocate from the circulation to extravascular tissues, whereas large PEGs translocate more slowly. In Colo-26 bearing mice, AlPc-PEG induced a similar tumor control rate, despite very low tumor uptake as compared to AlClPc and AlPc-PVA. This suggests that the residual amount of sensitizer in the tumor is distributed to sites of higher photodynamic sensitivity.

Hamblin *et al.* (104) studied the effect of pegylation of a polylysine-chlorin₆₆ conjugate, which was synthesized with a lysine:chlorin₆₆ molar ratio of 11:1. The molar ratio between PEG and the polylysine-chlorin₆₆ conjugate was not determined. Pegylated and non-pegylated conjugates were injected i.p. into nude mice bearing i.p. OVCAR-5 tumors. Tumor uptake of chlorin₆₆ was about 2 times higher for the pegylated conjugate, and also tumor:non-tumor ratios were higher. Neither the efficacy of the conjugates was determined, nor the biodistribution of i.v. injected conjugates.

e. pH-Responsive polymeric micelles

Taillefer *et al.* used this micelle approach for selective delivery of the sensitizer aluminum chloride phthalocyanine (AlClPc) to tumors. They incorporated the sensitizer in micelles consisting of alkylated *N*-isopropylacrylamide polymers (105). These micelles, which are formed due to the low water solubility of the polymers, are unstable at a lower pH. So this method combines the increased tumor selectivity of water-soluble polymer carriers, as described above, with pH-sensitivity. Both the lower pH as often found in the tumor interstitium, as well as the lower pH in endosomes and lysosomes (which take up the micelles after endocytosis), can lead to drug release by degradation of the micelles. A concomitant advantage is the ability of the polymers to destabilize the endosomal/lysosomal membrane after drug release.

Biodistribution and photodynamic experiments were performed in BALB/c mice bearing the mouse mammary tumor EMT-6. Sensitizer formulations were injected intravenously. Results showed that AlClPc-containing micelles were cleared more rapidly and accumulated less in the tumor than the standard AlClPc Cremophor formulation ($t_{1/2}$ in blood 15 vs. 23 min). However, despite this lower concentration in the tumor, similar phototoxicity was observed, illustrating the potential of polymeric micelles (106).

f. Photosensitizer-monoclonal antibody conjugates

The use of monoclonal antibodies directed against tumor-associated antigens for selective targeting has been studied for about 20 years. Until now, the proof of concept has only been delivered for photoimmunodetection. Pèlegri *et al.* (107) prepared fluorescein-anti-CEA MAb conjugates. For conjugates with a molar ratio of 10, the half-life in nude mice bearing human colon carcinoma T380 was reduced by about 40% compared to unconjugated MAb. Conjugates were shown to be more effective in tumor detection than Photofrin[®]: despite an injected dose of MAb-conjugated fluorescein which was 136 times lower than the

Photofrin® dose, the observed fluorescence intensity of the tumor was 8-fold greater with the conjugate. Folli *et al.* (108) confirmed the feasibility of these conjugates for tumor detection in 6 patients with primary colorectal carcinoma. However, because of its low excitation and emission wavelengths (488 and 515 nm, resp.), fluorescein has two major drawbacks: a low tissue penetration and interference of autofluorescence of normal tissue induced by the exciting laser light.

These problems have been overcome with indocyanin, a sensitizer with longer excitation and emission wavelengths (640 and 667 nm, resp.). The biodistribution and tumor localization of an indocyanin-MAb E48 conjugate with a molar ratio of 2 in A431 bearing nude mice was almost the same as for the unconjugated MAb. For example, tumor uptake 24 h p.i. was 15.5 and 18.2 %ID/g, resp. The indocyanin-MAb conjugates appeared to be superior for photoimmunodetection in comparison with the fluorescein-MAb conjugates (109): a conjugate with an indocyanin:MAb molar ratio of 2 was more efficient in tumor detection than a fluorescein-MAb conjugate with a ratio of 6.

Recently, Gutowski *et al.* (110) used indocyanin-MAb 35A7 conjugates with a molar ratio of 3 in nude mice bearing LS174T peritoneal carcinomatosis to assess the feasibility of intraoperative photoimmunodetection. Results were encouraging, as very small tumor nodules with a mass <1 mg and diameter <1 mm were detected. However, a decrease in sensitivity as a function of tumor mass was observed: sensitivity dropped from 100% for nodules >10 mg to 78% for nodules ≤1 mg.

Unfortunately, neither fluorescein nor indocyanin can be used therapeutically due to their very low yield of singlet oxygen. The first MAb-conjugates produced with a therapeutic aim were described in 1983, when Mew *et al.* developed a conjugation procedure for hematoporphyrin (111). The reproducibility of this procedure was a problem, while loss of antibody binding was significant, resulting in minimal *in vivo* efficacy of the conjugates. Therefore, the same research group developed a reproducible conjugation procedure for the sensitizer benzoporphyrin derivative monoacid ring A (BPD-MA). Polyvinyl alcohol was used as a linker between the sensitizer and the MAb (112). Data on the therapeutic potential of these conjugates have not been reported yet, although *in vitro* results appeared promising (113).

The group of Hasan studied MAb-conjugates with the photosensitizer chlorin_{e6} monoethylenediamine monoamide. Conjugation procedures for different linkers (dextran (114), polyglutamic acid (PGA, 115) and poly-L-lysine (116)), were developed. These linkers were used to increase the sensitizer:MAb ratio. With dextran (molecular weight 10 kDa) as

linker, ratios of 24–36 sensitizers per MAb were achieved. Such a heavy load resulted in slight impairment of the immunoreactivity (93% for the unconjugated MAb, 73% after conjugation). No data on the *in vivo* efficacy of these dextran-linked conjugates have been published. Photoimmunotherapy studies were performed with i.p. injected PGA-linked chlorin_{e6}-mMAb OC125 conjugates in a murine i.p. ovarian cancer model. Seven days after i.p. injection of 30 × 10⁶ NIH:OVCAR-3 cells, mice received 0.5 mg/kg sensitizer equivalent, and 5 J/cm² 24 h later. Treatment was repeated every 48 h, for a total of 3 and 4 treatments. The median survival for 3 and 4 times treated mice was 47 and 58 days, respectively, and 38 days for control mice.

The photoimmunoconjugates with poly-L-lysine, which is a positively charged linker, were most extensively studied. To determine the effect of charge of the conjugates on the uptake and phototoxicity negatively charged conjugates were also produced by polysuccinylation of the poly-L-lysine linker (116). The efficacy of these conjugates was determined in nude mice for several tumor types. In the i.p. ovarian cancer model described before (15 × 10⁶ NIH:OVCAR-5 cells, 1 mg/kg sensitizer equivalent, 25 J/cm² 24 h p.i.; 3 PDT treatments, repeated every 72 h), the cationic chlorin_{e6}-mMAb OC125F(ab')₂-conjugate (with a molar ratio chlorin_{e6}:F(ab')₂ of 15:1) showed after i.p. administration a higher tumor selectivity and phototoxicity, in comparison with the anionic conjugate and free sensitizer (117). The median survival for the cationic group was 41 days, compared with 35 days for the anionic group and 37 days for the free sensitizer. Because complete eradication of tumor cells was not consistently found, further refinement investigations are ongoing.

Interestingly, the anionic chlorin_{e6}-mMAb 17.1A conjugate performed better than the cationic one when administered i.v. instead of i.p.: In a hepatic metastasis model of colorectal cancer (118), tumor uptake of the anionic conjugate was about 7-fold higher than the cationic one (24 h p.i.), which was explained by the reduced serum half-life of the latter, and was about 3-fold higher than the free sensitizer. The tumor to normal liver ratio of the anionic conjugate, however, was lower than for the cationic conjugate and for the free sensitizer (1.5, 1.6 and 2.6, respectively at 24 h p.i.). PDT (0.25 mg/kg chlorin_{e6} equivalent, 80 J/cm² 3 h p.i.) with the i.v.-injected anionic chlorin_{e6}-mMAb 17.1A conjugate (with a molar ratio of 8.5:1) led to an increased median survival of 102 days in comparison to 77 days for the mice receiving free sensitizer and 63 days for the control mice (119). The efficacy of the cationic conjugate was not determined.

More recently, the group of Hasan performed a pilot study to investigate the photodynamic effect of a chlorin_{e6}-MAb C225 (an anti-EGFR MAb) conjugate on EGFR

expression in carcinogen-induced premalignant lesions of the hamster cheek pouch. The photodestruction of EGFR should result in inhibition of cellular proliferation. Photoimmunotherapy with an i.v. injected conjugate with a molar ratio of 4.8 reduced the overexpression of EGFR in dysplastic areas to background levels, as was determined by photoimmunodiagnosis with an indocyanine-MAb C225 conjugate (120).

Also the coupling of the sensitizer aluminium phthalocyanine tetrasulfonate (AlPc(SO₃H)₄) to MAbs has been described. Morgan *et al.* reported the coupling of AlPc(SO₃H)₄ via AlPc(SO₂Cl)₄ (121). Preliminary experiments with bladder carcinoma cell line 647C revealed limited phototoxicity of these conjugates *in vitro*. The IC₅₀, determined with the MTT assay, was about 0.5 μM (with a light dose of 3.2 J/cm²). Recently, Carcenac *et al.* reported on the preparation of AlPc(SO₃H)₄-MAb conjugates via a mono five-carbon spacer chain, but also in this case the *in vitro* efficacy of the conjugates was limited (122). The MTT assay revealed an IC₅₀ of about 0.35 μM (light dose 50 J/cm²).

AIM AND OUTLINE OF THE THESIS

As described in the introductory **Chapter 1**, PDT has been applied rather successfully for the treatment of superficially localized tumors, especially in head and neck cancer, locoregional breast cancer recurrences, and basal cell carcinoma. As most of the clinical PDT studies revealed a lack of tumor selectivity of the photosensitizers, increasing this selectivity remains to be a major issue. The use of monoclonal antibodies seems to be a realistic option, as was shown by Pèlerin *et al.* (107) with fluorescein-anti-CEA MAb conjugates. These conjugates were more efficient in tumor detection in nude mice than the free photosensitizer Photofrin®. However, therapeutically effective sensitizer-MAb conjugates are still not available, whereas research is mainly focused on conjugates to be used intraperitoneally. Therefore, the development of phototoxic conjugates suitable for systemic use forms a major challenge.

The availability in our lab of a panel of monoclonal antibodies with proven capacity for selective tumor targeting in head and neck cancer patients, as well as of several clinically promising sensitizers, gives us the opportunity to determine the full potential of photosensitizer-MAb conjugates. As a first step in this approach, this thesis addresses the development of conjugation routes to MAbs for these photosensitizers, as well as the *in vitro* and *in vivo* characterization of the conjugates. The main aim of the study is to develop photosensitizer-MAb conjugates capable of selective tumor targeting after i.v. administration.

This study starts with *m*THPC, considered to be one of the most promising sensitizers. In **Chapter 2** a procedure is described for conjugation of this very hydrophobic compound to MAbs. The capacity of a *m*THPC-MAb conjugate for selective tumor-targeting in nude mice is evaluated, and also preliminary results on PDT efficacy *in vitro* are reported.

TrisMPyP-ΦCO₂H, a hydrophilic porphyrin derivative, is used in **Chapter 3** as a model compound to assess the suitability of hydrophilic compounds for MAb-targeted PDT. The TrisMPyP-ΦCO₂H-MAb conjugates are characterized in the same way as for the conjugates described in the previous chapter.

In **Chapter 4** a conjugation procedure is described for AlPc(SO₃H)₄, also a hydrophilic sensitizer but with much better photochemical properties for PDT than TrisMPyP-ΦCO₂H. Also these conjugates are characterized with respect to their *in vivo* behavior, as well as, preliminary, their *in vitro* efficacy.

To rank the photosensitizer-MAb conjugates for their potential in photoimmunotherapy, **Chapter 5** describes an extensive *in vitro* evaluation of *m*THPC-MAB

and AIPcS₄-MAb conjugates. Five different SCC cell lines were used as target, and three different MAbs for tumor cell targeting.

REFERENCES

1. Raab, O. On the effect of fluorescent substances on infusoria. *Z. Biol.*, 39: 524-546, 1900.
2. Jodlbauer, A., and von Tappeiner, H. On the participation of oxygen in the photodynamic effect of fluorescent substances. *Münch. Med. Wochenschr.*, 52: 1139-1141, 1904.
3. Jesionek, A., and von Tappeiner, H. On the treatment of skin cancers with fluorescent substances. *Arch. Klin. Med.*, 82: 223-227, 1905.
4. Policard, A. Studies of experimental tumours under Wood's light. *Comp. Rend. Soc. Biol.*, 91: 1423-1428, 1924.
5. Auler, H., and Banzer, G. Investigations on the role of porphyrins in tumour-bearing humans and animals. *Z. Krebsforsch.*, 53: 65-68, 1942.
6. Lipson, R. L., and Baldes, E. J. The photodynamic properties of a particular haematoporphyrin derivative. *Arch. Dermatol.*, 82: 508-516, 1960.
7. Moan, J., and Berg, K. The photodegradation of porphyrins in cells can be used to estimate the lifetime of singlet oxygen. *Photochem. Photobiol.*, 53: 549-553, 1991.
8. Nilsson, R., Swanbeck, G., and Wennersten, G. Primary mechanisms of erythrocyte photolysis induced by biological sensitizers and phototoxic drugs. *Photochem. Photobiol.*, 22: 183-186, 1975.
9. Shulok, J. R., Wade, M. H., and Lin, C.-W. Subcellular localization of hematoporphyrin derivative in bladder tumor cells in culture. *Photochem. Photobiol.*, 51: 451-457, 1990.
10. Wilson, B. C., Olivo, M., and Singh, G. Subcellular localization of Photofrin[®] and aminolevulinic acid and photodynamic cross-resistance *in vitro* in radiation-induced fibrosarcoma cells sensitive or resistant to Photofrin-mediated photodynamic therapy. *Photochem. Photobiol.*, 65: 166-176, 1997.
11. Woodburn, K. W., Vardaxis, N. J., Hill, J. S., Kaye, A. H., and Phillips, D. R. Subcellular localization of porphyrins using confocal laser scanning microscopy. *Photochem. Photobiol.*, 54: 725-732, 1991.
12. Woodburn, K. W., Vardaxis, N. J., Hill, J. S., Kaye, A. H., Reiss, J. A., and Phillips, D. R. Evaluation of porphyrin characteristics required for photodynamic therapy. *Photochem. Photobiol.*, 55: 697-704, 1992.
13. Chiu, S.-M., Evans, H. H., Lam, M., Nieminen, A.-L., and Oleinick, N. L. Phthalocyanine 4 photodynamic therapy-induced apoptosis of mouse L5178Y-R cells results from a delayed but extensive release of cytochrome c from mitochondria. *Cancer Lett.*, 165: 51-58, 2001.
14. Fabris, C., Valduga, G., Miotto, G., Borsetto, L., Jori, G., Garbisa, S., and Reddi, E. Photosensitization with zinc (II) phthalocyanine as a switch in the decision between apoptosis and necrosis. *Cancer Res.*, 61: 7495-7500, 2001.
15. Ma, L., Moan, J., and Berg, K. Evaluation of a new photosensitizer, meso-tetra-hydroxyphenyl-chlorin, for use in photodynamic therapy: a comparison of its photobiological properties with those of two other photosensitizers. *Int. J. Cancer*, 57: 883-888, 1994.
16. Chen, J. Y., Mak, N. K., Wen, J. M., Leung, W. N., Chen, S. C., Fung, M. C., and Cheung, N. H. A comparison of the photodynamic effects of temoporfin (mTHPC) and MC540 on leukemia cells: efficacy and apoptosis. *Photochem. Photobiol.*, 68: 545-554, 1998.

17. Melnikova, V. O., Bezdetsnaya, L. N., Bour, C., Fester, E., Gramain, M.-P., Merlin, J.-L., Potapenko, A. Y., and Guillemin, F. Subcellular localization of meta-tetra(hydroxyphenyl)chlorin in human tumor cells subjected to photodynamic treatment. *J. Photochem. Photobiol. B: Biol.*, *49*: 96-103, 1999.
18. Yow, C. M. N., Chen, J. Y., Mak, N. K., Cheung, N. H., and Leung, A. W. N. Cellular uptake, subcellular localization and photodamaging effect of Temoporfin (mTHPC) in nasopharyngeal carcinoma cells: comparison with hematoporphyrin derivative. *Cancer Lett.*, *157*: 123-131, 2000.
19. Ramakrishnan, N., Oleinick, N. L., Clay, M. E., Horng, M. F., Antunez, A. R., and Evans, H. H. DNA lesions and DNA degradation in mouse lymphoma L5178Y cells after photodynamic treatment sensitized by chloroaluminium phthalocyanine. *Photochem. Photobiol.*, *50*: 373-378, 1989.
20. Dougherty, T. J., Gomer, C. J., Henderson, B. W., Jori, G., Kessel, D., Korbek, M., Moan, J., and Peng, Q. Photodynamic therapy. *J. Natl. Cancer Inst.*, *90*: 889-905, 1998.
21. Kessel, D. Determinants of photosensitization by purpurins. *Photochem. Photobiol.*, *50*: 169-174, 1989.
22. Fingar, V. H., Wieman, T. J., and Haydon, P. S. The effects of thrombocytopenia on vessel stasis and macromolecular leakage after photodynamic therapy using Photofrin. *Photochem. Photobiol.*, *66*: 513-517, 1997.
23. McMahon, K. S., Wieman, T. J., and Moore, P. H. Effects of photodynamic therapy using mono-L-aspartyl chlorin e₆ on vessel constriction, vessel leakage, and tumor response. *Cancer Res.*, *54*: 5374-5379, 1994.
24. Fingar, V. H., Wieman, T. J., and Karavolos, P. S. The effects of photodynamic therapy using differently substituted zinc phthalocyanines on vessel constriction, vessel leakage, and tumor response. *Photochem. Photobiol.*, *58*: 251-258, 1993.
25. Krosi, G., Korbek, M., and Dougherty, G. J. Induction of immune cell infiltration into murine SCCVII tumour by Photofrin-based photodynamic therapy. *Br. J. Cancer*, *71*: 549-555, 1995.
26. Lipson, R. L., Baldes, E. J., and Olsen, A. M. The use of a derivative of haematoporphyrin in tumor detection. *J. Natl. Cancer Inst.*, *26*: 1-11, 1961.
27. Dougherty, T. J., Grindey, G. B., Fiel, R., Weishaupt, K. R., and Boyle, D. G. Photoradiation therapy. II. Cure of animal tumours with hematoporphyrin and light. *J. Natl. Cancer Inst.*, *55*: 115-119, 1975.
28. Kelly, J. F., Snell, M. E., and Berenbaum, M. C. Photodynamic destruction of human bladder carcinoma. *Br. J. Cancer*, *31*: 237-244, 1975.
29. Berenbaum, M. C., Bonnett, R., and Scourides, P. A. *In vivo* biological activity of the components of haematoporphyrin derivative. *Br. J. Cancer*, *45*: 571-581, 1982.
30. Lightdale, C. J., Heier, S. K., Marcon, N. E., McCaughan J. S. Jr, Gerdes, H., Overholt, B. F., Sivak, M. V. Jr, Stiegmann, G. V., and Nava, H. R. Photodynamic therapy with porfimer sodium versus thermal ablation therapy with Nd:YAG laser for palliation of esophageal cancer: a multicenter randomized trial. *Gastrointest. Endosc.*, *42*: 507-512, 1995.
31. McCaughan, J. S., Williams, T. E., and Bethel, B. H. Photodynamic therapy of endobronchial tumors. *Lasers Surg. Med.*, *6*: 336-345, 1986.
32. Orenstein, A., Kostenich, G., Roitman, L., Shechtman, Y., Kopolovic, Y., Ehrenberg, B., and Malik, Z. A comparative study of tissue distribution and photodynamic therapy selectivity of chlorin e₆, Photofrin II and ALA-induced protoporphyrin IX in a colon carcinoma model. *Br. J. Cancer*, *73*: 937-944, 1996.
33. Bonnett, R., White, R. D., Winfield, U.-J., and Berenbaum, M. C. Hydroporphyrins of the meso-tetra(hydroxyphenyl)porphyrin series as tumour photosensitizers. *Biochem. J.*, *261*: 277-280, 1989.
34. Berenbaum, M. C., Bonnett, R., Chevetron, E. B., Akande-Adebakin, S. L., and Ruston, M. Selectivity of meso-tetra(hydroxyphenyl)porphyrins and chlorins and of Photofrin II in causing photodamage in tumour, skin, muscle and bladder. The concept of cost-benefit in analysing the results. *Lasers Med. Sci.*, *8*: 235-243, 1993.
35. Ronn, A. M., Nouri, M., Lofgren, L. A., Steinberg, B. M., Westerborn, A., Windahl, T., Shikowitz, M. J., and Abramson, A. L. Human tissue levels and plasma pharmacokinetics of Temoporfin (Foscan[®], mTHPC). *Lasers Med. Sci.*, *11*: 267-272, 1996.
36. Hettiaratchy, S., Clarke, J., Taubel, J., and Besa, C. Burns after photodynamic therapy. *BMJ*, *320*: 1245, 2000.
37. Bryce, R. Drug point gives misleading impression of incidence of burns with temoporfin (Foscan). *BMI*, *320*: 1731, 2000.
38. Kostenich, G. A., Zhuravkin, I. N., and Zhavrid, E. A. Experimental grounds for using chlorin e₆ in the photodynamic therapy of malignant tumors. *J. Photochem. Photobiol. B: Biol.*, *22*: 211-217, 1994.
39. Ambroz, M., Beeby, A., MacRobert, A. J., Simpson, M. S. C., Svensen, R. K., and Phillips, D. Preparative, analytical and fluorescence spectroscopic studies of sulphonated aluminum phthalocyanine photosensitizers. *J. Photochem. Photobiol. B: Biol.*, *9*: 87-95, 1991.
40. Berg, K., Bommer, J. C., and Moan, J. Evaluation of sulfonated aluminum phthalocyanines for use in photochemotherapy. A study on the relative efficiencies of photoinactivation. *Photochem. Photobiol.*, *49*: 587-594, 1989.
41. Paquette, B., Boyle, R. W., Ali, H., MacLennan, A. H., Truscott, T. G., and van Lier, J. E. Sulfonated phthalimidomethyl aluminum phthalocyanine: The effect of hydrophobic substituents on the *in vitro* phototoxicity of phthalocyanines. *Photochem. Photobiol.*, *53*: 323-327, 1991.
42. Boyle, R. W., Paquette, B., and van Lier, J. E. Biological activities of phthalocyanines XIV. Effect of hydrophobic phthalimidomethyl groups on the *in vivo* phototoxicity and mechanism of photodynamic action of sulphonated aluminium phthalocyanines. *Br. J. Cancer*, *65*: 813-817, 1992.
43. Pandey, R. K., Shiao, F.-Y., Sumlin, A. B., Dougherty, T. J., and Smith, K. M. Structure/activity relationships among photosensitizers related to pheophorbides and bacteriopheophorbides. *Bioorg. Med. Chem. Lett.*, *2*: 491-496, 1992.
44. El-Sharabasy, M. M., El-Waseef, A. M., Hafez, M. M., and Salim, S. A. Porphyrin metabolism in some malignant diseases. *Br. J. Cancer*, *65*: 409-412, 1992.
45. Leibovici, L., Schoenfeld, N., Yehoshua, H. A., Mamet, R., Rakowsky, E., Shindel, A., and Atsmon, A. Activity of porphobilinogen deaminase in peripheral blood mononuclear cells of patients with metastatic cancer. *Cancer*, *62*: 2297-2300, 1998.
46. Peng, Q., Berg, K., Moan, J., Kongshaug, M., and Nesland, J. M. 5-Aminolevulinic acid-based photodynamic therapy: principles and experimental research. *Photochem. Photobiol.*, *65*: 235-251, 1997.
47. Lofgren, L. A., Ronn, A. M., Nouri, M., Lee, C. J., Yoo, D., and Steinberg, B. M. Efficacy of intravenous delta-aminolevulinic acid photodynamic therapy on rabbit papillomas. *Br. J. Cancer*, *72*: 857-864, 1995.

48. Gaullier, J. M., Berg, K., Peng, Q., Anholt, H., Selbo, P. K., Ma, L. W., and Moan, J. Use of 5-aminolevulinic acid esters to improve photodynamic therapy on cells in culture. *Cancer Res.*, *57*: 1481-1486, 1997.
49. Brasseur, N., Menard, I., Forget, A., El Jastimi, R., Hamel, R., Molino, N. A., and van Lier, J. E. Eradication of multiple myeloma and breast cancer cells by TH9402-mediated photodynamic therapy: implication for clinical *ex vivo* purging of autologous stem cell transplants. *Photochem. Photobiol.*, *72*: 780-787, 2000.
50. Daziano, J.-P., Humeau, L., Henry, M., Mannoni, P., Chanon, M., Chabannon, C., and Julliard, M. Preferential photoinactivation of leukemia cells by aluminum phthalocyanine. *J. Photochem. Photobiol. B: Biol.*, *43*: 128-135, 1998.
51. Keller, G. S., Doiron, D. R., and Fisher, G. U. Photodynamic therapy in otolaryngology- head and neck surgery. *Arch. Otolaryngol.*, *111*: 758-761, 1985.
52. Zhao, F. Y., Zhang, K. H., Huang, H. N., Sun, K. H., Ling, Q. B., and Xu, B. Use of hematoporphyrin derivative as a sensitizer for radiotherapy of oral and maxillofacial tumors: a preliminary report. *Lasers Med. Sci.*, *1*: 253-256, 1986.
53. Grossweiner, L. I., Hill, J. H., and Lobraico, R. V. Photodynamic therapy of head and neck squamous cell carcinoma: optimal dosimetry and clinical trial. *Photochem. Photobiol.*, *46*: 911-917, 1987.
54. Monnier, Ph., Savary, M., Fontollet, Ch., Wagnières, G., Chatelain, A., Cornaz, P., Depeursinge, Ch., and van den Bergh, H. Photodetection and photodynamic therapy of 'early' squamous cell carcinomas of the pharynx, oesophagus and tracheobronchial tree. *Lasers Med. Sci.*, *5*: 149-169, 1990.
55. Gluckman, J. L. Hematoporphyrin photodynamic therapy: is there truly a future in head and neck oncology? Reflections on a 5-year experience. *Laryngoscope*, *101*: 36-41, 1991.
56. Grosjean, P., Savary, J. F., Mizeret, J., Wagnières, G., Woodtli, A., Theumann, J. F., Fontollet, C., van den Bergh, H., and Monnier P. Photodynamic therapy for cancer of the upper aerodigestive tract using Tetra(m-hydroxyphenyl)chlorin. *J. Clin. Laser Med. Surg.*, *14*: 281-287, 1996.
57. Savary, J.-F., Monnier, P., Fontollet, C., Mizeret, J., Wagnières, G., Braichotte, D., and van den Bergh, H. Photodynamic therapy for early squamous cell carcinomas of the esophagus, bronchi, and mouth with m-Tetra(hydroxyphenyl)chlorin. *Arch. Otolaryngol. Head Neck Surg.*, *123*: 162-168, 1997.
58. Fan, K. F. M., Hopper, C., Speight, P. M., Buonaccorsi, G., MacRobert, A. J., and Bown, S. G. Photodynamic therapy using 5-aminolevulinic acid for premalignant and malignant lesions of the oral cavity. *Cancer*, *78*: 1374-1383, 1996.
59. Biel, M. A. Photodynamic therapy and the treatment of head and neck neoplasia. *Laryngoscope*, *108*: 1259-1268, 1998.
60. Sutedja, T. G., and Postmus, P. E. Photodynamic therapy in lung cancer. A review. *J. Photochem. Photobiol. B: Biol.*, *36*: 199-204, 1996.
61. Hayata, Y., Kato, H., Konaka, C., Ono, J., and Takizawa, N. Hematoporphyrin derivative and laser photoradiation in the treatment of lung cancer. *Chest*, *81*: 269-277, 1982.
62. Konaka, C., Okunaka, T., and Kato, H. Combined use of photodynamic therapy and surgery. *Ann. Thorac Cardiovasc. Surg.*, *1*: 55-60, 1995.
63. Diaz-Jimenez, J. P., Martinez-Ballarin, J. E., Lluell, A., Farrero, E., Rodriguez, A., and Castro, M. J. Efficacy and safety of photodynamic therapy versus Nd-YAG laser resection in NSCLC with airway obstruction. *Eur. Respir. J.*, *14*: 800-805, 1999.
64. Moghissi, K., Dixon, K., Stringer, M., Freeman, T., Thorpe, A., and Brown, S. The place of bronchoscopic photodynamic therapy in advanced unresectable lung cancer: experience of 100 cases. *Eur. J. Cardiothorac Surg.*, *15*: 1-6, 1999.
65. Furuse, K., Fukuoka, M., Kato, H., Horai, T., Kubota, K., Kodama, N., Kusunoki, Y., Takifuji, N., Okunaka, T., and Konaka, C. A prospective phase II study on photodynamic therapy with Photofrin II for centrally located early-stage lung cancer. *J. Clin. Oncol.*, *11*: 1852-1857, 1993.
66. Nakamura, H., Kawasaki, N., Hagiwara, M., Ogata, A., and Kato, H. Endoscopic evaluation of centrally located early squamous cell carcinoma of the lung. *Cancer*, *91*: 1142-1147, 2001.
67. Van Boxcem, A. J. M., Westerga, J., Venmans, B. J. W., Postmus, P. E., and Sutedja, G. Photodynamic therapy, Nd-YAG laser and electrocautery for treating early-stage intraluminal cancer: which to choose? *Lung Cancer*, *31*: 31-36, 2001.
68. DeLaney, T. F., Sindelar, W. F., Tochner, Z., Smith, P. D., Friauf, W. S., Thomas, G., Dachowski, L., Cole, J. W., Steinberg, S. M., and Glatstein, E. Phase I study of debulking surgery and photodynamic therapy for disseminated intraperitoneal tumors. *Int. J. Radiat. Oncol. Biol. Phys.*, *25*: 445-457, 1993.
69. Bauer, T. W., Hahn, S. M., Spitz, F. R., Kachur, A., Glatstein, E., and Fraker, D. L. Preliminary report of photodynamic therapy for intraperitoneal sarcomatosis. *Ann. Surg. Oncol.*, *8*: 254-259, 2001.
70. Hendren, S. K., Hahn, S. M., Spitz, F. R., Bauer, T. W., Rubin, S. C., Zhu, T., Glatstein, E., and Fraker, D. L. Phase II trial of debulking surgery and photodynamic therapy for disseminated intraperitoneal tumors. *Ann. Surg. Oncol.*, *8*: 65-71, 2001.
71. Taber, S. W., Fingar, V. H., and Wieman, T. J. Photodynamic therapy for palliation of chest wall recurrence in patients with breast cancer. *J. Surg. Oncol.*, *68*: 209-214, 1998.
72. Wyss, P., Schwarz, V., Dobler-Girdziunaite, D., Hornung, R., Walt, H., Degen, A., and Fehr, M. K. Photodynamic therapy of locoregional breast cancer recurrences using a hlorin-type photosensitizer. *Int. J. Cancer*, *93*: 720-724, 2001.
73. Kostron, H., Obwegeser, A., and Jakober, R. Photodynamic therapy in neurosurgery: a review. *J. Photochem. Photobiol. B: Biol.*, *36*: 157-168, 1996.
74. Zimmermann, A., Ritsch-Marte, M., and Kostron, H. mTHPC-mediated photodynamic diagnosis of malignant brain tumors. *Photochem. Photobiol.*, *74*: 611-616, 2001.
75. Pass, H. I., Delaney, T., Tochner, Z., Smith, P. E., Temeck, B. K., Pogrebniak, H. W., Kranda, K. C., Russo, A., Friauf, W. S., Cole, J. W., Mitchell, J. B., and Thomas, G. Intrapleural photodynamic therapy: results of a phase I trial. *Ann. Surg. Oncol.*, *1*: 28-37, 1994.
76. Baas, P., Murrer, L., Zoetmulder, F. A. N., Stewart, F. A., Ris, H. B., van Zandwijk, N., Peterse, J. L., and Rutgers, E. J. Th. Photodynamic therapy as adjuvant therapy in surgically treated pleural malignancies. *Br. J. Cancer*, *76*: 819-826, 1997.
77. Schouwink, H., Rutgers, E. T., van der Sijp, J., Oppelaar, H., van Zandwijk, N., van Veen, R., Burgers, S., Stewart, F. A., Zoetmulder, F., and Baas, P. Intraoperative photodynamic therapy after pleuropneumectomy in patients with malignant pleural mesothelioma. Dose finding and toxicity results. *Chest*, *120*: 1167-1174, 2001.

78. Nseyo, U. O., Shumaker, B., Klein, E. A., and Sutherland, K. Photodynamic therapy using porfimer sodium as an alternative to cystectomy in patients with refractory transitional cell carcinoma in situ of the bladder. *J. Urol.*, *160*: 39-44, 1998.
79. Waidelich, R., Stepp, H., Baumgartner, R., Weninger, E., Hofstetter, A., and Kriegmair, M. Clinical experience with 5-aminolevulinic acid and photodynamic therapy for refractory superficial bladder cancer. *J. Urol.*, *165*: 1904-1907, 2001.
80. Grönlund-Pakkanen, S., Pakkanen, T. M., Koski, E., Talja, M., Ala-Opas, M., and Alhava, E. Effect of photodynamic therapy on urinary bladder function: an experimental study with rats. *Urol. Res.*, *29*: 205-209, 2001.
81. McCaughan, J. S. Jr, Guy, J. T., Hicks, W., Laufman, L., Nims, T. A., and Walker, J. Photodynamic therapy for cutaneous and subcutaneous malignant neoplasms. *Arch. Surg.*, *124*: 211-216, 1989.
82. Jeffes, E. W., McCullough, J. L., Weinstein, G. D., Fergin, P. E., Nelson, J. S., Shull, T. F., Simpson, K. R., Bukaty, L. M., Hoffman, W. L., and Fong, N. L. Photodynamic therapy of actinic keratosis with topical 5-aminolevulinic acid: a pilot dose ranging study. *Arch. Dermatol.*, *133*: 727-732, 1997.
83. Baas, P., Saarnak, A. E., Oppelaar, H., Neering, H., and Stewart, F. A. Photodynamic therapy with meta-tetrahydroxyphenylchlorin for basal cell carcinoma: a phase I/II study. *Br. J. Dermatol.*, *145*: 75-78, 2001.
84. Hsu, M. J., and Juliano, R. L. Interactions of liposomes with the reticuloendothelial system. II: Nonspecific and receptor-mediated uptake of liposomes by mouse peritoneal macrophages. *Biochim. Biophys. Acta*, *720*: 411-419, 1982.
85. Soncin, M., Polo, L., Reddi, E., Jori, G., Kenney, M. E., Cheng, G., and Rodgers, M. A. J. Effect of the delivery system on the biodistribution of Ge(IV) octabutoxy-phthalocyanines in tumour-bearing mice. *Cancer Lett.*, *89*: 101-106, 1995.
86. Jori, G., Reddi, E., Cozzani, I., and Tomio, L. Controlled targeting of different subcellular sites by porphyrins in tumour-bearing mice. *Br. J. Cancer*, *53*: 615-621, 1986.
87. Reddi, E., Zhou, C., Biolo, R., Menegaldo, E., and Jori, G. Liposome- or LDL- administered Zn(II)-phthalocyanine as a photodynamic agent for tumours. I. Pharmacokinetic properties and phototherapeutic efficiency. *Br. J. Cancer*, *61*: 407-414, 1990.
88. Sobolev, A. S., Akhlynina, T. V., Yachmenev, S. V., Rosenkranz, A. A., and Severin, E. S. Internalizable insulin-BSA-chlorin₆₆ conjugate is a more effective photosensitizer than chlorin₆₆ alone. *Biochem. Int.*, *26*: 445-450, 1992.
89. Akhlynina, T. V., Rosenkranz, A. A., Jans, D. A., and Sobolev, A. S. Insulin-mediated intracellular targeting enhances the photodynamic activity of chlorin₆₆. *Cancer Res.*, *55*: 1014-1019, 1995.
90. Akhlynina, T. V., Jans, D. A., Rosenkranz, A. A., Statsyuk, N. V., Balashova, I. Y., Toth, G., Pavo, I., Rubin, A. B., and Sobolev, A. S. Nuclear targeting of chlorin₆₆ enhances its photosensitizing activity. *J. Biol. Chem.*, *272*: 20328-20331, 1997.
91. Akhlynina, T. V., Jans, D. A., Statsyuk, N. V., Balashova, I. Y., Toth, G., Pavo, I., Rosenkranz, A. A., Naroditsky, B. S., and Sobolev, A. S. Adenoviruses synergize with nuclear localization signals to enhance nuclear delivery and photodynamic action of internalizable conjugates containing chlorin₆₆. *Int. J. Cancer*, *81*: 734-740, 1999.
92. Melgert, B. N., Wartna, E., Lebbe, C., Albrecht, C., Molema, G., Poelstra, K., Reichen, J., and Meijer, D. K. Targeting of naproxen covalently linked to HSA to sinusoidal cell types of the liver. *J. Drug Target.*, *5*: 329-342, 1998.
93. Gijssens, A., Missiaen, L., Merlevede, W., and de Witte, P. Epidermal growth factor-mediated targeting chlorin₆₆ selectively potentiates its photodynamic therapy. *Cancer Res.*, *60*: 2197-2202, 2000.
94. Suzuki, S., Takahashi, T., Nakamura, S., Koike, K., Ariyoshi, Y., Takahashi, T., and Ueda, R. Alterations of integrin expression in human lung cancer. *Jpn. J. Cancer Res.*, *84*: 168-174, 1993.
95. Allen, C. M., Sharman, W. M., La Madeleine, C., Weber, J. M., Langlois, R., Ouellet, R., and Van Lier, J. E. Photodynamic therapy: tumor targeting with adenoviral proteins. *Photochem. Photobiol.*, *70*: 512-523, 1999.
96. Gagnebin, J., Brunori, M., Otter, M., Juillerat-Jeanneret, L., Monnier, P., and Iggo, R. A photosensitizing adenovirus for photodynamic therapy. *Gene Ther.*, *6*: 1742-1750, 1999.
97. Shiah, J.-G., Sun, Y., Peterson, C. M., and Kopecek, J. Biodistribution of free and *N*-(2-hydroxypropyl)methacrylamide copolymer-bound mesochlorin₆₆ and adriamycin in nude mice bearing human ovarian carcinoma OVCAR-3 xenografts. *J. Control Rel.*, *61*: 145-157, 1999.
98. Shiah, J.-G., Sun, Y., Peterson, C. M., Straight, R. C., and Kopecek, J. Antitumor activity of *N*-(2-hydroxypropyl)methacrylamide copolymer-mesochlorin₆₆ and adriamycin conjugates in combination treatments. *Clin. Cancer Res.*, *6*: 1008-1015, 2000.
99. Westermann, P., Glanzmann, T., Andrejevic, S., Braichotte, D. R., Forrer, M., Wagnières, G. A., Monnier, P., van den Bergh, H., Mach, J.-P., and Folli, S. Long circulating half-life and high tumor selectivity of the photosensitizer meta-tetrahydroxyphenylchlorin conjugated to polyethylene glycol in nude mice grafted with a human colon carcinoma. *Int. J. Cancer*, *76*: 842-850, 1998.
100. Ris, H.-B., Im Hof, V., Stewart, C. M., Mettler, D., and Altermatt, H.-J. Endobronchial photodynamic therapy: Comparison of *m*THPC and polyethylene glycol-derived *m*THPC on human tumor xenografts and tumor-free bronchi of minipigs. *Lasers Surg. Med.*, *23*: 25-32, 1998.
101. Reuther, T., Kübler, A. C., Zillmann, U., Flechtenmacher, C., and Sinn, H. Comparison of the *in vivo* efficiency of Photofrin II-, *m*THPC-, *m*THPC-PEG- and *m*THPCnPEG-mediated PDT in a human xenografted head and neck carcinoma. *Lasers Surg. Med.*, *29*: 314-322, 2001.
102. Rovers, J. P., Saarnak, A. E., de Jode, M., Sterenborg, H. J. C. M., Terpstra, O. T., and Grahn, M. F. Biodistribution and bioactivity of tetra-pegylated meta-tetra(hydroxyphenyl)chlorin compared to native meta-tetra(hydroxyphenyl)chlorin in a rat liver tumor model. *Photochem. Photobiol.*, *71*: 210-217, 2000.
103. Brasseur, N., Ouellet, R., La Madeleine, C., and van Lier, J. E. Water-soluble aluminium phthalocyanine-polymer conjugates for PDT: photodynamic activities and pharmacokinetics in tumour-bearing mice. *Br. J. Cancer*, *80*: 1533-1541, 1999.
104. Hamblin, M. R., Miller, J. L., Rizvi, I., Ortel, B., Maytin, E. V., and Hasan, T. Pegylation of a chlorin₆₆ polymer conjugate increases tumor targeting of photosensitizer. *Cancer Res.*, *61*: 7155-7162, 2001.
105. Taillefer, J., Jones, M.-C., Brasseur, N., van Lier, J. E., and Leroux, J.-C. Preparation and characterization of pH-responsive polymeric micelles for the delivery of photosensitizing anticancer drugs. *J. Pharm. Sci.*, *89*: 52-62, 2000.

106. Taillefer, J., Brasseur, N., van Lier, J. E., Lenaerts, V., Le Garrec, D., and Leroux J.-C. In-vitro and in-vivo evaluation of pH-responsive polymeric micelles in a photodynamic cancer therapy model. *J. Pharm. Pharmacol.*, *53*: 155-166, 2001.
107. Pèlegriin, A., Folli, S., Buchegger, F., Mach, J.-P., Wagnières, G., and van den Bergh, H. Antibody-fluorescein conjugates for photoimmunodiagnosis of human colon carcinoma in nude mice. *Cancer*, *67*: 2529-2537, 1991.
108. Folli, S., Wagnières, G., Pèlegriin, A., Calmes J.-M., Braichotte, D., Buchegger, F., Chalandon, Y., Hardman, N., Heusser, N., Givel, J. C., Chapuis, G., Châtelain, A., van den Bergh, H., and Mach, J.-P. Immunophotodiagnosis of colon carcinomas in patients injected with fluoresceinated chimeric monoclonal antibodies against carcinoembryonic antigen. *Proc. Natl. Acad. Sci. USA*, *89*: 7973-7977, 1992.
109. Folli, S., Westermann, P., Braichotte, D., Pèlegriin, A., Wagnières, G., van den Bergh, H., and Mach, J.-P. Antibody-indocyanin conjugates for immunodetection of human squamous cell carcinoma in nude mice. *Cancer Res.*, *54*: 2643-2649, 1994.
110. Gutowski, M., Carcenac, M., Pourquier, D., Larroque, C., Saint-Aubert, B., Rouanet, P., and Pèlegriin, A. Intraoperative immunophotodetection for radical resection of cancers: Evaluation in an experimental model. *Clin. Cancer Res.*, *7*: 1142-1148, 2001.
111. Mew, D., Wat, C.-K., Towers, G. H. N., and Levy, J. G. Photoimmunotherapy: treatment of animal tumors with tumor-specific monoclonal antibody-hematoporphyrin conjugates. *J. Immunol.*, *130*: 1473-1477, 1983.
112. Jiang, F. N., Jiang, S., Liu, D., Richter, A., and Levy, J. G. Development of technology for linking photosensitizers to a model monoclonal antibody. *J. Immunol. Methods*, *134*: 139-149, 1990.
113. Jiang, F. N., Liu, D., Neyndorff, H., Chester, M., Jiang, S., and Levy, J. G. Photodynamic killing of human squamous cell carcinoma cells using a monoclonal antibody-photosensitizer conjugate. *J. Natl. Cancer Inst.*, *83*: 1218-1225, 1991.
114. Oseroff, A. R., Ohuoha, D., Hasan, T., Bommer, J. C., and Yarmush, M. L. Antibody-targeted photolysis: Selective photodestruction of human T-cell leukemia cells using monoclonal antibody-chlorin e_6 conjugates. *Proc. Natl. Acad. Sci. USA*, *83*: 8744-8748, 1986.
115. Goff, B. A., Blake, J., Bamberg, M. P., and Hasan, T. Treatment of ovarian cancer with photodynamic therapy and immunoconjugates in a murine ovarian cancer model. *Br. J. Cancer*, *74*: 1194-1198, 1996.
116. Hamblin, M. R., Miller, J. L., and Hasan, T. Effect of charge on the interaction of site-specific photoimmunoconjugates with human ovarian cancer cells. *Cancer Res.*, *56*: 5205-5210, 1996.
117. Molpus, K. L., Hamblin, M. R., Rizvi, I., and Hasan, T. Intraperitoneal photoimmunotherapy of ovarian carcinoma xenografts in nude mice using charged photoimmunoconjugates. *Gynecol. oncol.*, *76*: 397-404, 2000.
118. Hamblin, M. R., Del Governatore, M., Rizvi, I., and Hasan, T. Biodistribution of charged 17.1A photoimmunoconjugates in a murine model of hepatic metastasis of colorectal cancer. *Br. J. Cancer*, *83*: 1544-1551, 2000.
119. Del Governatore, M., Hamblin, M. R., Shea, C. R., Rizvi, I., Molpus, K. G., Tanabe, K. K., and Hasan, T. Experimental photoimmunotherapy of hepatic metastases of colorectal cancer with a 17.1A chlorin e_6 immunoconjugate. *Cancer Res.*, *60*: 4200-4205, 2000.
120. Soukos, N. S., Hamblin, M. R., Keel, S., Fabian, R. L., Deutsch, T. F., and Hasan, T. Epidermal growth factor receptor-targeted immunophotodiagnosis and photoimmunotherapy of oral precancer *in vivo*. *Cancer Res.*, *61*: 4490-4496, 2001.
121. Morgan, J., Lottman, H., Abbou, C. C., and Chopin, D. K. A comparison of direct and liposomal antibody conjugates of sulfonated aluminum phthalocyanines for selective photoimmunotherapy of human bladder carcinoma. *Photochem. Photobiol.*, *60*: 486-496, 1994.
122. Carcenac, M., Larroque, C., Langlois, R., van Lier, J. E., Artus, J.-C., and Pèlegriin, A. Preparation, phototoxicity and biodistribution studies of anti-carcinoembryonic antigen monoclonal antibody-phthalocyanine conjugates. *Photochem. Photobiol.*, *70*: 930-936, 1999.

Chapter 2

**DEVELOPMENT OF *m*THPC-MONOCLONAL ANTIBODY
CONJUGATES FOR PHOTOIMMUNOTHERAPY**

Maarten B. Vrouenraets, Gerard W.M. Visser, Fiona A. Stewart, Marijke Stigter,
Hugo Oppelaar, Pieter E. Postmus, Gordon B. Snow and Guus A.M.S. van Dongen

ABSTRACT

A limitation of photodynamic therapy (PDT) is the lack of tumor selectivity of the photosensitizer. To overcome this problem, a protocol was developed for coupling of *meta*-tetrahydroxyphenylchlorin (*m*THPC), one of the most promising photosensitizers, to tumor-selective monoclonal antibodies (MAbs). *m*THPC was radiolabeled with ^{131}I to facilitate the assessment of the *in vitro* and *in vivo* behavior. After the modification to ^{131}I -*m*THPC-($\text{CH}_2\text{CO-OH}$)₄, thus increasing the water solubility and creating a functional moiety suitable for coupling, conjugation was performed using a labile ester. Insoluble aggregates were not formed when *m*THPC-MAb conjugates with a molar ratio of up to 4 were prepared. These conjugates showed a minimal impairment of the integrity on SDS-PAGE, full stability in serum *in vitro*, and an optimal immunoreactivity.

To test the *in vivo* behavior of the *m*THPC-MAb conjugates, the head and neck squamous cell carcinoma (HNSCC) selective chimeric MAb (cMAb) U36 was used in HNSCC bearing nude mice. Biodistribution data showed that the tumor selectivity of cMAb U36-conjugated *m*THPC was increased in comparison with free *m*THPC, despite the fact that conjugates with a higher *m*THPC:MAb ratio were more rapidly cleared from the blood. Preliminary results on the *in vitro* efficacy of PDT with MAb-conjugated *m*THPC showed that *m*THPC coupled to the internalizing murine MAb (mMAb) 425 exhibited more phototoxicity than when coupled to the noninternalizing cMAb U36.

INTRODUCTION

Photodynamic therapy (PDT) is a therapeutic modality for the treatment of superficially localized tumors. In this approach, a photosensitive dye (photosensitizer) is injected intravenously, whereafter it accumulates more or less selectively in the tumor. After exposure to laser light in the red or near-infrared region, the sensitizer is excited and is able to produce singlet oxygen, a cytotoxic form of oxygen (1). Direct cell killing (2) and occlusion of tumor blood vessels (3), as well as a strong acute inflammatory reaction (4), can occur. These combined effects result in tumor necrosis. PDT has been applied for noninvasive treatment of many types of cancer, including colon, bladder, lung, and head and neck cancer (5-8).

Until now, Photofrin was one of the most frequently used photosensitizers. Photofrin,

which has an absorption maximum at 630 nm, is the commercially produced photosensitizer purified from hematoporphyrin derivative (HPD). However, this sensitizer has some drawbacks. The skin toxicity observed with Photofrin-based PDT is rather long lasting, 6-10 weeks. Moreover, Photofrin is a mixture of mono-, di- and oligomers, and it is not clear which components contribute to the photochemical effects (9).

Alternative photosensitizers have become available recently. One of the most promising second generation photosensitizers is *meta*-tetrahydroxyphenylchlorin (*m*THPC). *m*THPC is a pure and well-defined compound with better photochemical properties than those of Photofrin. It has a strong absorption band at 652 nm (absorption coefficient, $22400 \text{ l}\cdot\text{mol}^{-1}\cdot\text{cm}^{-1}$, compared with 3000 for Photofrin at 630 nm). The longer wavelength light used to excite *m*THPC can penetrate deeper into the tissue than 630 nm light, thus allowing treatment of larger tumors. The high photochemical efficiency of *m*THPC means that lower light doses (and shorter illumination times) are required for a tumoricidal PDT effect.

Preliminary results of PDT with *m*THPC in head and neck cancer patients are encouraging (10). The largest study has been performed by Savary *et al.* (11) using optimized protocols for PDT with *m*THPC for the treatment of early second primary squamous cell carcinoma of the esophagus, bronchi, and mouth. All lesions were carcinoma *in situ* or microinvasive carcinoma, which had been detected by rigid endoscopy and toluidine blue as a vital stain. Of the 33 lesions treated in this trial, 28 showed no recurrence during the mean follow-up of 14 months. In comparison to surgery and radiotherapy, PDT shows a low morbidity with little fibrosis and scarring.

Despite these promising results, *m*THPC-based PDT leaves room for improvement. A limitation is the lack of tumor selectivity, which can result in severe normal tissue damage after PDT of large surface areas. An option to overcome this problem is to couple *m*THPC to monoclonal antibodies (MAbs) directed against tumor-associated antigens. In this way, the photosensitizer will be targeted selectively to the tumor. These *m*THPC-MAb conjugates might be especially suitable for the treatment of multiple tumor foci in large areas, as is the case in minimal residual disease after surgical resection of thoracic and peritoneal tumors. The problem of phototoxicity will also be reduced because the accessibility of the skin is limited for MAbs.

The proof of concept for selective delivery of photosensitizers to tumors by MAbs was delivered by Pèlerin *et al.* (12) and Folli *et al.* (13). They showed the effectiveness of a fluorescein-anti-CEA MAb conjugate for photoimmunodetection of colon carcinoma in mice and in patients. More recently, they developed an indocyanin-MAb E48 conjugate and evaluated

these conjugates in nude mice bearing squamous cell carcinoma xenografts (14). These novel conjugates appeared to be superior for photoimmunodetection in comparison with the fluorescein-MAb conjugates, but unfortunately, neither of these conjugates is suitable for therapy because of their photochemical properties.

In the development of photoimmunoconjugates for therapy, the synthesis of *m*THPC-MAb conjugates has not yet been described. A serious problem in this respect is the poor water solubility of *m*THPC. Other factors expected to hamper the development of *m*THPC-MAb conjugates suitable for tumor targeting are the potential chemical cross-linkings during conjugation, as well as the impairment of the immunoreactivity and pharmacokinetic behavior of the MAb and the photochemical activity of the conjugates.

Our institute focuses on the use of MAbs for selective targeting of squamous cell carcinoma of the head and neck (HNSCC). To this end, MAbs E48 and U36 have been developed (15,16). Radioimmunosciintigraphy/biodistribution studies in HNSCC patients showed that these MAbs are highly capable of selective tumor targeting (17-19). This observation justifies a study for the use of these MAbs as transport vehicle for selective delivery of *m*THPC to HNSCC.

In this report, we describe a protocol for the reproducible synthesis of *m*THPC-MAb conjugates and their biodistribution after administration to HNSCC-bearing nude mice. Conjugation and biodistribution studies were performed with dual labeling using ¹³¹I-labeled *m*THPC and ¹²⁵I-labeled MAb. Preliminary data on the *in vitro* efficacy of *m*THPC-MAb-mediated PDT will be provided.

MATERIALS AND METHODS

*m*THPC

*m*THPC (M_r 680.76) was obtained from Scotia Pharmaceuticals (Surrey, UK) as a pure solid. [¹⁴C]*m*THPC (also provided by Scotia Pharmaceuticals) was synthesized by American Radiolabeled Chemicals, Inc. (St. Louis, MO).

Monoclonal antibodies

Selection and production of MAb U36 and its chimeric (mouse/human) IgG1 derivative (cMAb U36) have been described previously (16,20). MAb U36 recognizes the v6 domain of the M_r 200,000 CD44 splice variant epican (21), which is highly expressed in squamous cell

carcinoma of the head and neck, lung, skin, esophagus, and cervix, adenoma carcinomas of breast and lung, as well as in normal stratified epithelium. A clinical radioimmunosciintigraphy study with ^{99m}Tc-labeled U36 revealed that U36 IgG accumulates selectively and to a high level in HNSCC (19), and therefore, the MAb is presently evaluated in radioimmunotherapy studies.

Murine monoclonal antibody 425 (mMAb 425) is an IgG2a MAb developed and characterized by Murthy *et al.* (22). The epitope recognized by mMAb 425 is localized on the external domain of the EGF receptor (EGFR), which has been shown to be highly expressed by various tumor types including HNSCC, renal cell cancer, gliomas, and carcinoma of the esophagus, bladder, cervix, stomach, lung, and breast (23-30). After binding to this antigen, anti-EGFR MAbs are internalized and catabolized by A431 cells (31). Anti-EGFR MAbs, MAb 425 included, have been studied extensively in clinical trials (32,33).

Cell lines

Characteristics of the squamous cell carcinoma cell lines UM-SCC-11B, UM-SCC-22A, and A431 and their culturing conditions have been described previously (34).

Analyses

HPLC analysis was performed by using an LKB 2150 HPLC-pump (Pharmacia Biotech, Roosendaal, the Netherlands), an LKB 2152 LC controller (Pharmacia Biotech), and a 25-cm Lichrosorb 10 RP 18 column (Chrompack, Middelburg, the Netherlands) at a flow rate of 2 ml/min. The eluent consisted of a 9:1 (v/v) mixture of MeCN and 0.1% trifluoroacetic acid. Absorption was measured at 230 and 415 nm by a Pharmacia LKB VWM 2141 UV detector. Radioactivity was measured by an Ortec 406A single-channel analyzer connected to a Drew 3040 data collector (Becton Scientific, Rotterdam, the Netherlands).

¹H-NMR spectra were recorded in [²H₆]Me₂SO on a Bruker ARX 400 (400.14 MHz) spectrometer and a Bruker AC 200 (200.13 MHz) spectrometer. Chemical shifts (δ) are given in ppm relative to tetramethylsilane as the internal standard. For description of the NMR spectra of *m*THPC and its derivatives, see Table 1.

The absorption spectra of *m*THPC and *m*THPC-MAb conjugates were measured using a Ultrospec III spectrophotometer (Pharmacia Biochrom). The *m*THPC concentration in the conjugate preparations was assessed with the same apparatus at a wavelength of 415 nm. The absorption of a range of dilutions (1-9 μ g/ml) of *m*THPC in MeCN was measured and graphically depicted using the least square method. The *m*THPC concentration in the conjugate preparations

was determined using this calibration curve.

The integrity of the *m*THPC-MAb conjugates was analyzed by electrophoresis on a Phastgel System (Pharmacia Biotech) using preformed 7.5% SDS-PAGE gels under nonreducing conditions. After running, gels were stained with 0.2% Coomassie Brilliant Blue (Sigma) and exposed to a Phosphor plate for 1-3 h and analyzed with a Phosphor Imager (B&L-Isogen Service Laboratory, Amsterdam, the Netherlands) for localization of the protein bands. Quantitative information was obtained by cutting the lanes into pieces and dual label counting in a gamma counter (LKB-Wallac 1282 CompuGamma; Pharmacia, Woerden, the Netherlands).

Dual label counting of ^{125}I and ^{131}I

The amounts of ^{125}I (E_γ 35 keV) and ^{131}I (E_γ 364 keV) were measured simultaneously in a gamma counter in the corresponding window settings (channels 35-102 and 155-185, respectively) with automatic correction for the ^{131}I -comptongammas in the ^{125}I -window setting; in our case, this correction corresponded to 15.2% of the ^{131}I -photopeak counts present in the sample.

^{125}I -Labeling of MAbs

Radio-iodination of cMAb U36 and mMAb 425 with ^{125}I was performed using Iodogen (Brunschwig Chemie, Amsterdam) as described by Haisma *et al.* (35). One to 2 mg of MAb dissolved in 500 μl of PBS (pH 7.4) and 1 mCi of ^{125}I (100 mCi/ml; Amersham, Aylesbury, England) were mixed in a vial coated with 50 μg of Iodogen. After 5 min incubation at room temperature, the reaction mixture was filtered through a 0.22 μm Acrodisc filter (Gelman Sciences, Inc., Ann Arbor, MI), and unbound ^{125}I was removed using a PD-10 column (Pharmacia Biotech, Woerden) with 0.9% NaCl as eluent. After removal of unbound ^{125}I , the radiochemical purity always exceeded 98%.

^{131}I -Labeling of *m*THPC

To facilitate the analysis of the stability of the *m*THPC-MAb conjugates *in vitro* and *in vivo* and their pharmacokinetic behavior, in most of the experiments *m*THPC was trace-labeled with ^{131}I . This labeling and subsequent reaction steps with *m*THPC were carried out in the dark and under a N_2 atmosphere to prevent unwanted photochemical reactions during the synthesis of the *m*THPC-MAb conjugates.

^{131}I -Labeling of *m*THPC was performed using Iodo-beads (Brunschwig Chemie) as

follows. The appropriate amount of ^{131}I was added to 50 μl of 1 mM NaOH containing 10 μg of Na_2SO_3 . This ^{131}I solution was added to 4 Iodo-beads covered with 450 μl of a MeCN/ H_2O mixture (10:1; v/v), followed by 100 μl (734 nmol) of a *m*THPC solution (5 mg/ml in MeCN). After labeling during 30 min, the reaction mixture was diluted with 400 μl of H_2O , loaded on a conditioned Sep-pak C_{18} cartridge (Waters, Millipore, MA) and washed with 50 ml of H_2O . The ^{131}I -labeled *m*THPC (actually consisting of a small proportion of ^{131}I -*m*THPC and an excess of unlabeled *m*THPC) was eluted with 3 ml of MeCN. The solvent was evaporated under a stream of N_2 .

The radiochemical purity of ^{131}I -*m*THPC was determined by HPLC analysis. The HPLC retention times were 9.8 min for ^{131}I -*m*THPC, between 5-9 min for ^{131}I -labeled minor impurities, and 9.6 min for *m*THPC (for the ^1H -NMR data of *m*THPC, see Table 1).

Preparation of the tetrafluorophenol (TFP) ester

Preparation of the ester (either in labeled or unlabeled form) was performed in two steps. The first step was tetracarboxymethylation of ^{131}I -*m*THPC/*m*THPC. To ^{131}I -*m*THPC/*m*THPC, dissolved in 600 μl of a DMF: H_2O mixture (5:1; v/v), 150 mg (3.7 mmol) of powdered NaOH were added, and the mixture was stirred until the solution was green (2-3 min). Hereafter, 70 mg (380 μmol) of iodoacetic acid (Janssen Chimica, Beerse, Belgium) were added, and stirring was continued for another 90 min. The pH was adjusted to 5.0 with 3 ml of 1 N HCl, and the tetracarboxymethylated product was isolated by extraction with four portions of 0.5 ml of CH_2Cl_2 . The HPLC retention times were 7.1 min for ^{131}I -*m*THPC- $(\text{CH}_2\text{COOH})_4$ and 7.3 min for *m*THPC- $(\text{CH}_2\text{COOH})_4$ (^1H -NMR data of *m*THPC- $(\text{CH}_2\text{COOH})_4$ are given in Table 1).

In the next reaction step, the four carboxylic acid groups were esterified using an excess of TFP (Janssen Chimica). To the tetracarboxymethylated product in CH_2Cl_2 , 150 μl of a TFP solution (100 mg/ml in DMF) and 50 mg of solid EDC (Janssen Chimica) were added. The pH was adjusted to 5.7-5.9 with 1 N Na_2CO_3 . After reaction for 30 min, column chromatography was performed to remove all impurities. This purification was performed with a 24-cm LiChroprep Si 60 (40-63 μm) column (Merck, Darmstadt, Germany) using $\text{CH}_2\text{Cl}_2/\text{MeCN}$ (97:3, v/v) as the eluent (flow rate of 1 ml/min). Fractions of 0.5 ml were collected and analyzed by HPLC with absorption measurement at 230 and 415 nm. The pure tetraester fractions (under our conditions, fractions 20-23) were pooled, and the solvent was evaporated. The HPLC retention times were 17.2 min for ^{131}I -*m*THPC- $(\text{CH}_2\text{CO-TFP})_4$ (Fig. 1B) and 15.9 min for *m*THPC- $(\text{CH}_2\text{CO-TFP})_4$ (Fig. 1A; ^1H -NMR data of *m*THPC- $(\text{CH}_2\text{CO-TFP})_4$ are given in Table 1).

	OH (s) ^a	pyrrole-CH	TFP-H (m)	benz.-H (m)	-CH ₂ CO- (d)	pyrrole-CH ₂ (s)	NH (s)
Number of protons	4	6	4	16	8	4	2
<i>m</i> THPC	9.81	8.68 ^b /8.42/8.28 ^c (d/s/d)		7.65–7.12		4.20	-1.60
<i>m</i> THPC-(CH ₂ COOH) ₄	11.30	8.62 ^d /8.37/8.24 ^e (d/s/d)		7.66–7.20	4.83 ^f	4.17	-1.64
<i>m</i> THPC-(CH ₂ CO-TFP) ₄		8.60 ^g /8.35 ^h /8.21 ⁱ (dd/d/dd)	7.96	7.79–7.39	5.57 ^j	4.13	-1.60

Table 1. Chemical shifts (ppm) of *m*THPC, *m*THPC-(CH₂COOH)₄ and *m*THPC-(CH₂CO-TFP)₄

^as, singlet; d, doublet; dd, double doublet; m, multiplet.

^{b,j} Observed coupling constants (Hz): ^b*J* = 4.9; ^c*J* = 4.9; ^d*J* = 5.4; ^e*J* = 5.4; ^f*J* = 10.1; ^g*J* = 5.2; ^h*J* = 4.3; ⁱ*J* = 5.1; ^j*J* = 12.7.

Preparation of ¹³¹I-*m*THPC-(CH₂COOH)₃CH₂CONH-¹²⁵I-Mab conjugates

For the coupling reaction with the ¹²⁵I-labeled MAb, the ¹³¹I-*m*THPC-(CH₂CO-TFP)₄ (Fig. 1, A and B) was partly hydrolyzed to leave one reactive ester function, thus preventing cross-linking of MAbs during conjugation. The partial hydrolysis was performed by dissolving the tetraester in 300 μl of MeCN and by stepwise addition of 10–25 μl of 10 mM Na₂CO₃. The degree of hydrolysis was monitored by radio-HPLC analysis with simultaneous absorption measurement at 415 nm (Fig. 1, C and D). When the percentage of monoester was optimal for conjugation (no tetra- and triester, <5% diester, 45% monoester together with 50% completely hydrolyzed ¹³¹I-*m*THPC-(CH₂COOH)₄; Fig. 1, E and F), this mixture was added to 2 mg of ¹²⁵I-labeled MAb in 1 ml of 0.9% NaCl at pH 9.5. After 30 min of incubation, the ¹³¹I-*m*THPC-(CH₂COOH)₃CH₂CONH-¹²⁵I-MAb conjugate was purified by gel filtration using a PD-10 column with 0.9% NaCl as eluent.

The conjugation efficiency was determined from the ¹²⁵I:¹³¹I ratio before and after PD-10 purification using dual label counting in a gamma counter. The ¹³¹I-*m*THPC:¹²⁵I-MAb molar ratio was determined by measuring the absorbance at 415 nm to calculate *m*THPC concentration and ¹²⁵I measurement for MAb quantitation. The integrity of the conjugate was checked by gel electrophoresis.

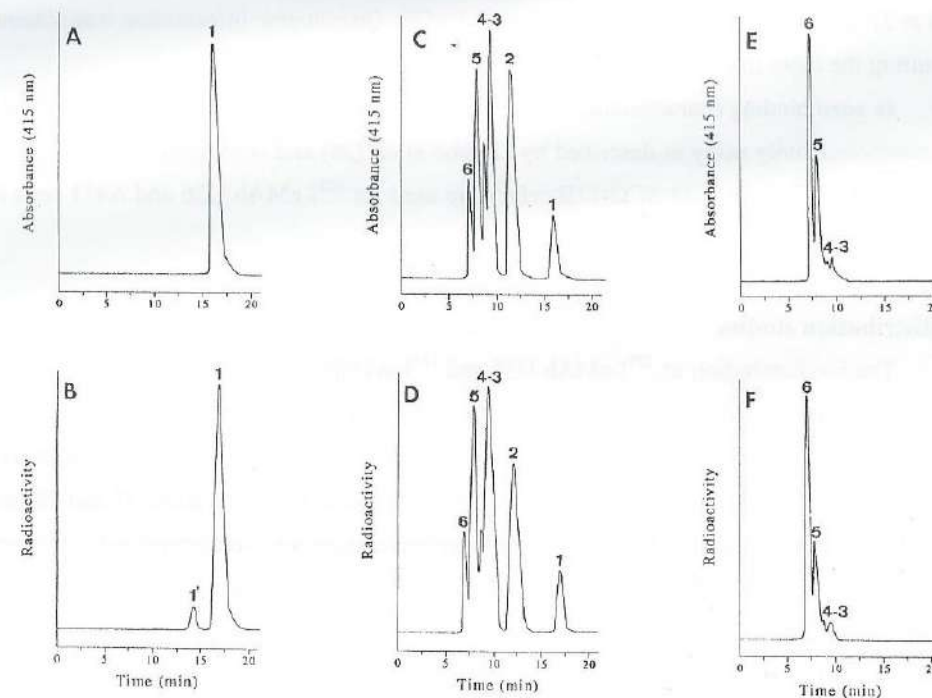


Figure 1. HPLC profiles (absorbance (415 nm) and radioactivity) during the partial hydrolysis of ¹³¹I-*m*THPC-(CH₂CO-TFP)₄. At the start, HPLC analysis showed: A (peak 1: *m*THPC-(CH₂CO-TFP)₄) and B (peak 1: ¹³¹I-*m*THPC-(CH₂CO-TFP)₄ and peak 1': ¹³¹I-*m*THPC-(CH₂CO-TFP)₃). During hydrolysis: C (peak 1: *m*THPC-(CH₂CO-TFP)₄, peak 2: *m*THPC-(CH₂COOH)(CH₂CO-TFP)₃, peak 3/4: two isomers of *m*THPC-(CH₂COOH)₂(CH₂CO-TFP)₂, peak 5: *m*THPC-(CH₂COOH)₃CH₂CO-TFP, and peak 6: *m*THPC-(CH₂COOH)₄) and D (identical to C, corresponding ¹³¹I-labeled compounds). Conjugations were performed with mixtures: E (peak 3/4: two isomers of *m*THPC-(CH₂COOH)₂(CH₂CO-TFP)₂, peak 5: *m*THPC-(CH₂COOH)₃CH₂CO-TFP, and peak 6: *m*THPC-(CH₂COOH)₄) and F (identical to E, corresponding ¹³¹I-labeled compounds).

In vitro stability and immunoreactivity of ¹³¹I-*m*THPC-¹²⁵I-MAb conjugates^l

For measurement of the serum stability of the ¹³¹I-*m*THPC-¹²⁵I-MAb conjugates, 0.5 μg

^l*m*THPC-(CH₂COOH)₃CH₂CONH-MAb conjugates are designated as *m*THPC-MAb conjugates if the modification of *m*THPC is not relevant for understanding.

of conjugate in 10 μ l of 0.9% NaCl was added to 40 μ l of serum. Stability was measured in mouse and human serum, whereas 0.9% NaCl served as a control. After a 20-h incubation in the dark at 37°C, samples were analyzed with SDS-PAGE. Quantitative information was obtained by cutting the lanes into pieces and dual label counting.

In vitro binding characteristics of ^{131}I -*m*THPC- ^{125}I -MAb conjugates were determined in an immunoreactivity assay as described by Lindmo *et al.* (36) and compared with those of the unconjugated ^{125}I -MAb. UM-SCC-11B cells were used for ^{125}I -cMAB U36 and A431 cells for ^{125}I -mMAB 425.

Biodistribution studies

The biodistribution of ^{125}I -cMAB U36 and ^{131}I -*m*THPC- ^{125}I -cMAB U36 conjugate was studied in nude mice bearing s.c. xenografts of the HNSCC cell line HNX-OE, with a tumor size ranging from 50 to 200 mm^3 . For a comparison the distribution of ^{131}I -*m*THPC-(CH_2COOH)₄, ^{123}I -*m*THPC and [^{14}C]*m*THPC (as a reference compound used by others; Refs. 37 and 38) was studied in the same animal model. Because the latter two compounds were coinjected in the same group of animals, the short-living ^{123}I isotope was used instead of ^{131}I to facilitate the assessment of the ^{14}C activity.

The cMAB U36 samples were injected i.v. in 0.9% NaCl; the ^{123}I - and [^{14}C]*m*THPC derivatives were injected in a mixture consisting of 20% ethanol, 30% polyethylene glycol 400, and 50% water (v/v). At indicated time points postinjection, mice were anesthetized, bled, killed and dissected. The urine was collected, and the organs were removed. After weighing, the amount of gamma-emitting radioactivity in organs, blood, and urine was measured in a gamma counter.

For the weak β -emitter ^{14}C , the blood, urine, and organs were treated as follows. After complete decay of ^{123}I , tissue samples were placed in counting vials, and 1 ml of Soluene-350 (Packard Instrument Company, Groningen, the Netherlands) was added to dissolve the organs. The vials were subsequently heated at 50°C for 24 h, after which 250 μ l of a 1:1 (v/v) mixture of 30% H_2O_2 and acetic acid were added for decolorization of the solutions. After 1 h, Ultima Gold liquid scintillation mixture (15 ml; Packard Instrument Company) was added to the samples prior to counting in an LKB-Wallac 1410 Liquid Scintillation Counter (Pharmacia, Woerden). Radioactivity uptake in the tissues was expressed as the percentage of the %ID/g.

Photoimmunotherapy *in vitro*

Phototoxicity of the *m*THPC-cMAB U36 conjugates and the unconjugated *m*THPC was assessed in UM-SCC-22A cells using the SRB (Sigma) assay, which measures the cellular protein content (39). Cells were plated in 96-well plates (2500/well) and grown for 3 days before incubating with *m*THPC or *m*THPC-cMAB U36 conjugates (0.1 nM to 1.0 μ M *m*THPC equivalent) in DMEM supplemented with 2 mM L-glutamine, 5% FCS, and 25 mM HEPES at 37 °C. After 20 h, remaining free *m*THPC-cMAB U36 and *m*THPC were removed by washing twice with medium. Fresh medium was added, and cells were illuminated at 652 nm with a 6 W Diode Laser (AOC Medical Systems) at a dose of 25 J/cm^2 . Three days after illumination, growth was assessed by staining the cellular proteins with SRB and spectrophotometric measurement of the absorption at 540 nm with a microplate reader. IC_{50} s were estimated based on the absorption values and defined as the concentration that corresponded to a reduction in growth of 50% compared with values for control cells (no *m*THPC-MAB conjugates or *m*THPC added but illuminated in the same way). Phototoxicity of the *m*THPC-mMAB 425 conjugates was assessed in A431 cells (2000 cells/well) in a similar way.

RESULTS

Iodination of *m*THPC

The first step in the synthesis of ^{131}I -*m*THPC-(CH_2COOH)₃ CH_2CONH - ^{125}I -MAb conjugates (Fig. 2, *scheme 5*) was trace labeling of *m*THPC with ^{131}I using Iodo-beads. After 30 min incubation at room temperature, HPLC analysis revealed 70-75% ^{131}I -*m*THPC (Fig. 2, *scheme 1*), <10% ^{131}I -labeled impurities, and about 20% unreacted ^{131}I . After purification on a Sep-pak cartridge, the final preparation contained >94% ^{131}I -*m*THPC, <4% impurities, and about 2% unbound ^{131}I .

Synthesis of ^{131}I -*m*THPC-($\text{CH}_2\text{CO-TFP}$)₄

In the next step, ^{131}I -*m*THPC was tetracarboxymethylated. The reaction, with an excess of iodoacetic acid at pH 13, followed by extraction with CH_2Cl_2 , gave 95% \pm 5% (HPLC analysis) tetracarboxymethylated product (Fig. 2, *scheme 2*). Esterification was performed with TFP, and purification of the crude product with a LiChroprep column gave the desired product (Fig. 2, *scheme 3*) with >95% purity, also containing <5% ^{131}I -*m*THPC-($\text{CH}_2\text{CO-TFP}$)₃.

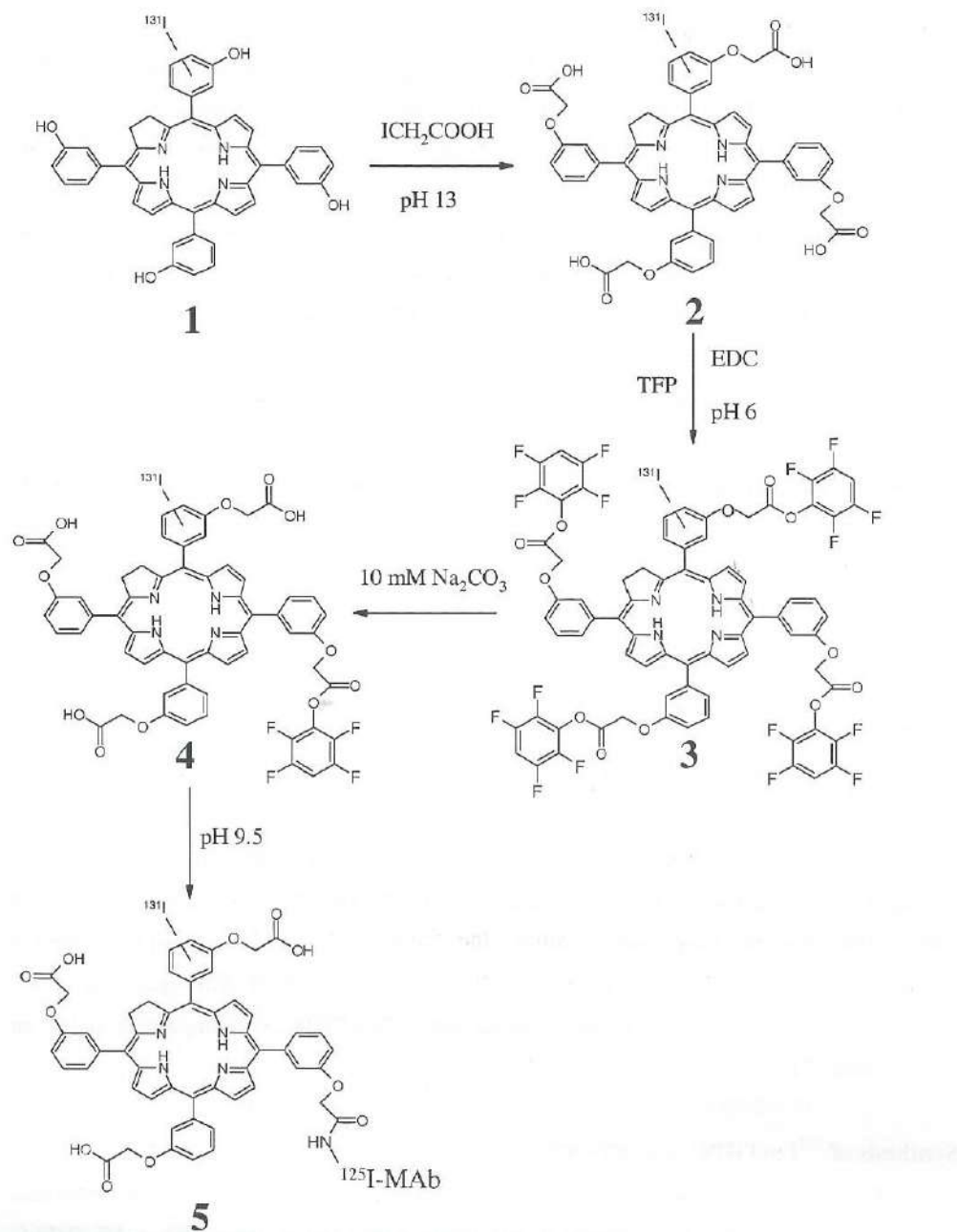


Figure 2. Schematic representation of the synthesis of ^{131}I -*m*THPC-(CH_2COOH)₄, its esterification, partial hydrolysis, and conjugation to a ^{125}I -labeled MAb. It is of note that ^{131}I can occupy 12 positions (both *ortho* positions and the *para* position relative to the OH, in each of the four phenyl rings). In the mono-TFP ester 4, one of the four possible mono-TFP esters is depicted.

The purity of the fractions (0.5 ml) that were recovered from the LiChrorep column was analyzed using HPLC analysis at 415 nm for detection of *m*THPC-($\text{CH}_2\text{CO-TFP}$)₄ and at 230 nm for detection of $\text{ICH}_2\text{CO-TFP}$, formed as a sideproduct. On the LiChrorep column, this latter ester had a retention time slightly longer than *m*THPC-($\text{CH}_2\text{CO-TFP}$)₄. The fractions that only contained *m*THPC-($\text{CH}_2\text{CO-TFP}$)₄ (under our conditions, fractions 20-23) were, after collection, evaporated under a stream of N_2 and stored in the dark at 4 °C until use. The LiChrorep purification also removed unbound ^{131}I and any unreacted TFP, EDC, or ICH_2COOH . As a result, the *m*THPC-ester was obtained in an overall yield of 60% with a purity >95%.

Conjugation

The ^{131}I -*m*THPC-($\text{CH}_2\text{CO-TFP}$)₄ ester was dissolved in 300 μl MeCN before starting of the HPLC-monitored hydrolysis with 10 mM Na_2CO_3 -buffer. This base was added in portions of 10-25 μl with intervals of 10 min. Approximately 125-150 μl of this buffer were used to reach the optimum mixture for conjugation (Fig. 2, *scheme 4*).

For conjugation, the mixture was added to a solution of ^{125}I -MAB in 0.9% NaCl at pH 9.5. After 30 min at room temperature, the ^{131}I -*m*THPC-(CH_2COOH)₃ $\text{CH}_2\text{CONH-}^{125}\text{I}$ -MAB conjugate (Fig. 2, *scheme 5*) was purified on a PD-10 column. When 2 mg of ^{125}I -MAB in a conjugation volume of 1.8 ml were used, the ^{131}I -*m*THPC: ^{125}I -MAB molar ratio was ~2.0-2.5. The conjugation efficiency was $60\% \pm 10\%$ (corrected for completely hydrolyzed ester, which is unable to couple), whereas the recovery of the MAB always exceeded 95% (measured by ^{125}I activity).

By adapting the ester concentration during conjugation, conjugates with a ratio >4 could be obtained. However, under these conditions, the recovery of the MAB from the PD-10 column dropped significantly, indicating an impairment of the solubility of the MAB.

SDS-PAGE analysis of ^{131}I -*m*THPC- ^{125}I -Mab conjugates

SDS-PAGE and subsequent Coomassie Brilliant Blue staining and Phosphor Imager analysis (Fig. 3) of the conjugate revealed one major protein band and a minor band, probably consisting of high molecular weight complexes. Cutting of the gel and dual label counting of the gel pieces showed >90% of the ^{125}I -MAB and >80% of the ^{131}I -*m*THPC to be localized in the main band, when conjugates with a ratio of up to 4 were analyzed. The remaining radioactivity was predominantly localized in the high molecular weight band. A typical example is shown by Fig. 3.

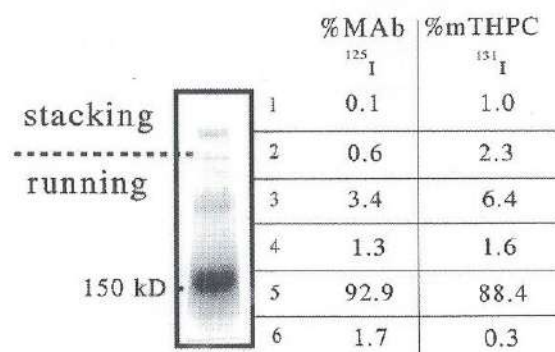


Figure 3. Example of an SDS-PAGE and Phosphor Imager analysis of a ¹³¹I-*m*THPC-¹²⁵I-cMAb U36 conjugate with ratio 1.8. Quantitative assessment of the radioactivity was obtained by cutting the lane and dual label counting.

In vitro stability and immunoreactivity of ¹³¹I-*m*THPC-¹²⁵I-MAb conjugates

After 20 h incubation in serum, the ¹³¹I-*m*THPC-¹²⁵I-MAb conjugates were analyzed by SDS-PAGE. Cutting of the gel and subsequent dual label counting showed that the ¹²⁵I:¹³¹I ratio of the IgG peak after incubation in mouse and human serum did not differ from that of the control incubation in 0.9% NaCl. Therefore, ¹³¹I-*m*THPC-¹²⁵I-MAb conjugates were fully stable in both serum sources.

Lindmo assays were performed to determine whether coupling of *m*THPC to cMAb U36 or mMAb 425 influenced the immunoreactivity of the MAb. For conjugates with a *m*THPC:MAB ratio of up to 4, no effect on the immunoreactivity was seen in comparison to the unconjugated MAb. Immunoreactivity was >93% in all cases, irrespective of whether assessed by ¹²⁵I or ¹³¹I counting.

Biodistribution of ¹³¹I-*m*THPC-¹²⁵I-cMAb U36 conjugates

Dual label experiments were performed to determine whether coupling of ¹³¹I-*m*THPC-(CH₂COOH)₄ to ¹²⁵I-cMAb U36 resulted in improved targeting of the sensitizer to the tumor. To this end, the biodistribution of unconjugated ¹²⁵I-cMAb U36 and ¹³¹I-*m*THPC-(CH₂COOH)₄ were first determined. For evaluation of ¹²⁵I-cMAb U36, 5 μCi of ¹²⁵I-cMAb U36 (100 μg) were injected in five HNX-OE xenograft-bearing nude mice. The mice were sacrificed 48 h after

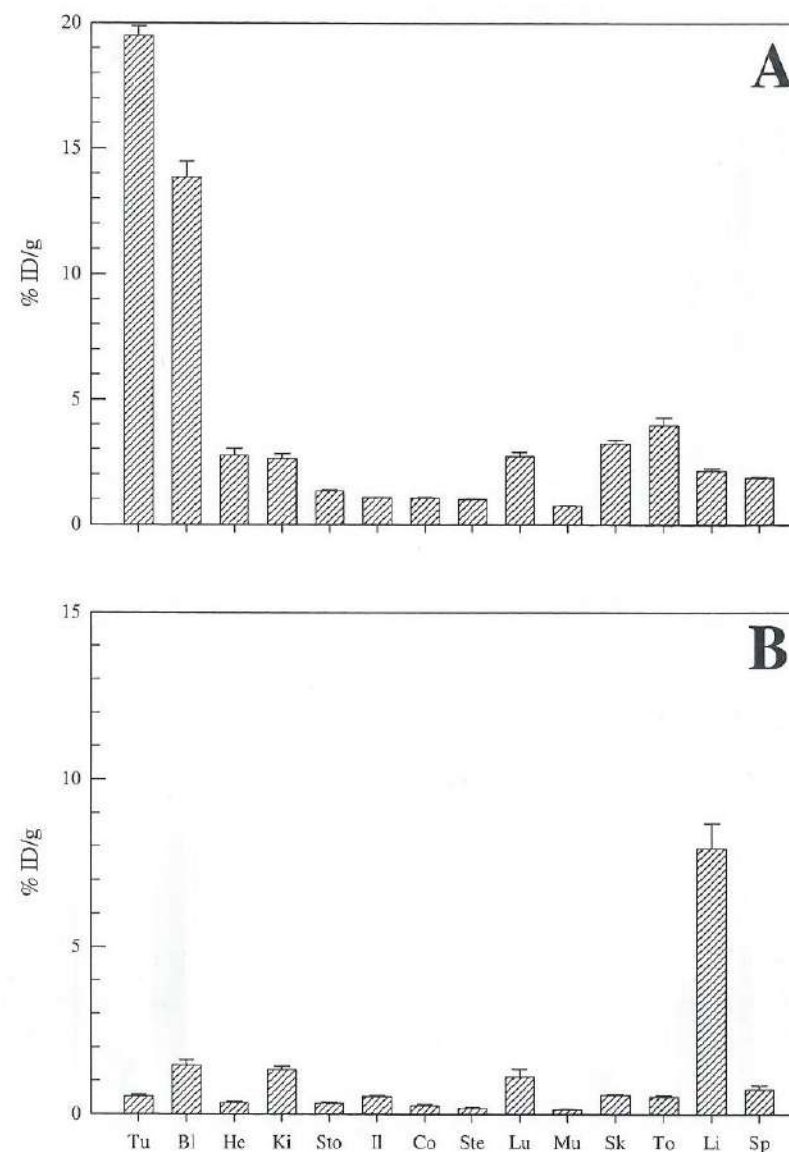


Figure 4. Biodistribution of ¹²⁵I-cMAb U36 and ¹³¹I-*m*THPC-(CH₂COOH)₄ before conjugation. Each preparation was intravenously injected in six HNX-OE bearing nude mice. **A:** 48 h p.i. of ¹²⁵I-cMAb U36 (100 μg; 5 μCi). **B:** 24 h p.i. of ¹³¹I-*m*THPC-(CH₂COOH)₄ (5 μg; 10 μCi). At indicated time points, mice were bled, sacrificed, and dissected, and the radioactivity levels (%ID/g + SE) of blood, tumor and several organs were assessed. Tu: tumor, Bl: blood, He: heart, Ki: kidney, Sto: stomach, Il: ileum, Co: colon, Ste: sternum, Lu: lung, Mu: muscle, Sk: skin, To: tongue, Li: liver, Sp: spleen.

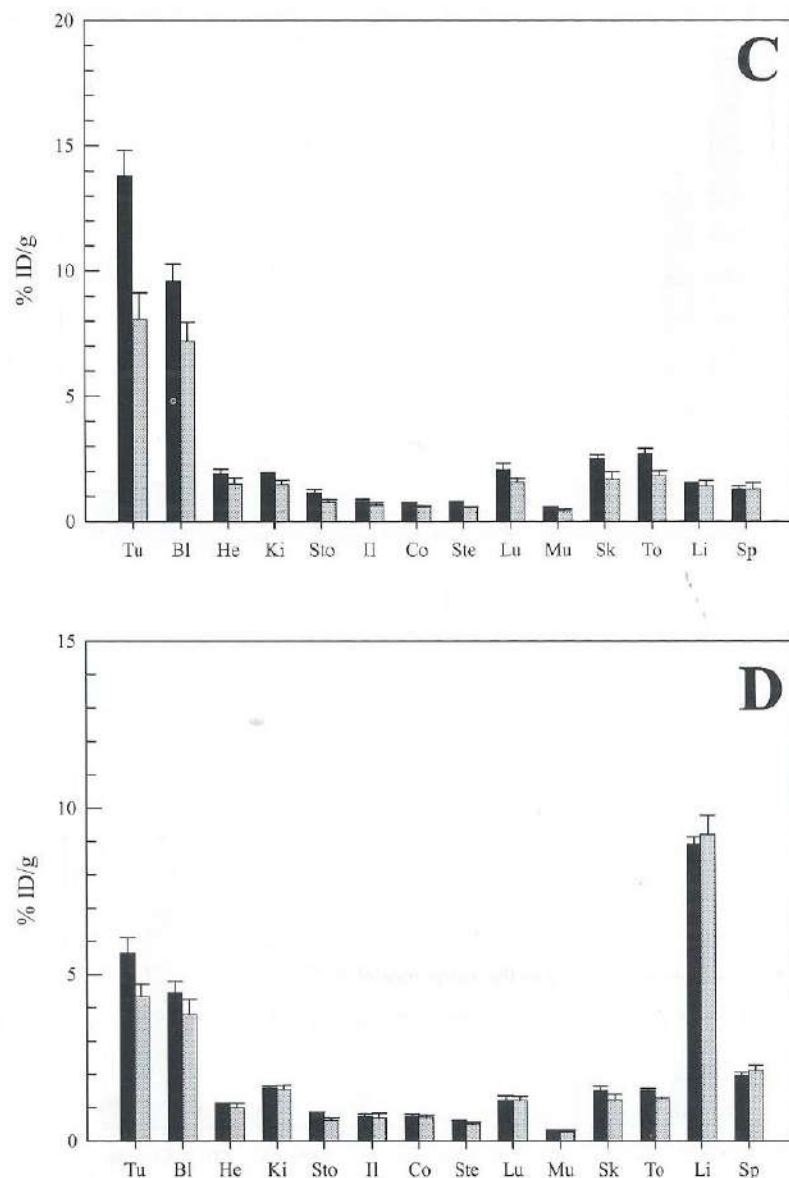


Figure 4. Biodistribution of ^{125}I -cMAb U36 and ^{131}I -*m*THPC-(CH₂COOH)₄ after conjugation (continued). Each preparation was intravenously injected in six HNX-OE bearing nude mice. C (^{125}I) and D (^{131}I): 48 h p.i. of ^{131}I -*m*THPC-(CH₂COOH)₃CH₂CONH- ^{125}I -cMAb U36 (100 μg ; 5 μCi ^{125}I , 1 μCi ^{131}I) at a molar ratio of 0.9 (black bars) or 1.8 (grey bars). At indicated time points mice were bled, sacrificed, and dissected, and the radioactivity levels (%ID/g + SE) of blood, tumor and several organs were assessed. Tu: tumor, Bl: blood, He: heart, Ki: kidney, Sto: stomach, Il: ileum, Co: colon, Ste: sternum, Lu: lung, Mu: muscle, Sk: skin, To: tongue, Li: liver, Sp: spleen.

injection, and the biodistribution was determined. The mean uptake in tumor tissue was 19.5 %ID/g, whereas the mean blood level was 13.9 %ID/g. Uptake in all other organs was <4 %ID/g (Fig. 4A).

For evaluation of *m*THPC-(CH₂COOH)₄, 2.5 μCi (5 μg) of ^{131}I -*m*THPC-(CH₂COOH)₄ were injected in five HNX-OE xenograft-bearing nude mice. Fig. 4B shows the biodistribution after 24 h. The compound was cleared very rapidly from the circulation. The mean blood level was 1.5 %ID/g, whereas the uptake in the tumor was 0.5 %ID/g. Uptake in all other organs was <1.5 %ID/g, except for the liver. Because the levels of ^{131}I were already very low after 24 h, the biodistribution after 48 h was not determined.

The biodistribution of ^{131}I -*m*THPC- ^{125}I -cMAb U36 conjugates with a ratio of 0.9 and 1.8 is shown in Fig. 4C (^{125}I data) and D (^{131}I data). Conjugates (100 μg ; 10 μCi ^{125}I :2.5 μCi ^{131}I) were injected in two groups of five mice, and mice were killed 48 h after receiving injections.

The results depicted in Fig. 4 revealed that coupling of *m*THPC-(CH₂COOH)₄ to cMAb U36 resulted in selective targeting of the sensitizer to the tumor (Fig. 4D and B). However, tumor uptake levels of the sensitizer appeared to be lower than could be expected on the basis of the biodistribution of the unconjugated MAb (Fig. 4A and D). The fact that tumor uptake of the transporter of the sensitizer, *i.e.*, the conjugated MAb, was also lower than expected indicated that a proportion of the conjugate became rapidly eliminated from the blood (blood levels Fig. 4A and C). This elimination was more pronounced for conjugates with the higher *m*THPC:MAb ratio. For both the free *m*THPC-(CH₂COOH)₄ and the conjugate, high *m*THPC levels were found in the liver (Fig. 4B and D).

To establish the overall efficiency of sensitizer targeting by the MAb, the biodistribution of unmodified *m*THPC was assessed in the same model as ^{131}I -*m*THPC-(CH₂COOH)₄. Externally labeled ^{123}I -*m*THPC (5.0 $\mu\text{g}/\text{mouse}$; specific activity, 11.3 Ci/mmol) and internally labeled [^{14}C]*m*THPC (5.0 $\mu\text{g}/\text{mouse}$; specific activity, 74 mCi/mmol) were coinjected in six HNX-OE-bearing nude mice. As found previously by others in BALB/c mice (37), the free sensitizer showed a random distribution in the organs and no selective tumor uptake (Fig. 5). For both *m*THPC compounds, the highest accumulation was observed in liver, spleen, and lung, and the lowest uptake was observed in muscle. Besides this, small differences were observed in the distribution pattern of the compounds, partly originating from the difficulty to assess the [^{14}C] radioactivity in solid/colored tissue.

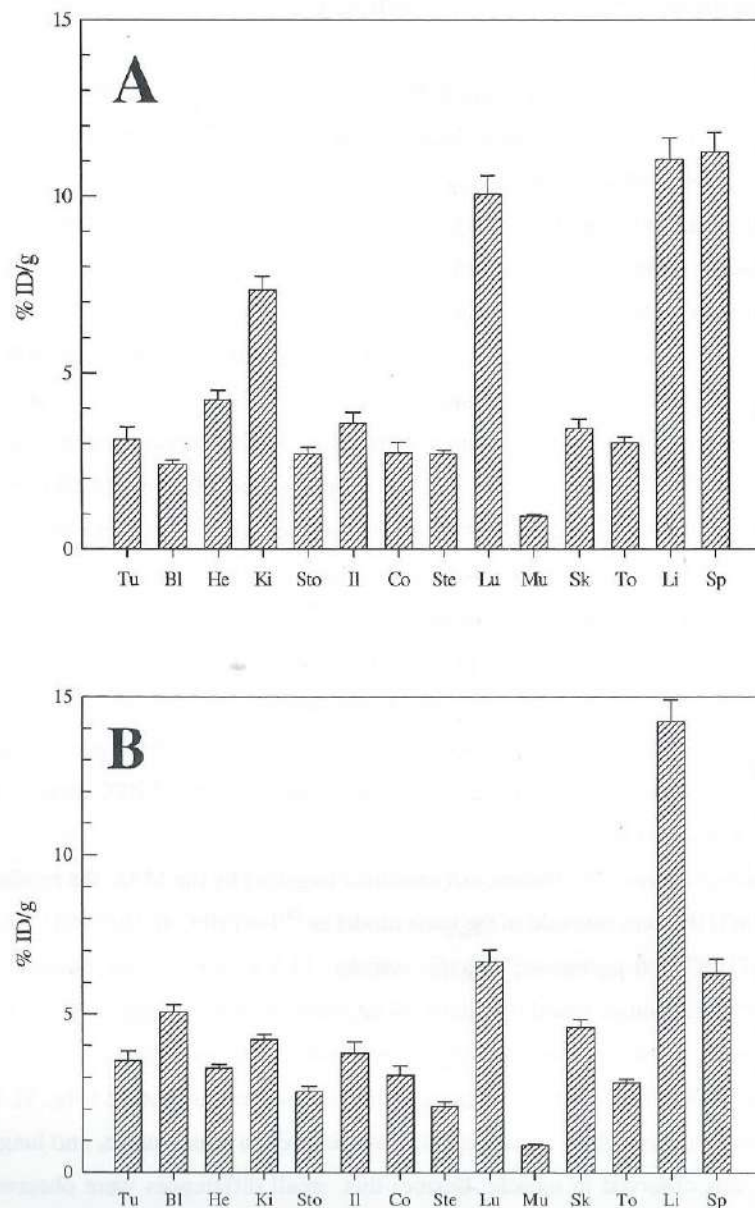


Figure 5. Comparison of the biodistribution of [^{14}C]mTHPC (A) and ^{123}I -mTHPC (B), 24 h after intravenous injection. Six mice received [^{14}C]mTHPC (5.0 μg ; 0.54 μCi) and ^{123}I -mTHPC (5.0 μg ; 83 μCi). At 24 h p.i. mice were bled, sacrificed, and dissected, and the radioactivity levels (%ID/g + SE) of blood, tumor and several organs were assessed. For abbreviations, see the legend to Figure 4.

Photoimmunotherapy *in vitro*

The efficacy of photoimmunotherapy with *m*THPC-cMAb U36 conjugates was tested in 22A cells using the SRB assay. After exposure to the relatively high concentration of 1 μM conjugated *m*THPC, ~25% growth inhibition was observed (Fig. 6A). In the same assay, unconjugated *m*THPC showed an IC_{50} of 0.75 nM. Conjugated and free *m*THPC appeared to be nontoxic without illumination.

To investigate the possibility that the sensitizer must be internalized for phototoxicity to occur, we coupled *m*THPC to mMAb 425, an internalizing MAb directed against EGFR. Internalization of the *m*THPC-MAb 425 conjugate was confirmed according to a method described before (40, 41). The efficacy of these conjugates was tested in A431 cells. The IC_{50} using *m*THPC-mMAb 425 conjugates was 7.3 nM, whereas in this cell line, the IC_{50} for free *m*THPC was 2.0 nM (Fig. 6B). Once again, conjugated and free *m*THPC were nontoxic without illumination. Unconjugated cMAb U36 or mMAb 425 did not result in growth inhibition with or without illumination (data not shown).

DISCUSSION

Several attempts to use MAbs for selective delivery of photosensitizers to tumors have been made. However, none of these has led to conjugates suitable for therapeutic use. In 1983, Mew *et al.* (42) described the synthesis of hematoporphyrin-MAb conjugates, but the *in vivo* efficacy of these conjugates appeared to be minimal. The same research group developed benzoporphyrin derivative monoacid ring A (BPD)-MAb conjugates, using polyvinyl alcohol as a linker (43), but no data on the therapeutic applicability of these conjugates have been reported. The photosensitizer chlorin e_6 was conjugated to MAbs by Goff *et al.* (44) using polyglutamic acid as a linker. Preliminary results of PDT after i.p. injection of these conjugates in a murine i.p. ovarian cancer model showed an improved survival. No data on the i.v. use of these conjugates or for chlorin e_6 -MAb conjugates using a dextran polymer linker (45) have been published thus far.

Although *m*THPC is one of the most promising photosensitizers available for clinical use, no reports on *m*THPC-MAb conjugates have been published. In this report, a reproducible procedure for conjugation of *m*THPC to MAbs is provided in detail. Of major importance is that all reactions, including the modification of *m*THPC, conjugation, and subsequent purification,

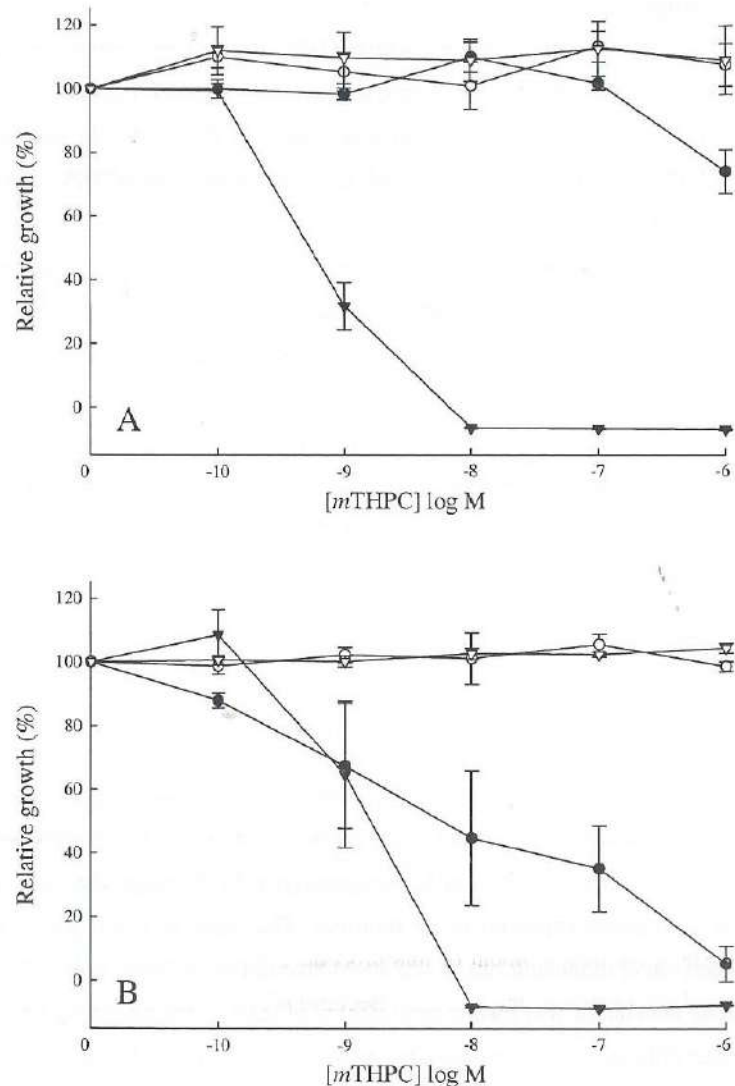


Figure 6. The SRB assay was used to assess the antiproliferative effect of *m*THPC and *m*THPC-MAb conjugates upon illumination. A) 22A cells, *m*THPC + 25 J/cm² (▼), *m*THPC not illuminated (▽), *m*THPC-cMAb U36 + 25 J/cm² (●), *m*THPC-cMAb U36 not illuminated (○). B) A431 cells, *m*THPC + 25 J/cm² (▼), *m*THPC not illuminated (▽), *m*THPC-mMAb 425 + 25 J/cm² (●), *m*THPC-mMAb 425 not illuminated (○). Results of three experiments are indicated as means ± SD.

are performed in the dark, and that solvents used are saturated with nitrogen. Fig. 7 illustrates the phototoxic effect of free *m*THPC, when these precautions are not taken. In this case, the integrity of the MAb was impaired in such a way that it could not penetrate a 7.5% SDS-PAGE gel.

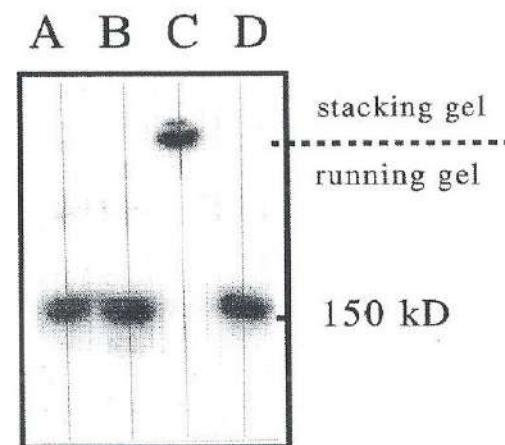


Figure 7. Illustration of the phototoxicity of *m*THPC to the integrity of ¹²⁵I-cMAb U36. 50 µg of ¹²⁵I-cMAb U36 were incubated in 500 µl of MeCN/0.9% NaCl (1:4, v/v) at pH 9.5: with 25 µg *m*THPC in the dark (lane A), with 25 µg of *m*THPC in the light under a N₂ atmosphere (lane B), with 25 µg of *m*THPC in the light (lane C), and without *m*THPC in the light as a control (lane D). After 1 h of incubation, SDS-PAGE and Phosphor Imager analysis was performed.

As anticipated, the development of this procedure was hampered by the necessity for modification of *m*THPC and its hydrophobicity. Because *m*THPC lacks a functional moiety for direct coupling to a MAb, *m*THPC was carboxymethylated. In our initial attempts to produce *m*THPC-MAb conjugates, monocarboxymethylated *m*THPC was synthesized. With such a derivative, after esterification no cross-linking can occur during conjugation. However, the TFP ester of this compound did not chemically conjugate to the MAb. The reason was found to be that, after esterification, the compound is poorly water soluble. The ester, once brought in aqueous medium, immediately adheres to the MAb without forming covalent bonds.

To obtain a water-soluble *m*THPC-TFP ester derivative, *m*THPC was tetracarboxymethylated. Attempts were made to form the monoester of this compound directly, which would be the optimal compound for conjugation. However, the synthesis of this

monoester, implying the combination of 1 molar equivalent TFP and EDC, led to an intractable mixture of products, which were not identified further.

The final route to the reproducible production of *m*THPC-(CH₂COOH)₃CH₂CO-TFP was the synthesis of the tetraesterified compound, followed by partial hydrolysis to leave the monoester. The esterification of *m*THPC-(CH₂COOH)₄ using an excess of TFP and EDC gave, after column chromatography, pure *m*THPC-(CH₂CO-TFP)₄ in a reasonable yield (60%). During the following partial hydrolysis procedure, the formation of fully hydrolyzed *m*THPC-(CH₂COOH)₄ is unavoidable. When hydrolysis was performed until no diester was left, only 20% of the mixture consisted of monoester. In our experiments, we hydrolyzed until 45% of the mixture consisted of monoester. Under these conditions, less than 5% diester was left, which was judged acceptable for conjugation. As a result, the overall amount of *m*THPC available for conjugation was about 30%, owing to the loss during the modification, esterification, and subsequent hydrolysis.

It was possible to couple four *m*THPC molecules to one MAb molecule without impairment of its solubility. When conjugates with a higher ratio were made, the MAbs formed insoluble aggregates during the conjugation. These aggregates were not recovered from the PD-10 column. Aggregate formation was also observed by the group of Mach when making indocyanin-MAb conjugates at a ratio of 2 (14). After the synthesis and purification of these conjugates, a small proportion of the MAbs aggregated during a subsequent 24-h storage period.

*m*THPC-MAb conjugates prepared according to the method described herein showed a minimal impairment of the integrity on SDS-PAGE (<10% aggregate formation), full stability in serum *in vitro*, and an optimal immunoreactivity, provided that not more than four *m*THPC molecules were coupled to the MAb. Nevertheless, the pharmacokinetics of *m*THPC-MAb conjugates in xenograft-bearing nude mice differed from that of unconjugated MAb. For conjugates with a mean ratio of 0.9 and 1.8, the ¹²⁵I-levels of the ¹³¹I-*m*THPC-¹²⁵I-MAb in the blood at 48 h p.i. were 69 and 52%, respectively, of that of an unconjugated ¹²⁵I-MAb. In addition, the ¹³¹I-levels decreased more extensively than the ¹²⁵I-levels. These data indicate that conjugates with a higher ratio are more susceptible for removal from the blood. Our biodistribution data, therefore, indicate hepatic extraction with retention of the sensitizer in this organ after catabolism. Rapid blood clearance and extensive liver accumulation have also been observed for MAbs coupled with other chemical groups to their lysine residues (12, 46-48).

¹³¹I-*m*THPC-(CH₂COOH)₄ was cleared more rapidly from the circulation than the unmodified *m*THPC. The tumor selectivity of MAb-conjugated *m*THPC was increased in

comparison with both of these, despite the more rapid elimination of the conjugates with a higher ratio. For the conjugates with a ratio of 0.9 and 1.8, the tumor levels of ¹³¹I-*m*THPC were 5.7 and 4.4 %I.D./g, respectively. In absolute amounts, this corresponds with 23 and 36 ng/g tumor, respectively. Given the fact that increasing the MAb dose to 400 μg/mouse does not result in antigen saturation, this implies that about 150 ng of *m*THPC per g of tumor can be delivered.

Another aspect of evaluation is the uptake in the skin, in view of the problem of skin photosensitization. At 48 h after injection, the levels of the MAb-conjugated *m*THPC in the skin were much lower than in the tumor (tumor:skin ratios were 3.5; Fig. 4D). For the unconjugated ¹²³I-*m*THPC and the reference compound [¹⁴C]*m*THPC, the levels in the skin and tumor were almost the same 24 h after injection (tumor:skin ratios were 0.8 and 0.9, respectively; Fig. 5). This is in agreement with data of Whelpton *et al.*, who showed that tumor:skin ratios remained about 1 between 1 and 4 days after administration of [¹⁴C]*m*THPC to Colo 26-bearing mice (37). Westermann *et al.* showed that in colon carcinoma-bearing nude mice, these ratios were improved by using ¹²⁵I-*m*THPC-PEG conjugates instead of ¹²⁵I-*m*THPC (49).

The improved selectivity of *m*THPC directed by the MAb does not guarantee improved efficacy. Therefore, *in vitro* studies were performed to compare the phototoxicity of internalizing and noninternalizing MAb-conjugated *m*THPC with that of free *m*THPC at equimolar doses. Our data on the photodynamic efficacy of the *m*THPC-MAb conjugates revealed a remarkable difference between internalizing and noninternalizing MAbs. When coupled to mMab 425, which was internalized by the cell after conjugation, *m*THPC exhibited more phototoxicity than when coupled to the noninternalizing cMab U36. Sobolev *et al.* also reported that the photosensitizer chlorin *e*₆ was more effective when localized intracellularly (50). For BPD-MAb conjugates, produced by Jiang *et al.*, internalization enhanced the cell killing by 10-fold (51). These data strongly suggest that the critical target for photodynamic damage is localized intracellularly. When this is true, it is clear that the kinetics of cellular uptake of free *m*THPC versus mMab 425-conjugated *m*THPC are crucial parameters and might have influenced the relative efficacy as observed in our SRB experiments (Fig. 6). For the same reason, at this moment it is difficult to speculate about the relative efficacy *in vivo*. Therapy experiments with the use of *m*THPC-mMab 425 conjugates in HNSCC-bearing nude mice will be started shortly.

REFERENCES

1. Weishaupt, K. R., Gomer, C. J., and Dougherty, T. J. Identification of singlet oxygen as the cytotoxic agent in photoinactivation of a murine tumor. *Cancer Res.*, *36*: 2326-2329, 1976.
2. Penning, L. C., Tijssen, K., Boegheim, J. P. J., van Steveninck, J., and Dubbelman, T. M. A. R. Relationship between photodynamically induced damage to various cellular parameters and loss of clonogenicity in different cell types with hematoporphyrin derivative as sensitizer. *Biochim. Biophys. Acta*, *1221*: 250-258, 1994.
3. Henderson, B. W., Waldow, S. M., Mang, T. S., Potter, W. R., Malone, P. B., and Dougherty, T. J. Tumor destruction and kinetics of tumor cell death in two experimental mouse tumors following photodynamic therapy. *Cancer Res.*, *45*: 572-576, 1985.
4. Kros, G., Korbek, M., and Dougherty, G. J. Induction of immune cell infiltration into murine SCCVII tumour by Photofrin-based photodynamic therapy. *Br. J. Cancer*, *71*: 549-555, 1995.
5. Fromm, D., Kessel, D., and Webber, J. Feasibility of photodynamic therapy using endogenous photosensitization for colon cancer. *Arch. Surg.*, *131*: 667-669, 1996.
6. Nseyo, U. O., and Lamm, D. L. Therapy of superficial bladder cancer. *Sem. Oncol.*, *23*: 598-604, 1996.
7. Furuse, K., Fukuoka, M., Kato, H., Horai, T., Kubota, K., Kodama, N., Kusunoki, Y., Takifuji, N., Okunaka, T., Konaka, C., Wada, H., and Hayata, Y. A prospective phase II study on photodynamic therapy with Photofrin II for centrally located early-stage lung cancer. *J. Clin. Oncol.*, *11*: 1852-1857, 1993.
8. Lofgren, L. A., Hallgren, S., Nilsson, E., Westerborn, A., Nilsson, C., and Reizenstein, J. Photodynamic therapy for recurrent nasopharyngeal cancer. *Arch. Otolaryngol. Head Neck Surg.*, *121*: 997-1002, 1995.
9. Bonnett, R. Photosensitizers of the porphyrin and phthalocyanine series for photodynamic therapy. *Chem. Soc. Rev.*, *24*: 19-33, 1995.
10. Dilkes, M. G., DeJode, M. L., Rowntree-Taylor, A., McGilligan, J. A., Kenyon, G. S., and McKelvie, P. mTHPC photodynamic therapy for head and neck cancer. *Lasers Med. Sci.*, *11*: 23-29, 1996.
11. Savary, J-F., Monnier, P., Fontollet, C., Wagnières, G., Braichotte, D., and van den Bergh, H. Photodynamic therapy for early squamous cell carcinomas of the esophagus, bronchi, and mouth with *meta*-tetrahydroxyphenylchlorin. *Arch. Otolaryngol. Head Neck Surg.*, *123*: 162-168, 1997.
12. Pèlegrin, A., Folli, S., Buchegger, F., Mach, J-P., Wagnières, G., and van den Bergh, H. Antibody-fluorescein conjugates for photoimmunodiagnosis of human colon carcinoma in nude mice. *Cancer*, *67*: 2529-2537, 1991.
13. Folli, S., Wagnières, G., Pèlegrin, A., Calmes J-M., Braichotte, D., Buchegger, F., Chalandon, Y., Hardman, N., Heusser, N., Givel, J. C., Chapuis, G., Châtelain, A., van den Bergh, H., and Mach, J-P. Immunophotodiagnosis of colon carcinomas in patients injected with fluoresceinated chimeric monoclonal antibodies against carcinoembryonic antigen. *Proc. Natl. Acad. Sci. USA*, *89*: 7973-7977, 1992.
14. Folli, S., Westermann, P., Braichotte, D., Pèlegrin, A., Wagnières, G., van den Bergh, H., and Mach, J-P. Antibody-indocyanin conjugates for immunodetection of human squamous cell carcinoma in nude mice. *Cancer Res.*, *54*: 2643-2649, 1994.
15. Quak, J. J., van Dongen, G. A. M. S., Balm, A. J. M., Brakkee, J. P. G., Scheper, R. J., Snow, G. B., and Meijer, C. J. L. M. A 22-kDa surface antigen detected by monoclonal antibody E48 is exclusively expressed in stratified squamous and transitional epithelia. *Am. J. Pathol.*, *136*: 191-197, 1990.
16. Schrijvers, A. H. G. J., Quak, J. J., Uyterlinde, A. M., van Walsum, M., Meijer, C. J. L. M., Snow, G. B., and van Dongen, G. A. M. S. MAb U36, a novel monoclonal antibody successful in immunotargeting of squamous cell carcinoma of the head and neck. *Cancer Res.*, *53*: 4383-4390, 1993.
17. De Bree, R., Roos, J. C., Quak, J. J., den Hollander, W., van den Brekel, M. W. M., van de Wal, J. E., Snow, G. B., and van Dongen, G. A. M. S. Clinical imaging of head and neck cancer with ^{99m}Tc-labeled monoclonal antibody E48 IgG or F(ab')₂. *J. Nucl. Med.*, *35*: 775-783, 1994.
18. De Bree, R., Roos, J. C., Quak, J. J., den Hollander, W., Wilhelm, A. J., van Lingem, A., Snow, G. B., and van Dongen, G. A. M. S. Biodistribution of radiolabeled monoclonal antibody E48 IgG and F(ab')₂ in patients with head and neck cancer. *Clin. Cancer Res.*, *1*: 277-286, 1995.
19. De Bree, R., Roos, J. C., Quak, J. J., den Hollander, W., Snow, G. B., and van Dongen, G. A. M. S. Radioimmunoscintigraphy with ^{99m}Tc-labeled monoclonal antibody U36 and its biodistribution in patients with head and neck cancer. *Clin. Cancer Res.*, *1*: 591-598, 1995.
20. Brakenhoff R. H., van Gog, F. B., Looney J. E., van Walsum, M., Snow G. B., and van Dongen G. A. M. S. Construction and characterization of the chimeric monoclonal antibody E48 for therapy of head and neck cancer. *Cancer Immunol. Immunother.*, *40*: 191-200, 1995.
21. Van Hal N. L. W., van Dongen, G. A. M. S., Rood-Knippels, E. M. C., van der Valk, P., Snow, G. B., and Brakenhoff, R. H. Monoclonal antibody U36, a suitable candidate for clinical immunotherapy of squamous-cell carcinoma, recognizes a CD44 isoform. *Int. J. Cancer*, *68*: 520-527, 1996.
22. Murthy, U., Basu, A., Rodeck, U., Herlyn, M., Ross, A. H., and Das, M. Binding of an antagonistic monoclonal antibody to an intact and fragmented EGR-receptor polypeptide. *Arch. Biochem. Biophys.*, *252*: 549-560, 1987.
23. Stanton, P., Richards, S., Reeves, J., Nikolic, M., Edington, K., Clark, L., Robertson, G., Souter, D., Mitchell, R., Hendler, F. J., Cooke, T., Parkinson, E. K., and Ozanne, B. W. Epidermal growth factor receptor expression by human squamous cell carcinomas of the head and neck, cell lines and xenografts. *Br. J. Cancer*, *70*: 427-433, 1994.
24. Atlas, I., Mendelsohn, J., Baselga, J., Masui, H., Fair, W. R., and Kumar, R. Growth regulation of human renal carcinoma cells: role of transforming growth factor- α . *Cancer Res.*, *52*: 3335-3339, 1992.
25. Liberman, T. A., Razon, N., Bartal, A. D., Yarden, Y., Schlessinger, J., and Soreq, H. Expression of EGF receptors in human brain tumors. *Cancer Res.*, *44*: 753-760, 1984.
26. Yoshida, K., Kyo, E., Tsuda, T., Tsujino, T., Ito, M., and Tahara, E. EGF and TGF- α , the ligands of hyperproduced EGFR in human esophageal carcinoma cells, act as autocrine growth factors. *Int. J. Cancer*, *45*: 131-135, 1990.
27. Neal, D. E., Bennet, M. K., Hall, R. R., Marsh, C., Abel, P. D., Sainsbury, J. R. C., and Harris, A. L. Epidermal growth factor receptors in human bladder cancer: comparison of invasive and superficial tumors. *Lancet*, *1*: 366-368, 1985.
28. Gullick, W. J., Marsden, J. J., Whittle, N., Ward, B., Bobrow, L., and Waterfield, M. D. Expression of epidermal growth factor receptors on human cervical, ovarian, and vulval carcinomas. *Cancer Res.*, *46*: 285-292, 1986.
29. Hendler, F. J., and Ozanne, B. W. Human squamous cell lung cancers express increased epidermal growth

- factor receptors. *J. Clin. Invest.*, *74*: 647-651, 1984.
30. Fitzpatrick, S. L., Brightwell, J., Wittliff, J. L., Barrows, G. H., and Schultz, G. S. Epidermal growth factor binding by breast tumor biopsies and relationship to estrogen and progesterone receptor levels. *Cancer Res.*, *44*: 3448-3453, 1984.
 31. Sunada, H., Magun, B. E., Mendelsohn, J., and MacLeod, C. L. Monoclonal antibody against epidermal growth factor receptor is internalized without stimulating receptor phosphorylation. *Proc. Natl. Acad. Sci. USA*, *83*: 3825-3829, 1986.
 32. Modjtahedi, H., Hickish, T., Nicolson, M., Moore, J., Styles, J., Eccles, S., Jackson, E., Salter, J., Sloane, J., Spencer, L., Priest, K., Smith, I., Dean, C., and Gore, M. Phase I trial and tumour localisation of the anti-EGFR monoclonal antibody ICR62 in head and neck or lung cancer. *Br. J. Cancer*, *73*: 228-235, 1996.
 33. Bier, H., Reiffen, K. A., Haas, I., and Stasiecki, P. Dose-dependent access of murine anti-epidermal growth factor receptor monoclonal antibody to tumor cells in patients with advanced laryngeal and hypopharyngeal carcinoma. *Eur. Arch. Otorhin.*, *252*: 433-439, 1995.
 34. Brakenhoff R. H., Gerretsen, M., Knippels, E. M. C., van Dijk, M., van Essen, H., Olde Weghuis, D., Sinke, R. J., Snow, G. B., and van Dongen, G. A. M. S. The human E48 antigen, highly homologous to the murine Ly-6 antigen ThB, is a GPI-anchored molecule apparently involved in keratinocyte cell-cell adhesion. *J. Cell Biol.*, *129*: 1677-1689, 1995.
 35. Haisma, H. J., Hilgers, J., and Zurawski, V. R. Iodination of monoclonal antibodies for diagnosis and therapy using a convenient one-vial method. *J. Nucl. Med.*, *27*: 1890-1895, 1986.
 36. Lindmo, T., Boven, E., Luttit, F., Fedorko, J., and Bunn Jr, P. A. Determination of the immunoreactive fraction of radiolabeled monoclonal antibodies by linear extrapolation to binding at infinite antigen excess. *J. Immunol. Methods*, *72*: 77-89, 1984.
 37. Whelpton, R., Michael-Titus, A. T., Jamdar, R. P., Abdillahl, K., and Grahn, M. F. Distribution and excretion of radiolabeled Temoporfin in a murine tumor model. *Photochem. Photobiol.*, *63*: 885-891, 1996.
 38. Veenhuizen, R., Oppelaar, H., Ruevekamp, M., Schellens, J., Dalesio, O., and Stewart, F. Does tumour uptake of Foscan determine PDT efficacy? *Int. J. Cancer*, *73*: 236-239, 1997.
 39. Skehan, P., Storeng, R., Scudiero, D., Monks, A., McMahon, J., Vistica, D., Warren, J. T., Bokesch, H., Kenney, S., and Boyd, M. R. New colorimetric cytotoxicity assay for anticancer-drug screening. *J. Natl. Cancer Inst.*, *82*: 1107-1112, 1990.
 40. Reist, C. J., Garg, P. K., Alston, K. L., Bigner, D. D., and Zalutsky, M. R. Radioiodination of internalizing monoclonal antibodies using *N*-succinimidyl 5-iodo-3-pyridinecarboxylate. *Cancer Res.*, *56*: 4970-4977, 1996.
 41. Wargalla, U. C., Reisfeld, R. A. Rate of internalization of an immunotoxin correlates with cytotoxic activity against human tumor cells. *Proc. Natl. Acad. Sci. USA*, *86*: 5146-5150, 1989.
 42. Mew, D., Wat, C.-K., Towers, G. H. N., and Levy, J. G. Photoimmunotherapy: treatment of animal tumors with tumor-specific monoclonal antibody-hematoporphyrin conjugates. *J. Immunol.*, *130*: 1473-1477, 1983.
 43. Davis, N., Liu, D., Jain, A. K., Jiang, S.-Y., Jiang, F., Richter, A., and Levy, J. G. Modified polyvinyl alcohol-benzoporphyrin derivative conjugates as phototoxic agents. *Photochem. Photobiol.*, *57*: 641-647, 1993.
 44. Goff, B. A., Blake, J., Bamberg, M. P., and Hasan, T. Treatment of ovarian cancer with photodynamic therapy and immunoconjugates in a murine ovarian cancer model. *Br. J. Cancer*, *74*: 1194-1198, 1996.
 45. Oseroff, A. R., Ohuoha, D., Hasan, T., Bommer, J. C., and Yarmush, M. L. Antibody-targeted photolysis: Selective photodestruction of human T-cell leukemia cells using monoclonal antibody-chlorin *e*₆ conjugates. *Proc. Natl. Acad. Sci. USA*, *83*: 8744-8748, 1986.
 46. Boniface, G. R., Izard, M. E., Walker, K. Z., McKay, D. R., Soby, P. J., Turner, J. H., and Morris, J. G. Labeling of monoclonal antibodies with Samarium-153 for combined radioimmunoscintigraphy and radioimmunotherapy. *J. Nucl. Med.*, *30*: 683-691, 1989.
 47. Smith, A., Zangemeister-Wittke, U., Waibel, R., Schenker, T., Schubiger, P. A., and Stahel, R. A. A comparison of ⁶⁷Cu- and ¹³¹I-labeled forms of monoclonal antibodies SEN7 and SWA20 directed against small-cell lung cancer. *Int. J. Cancer*, *8*: 43-48, 1994.
 48. Van Gog, F. B., Visser, G. W. M., Klok, R., van der Schors, R., Snow, G. B., and van Dongen, G. A. M. S. Monoclonal antibodies labeled with Rhenium-186 using the MAG3 chelate: relationship between the number of chelated groups and biodistribution characteristics. *J. Nucl. Med.*, *37*: 352-362, 1996.
 49. Westermann, P., Glanzmann, T., Andrejevic, S., Braichotte, D. R., Forrer, M., Wagnières, G. A., Monnier, P., van den Bergh, H., Mach, J.-P., and Folli, S. Long circulating half-life and high tumor selectivity of the photosensitizer *meta*-tetrahydroxyphenylchlorin conjugated to polyethylene glycol in nude mice grafted with a human colon carcinoma. *Int. J. Cancer*, *76*: 842-850, 1998.
 50. Sobolev A. S., Akhlylina, T. V., Yachmenev, S. V., Rosenkranz, A. A., and Severin, E. S. Internalizable insulin-BSA-chlorin *e*₆ conjugate is a more effective photosensitizer than chlorin *e*₆ alone. *Biochem. Int.*, *26*: 445-450, 1992.
 51. Jiang, F. N., Allison, B., Liu, D., and Levy J. G. Enhanced photodynamic killing of target cells by either monoclonal antibody or low density lipoprotein mediated delivery systems. *J. Controlled Release*, *19*: 41-58, 1992.

Chapter 3

**TARGETING OF A HYDROPHILIC PHOTSENSITIZER
BY USE OF INTERNALIZING MONOCLONAL ANTIBODIES:
A NEW POSSIBILITY FOR USE IN PHOTODYNAMIC THERAPY**

Maarten B. Vrouenraets, Gerard W.M. Visser, Christophe Loup,
Bernard Meunier, Marijke Stigter, Hugo Oppelaar,
Fiona A. Stewart, Gordon B. Snow and Guus A.M.S. van Dongen

International Journal of Cancer, 88: 108-114, 2000

ABSTRACT

Coupling of photosensitizers to tumor-selective monoclonal antibodies (MAbs) is an attractive option for improving the selectivity of photodynamic therapy (PDT). For this purpose, hydrophilic sensitizers would be most suitable because of their solubility in water. However, such sensitizers are known to be ineffective in PDT, probably because they cannot readily pass the cell membrane and reach the critical intracellular target. We used the model compound TrisMPyP- Φ CO₂H, a hydrophilic porphyrin derivative, to test the hypothesis that hydrophilic photosensitizers might become of therapeutic value when directed into the tumor cell by use of internalizing MAbs.

TrisMPyP- Φ CO₂H was conjugated using a labile ester. Conjugates showed no impairment of integrity on SDS-PAGE, full stability in serum *in vitro*, and optimal immunoreactivity when the sensitizer:MAB ratio was ≤ 3 . At higher molar ratios, the solubility of the conjugates decreased. *In vitro* internalization experiments showed that TrisMPyP- Φ CONH-¹²⁵I-cMAB U36 and TrisMPyP- Φ CONH-¹²⁵I-mMAB 425 conjugates were internalized by A431 cells, in contrast to TrisMPyP- Φ CONH-¹²⁵I-mMAB E48 conjugates. Data on the *in vitro* efficacy of PDT with MAB-conjugated TrisMPyP- Φ CO₂H showed that the internalizing cMAB U36 and mMAB 425 conjugates were phototoxic to A431 cells, while the non-internalizing E48 conjugate and the unconjugated sensitizer were not. Biodistribution data of conjugates with sensitizer:¹²⁵I-cMAB U36 ratios varying from 1:1 to 3:1 in tumor-bearing nude mice revealed selective accumulation in the tumor. Conjugates with higher molar ratios were cleared more rapidly from the blood than the unconjugated ¹²⁵I-cMAB U36, resulting in lower tumor uptake but similar tumor-to-blood ratios. Our data suggest that hydrophilic photosensitizers might have therapeutic value when targeted to tumors by internalizing MAbs.

INTRODUCTION

Photodynamic therapy (PDT) is a non-invasive therapeutic modality for the treatment of superficially localized tumors. In this approach, a photosensitizer, in most cases a porphyrin derivative, is injected i.v. and accumulates in the tumor. The tumor area is then illuminated with light of 600 to 700 nm, depending on the sensitizer used. This light causes excitation of the photosensitizer, and in this excited state the sensitizer produces singlet

oxygen, a cytotoxic form of oxygen, which eradicates tumor cells (1). Tumor necrosis is a combined result of direct cell killing (2), occlusion of tumor blood vessels (3), and an acute inflammatory reaction (4). PDT has been used to treat many types of cancer, including colon, bladder, lung, esophageal, and head-and-neck cancers (5-8).

A limitation of this approach is the lack of tumor selectivity of the photosensitizers. This can result in severe normal tissue damage after PDT of large surface areas. A possible way to overcome this problem is to target photosensitizers by monoclonal antibodies (MAbs) directed against tumor-associated antigens. Since expression of such antigens on normal tissues is limited, it can be anticipated that these tissues are spared. A serious problem in the development of photosensitizer-MAB conjugates, however, is the poor water solubility of most of the effective photosensitizers, as we described in our previous study on the development of *meta*-tetrahydroxyphenylchlorin (*m*THPC)-MAB conjugates (9). From this study, the following conclusions were drawn: (i) the tumor selectivity of *m*THPC was improved by coupling to tumor-selective MAbs, as demonstrated in tumor-bearing nude mice; (ii) in the same model, *m*THPC-conjugated MAB molecules were cleared more rapidly from the blood than unconjugated MAB molecules; (iii) *m*THPC-MAB conjugates were effective in *in vitro* photoimmunotherapy but significantly less effective, at equimolar doses, than free *m*THPC; and (iv) *in vitro* phototoxicity with *m*THPC-MAB conjugates was observed only when these were internalized. From this latter observation, we concluded that the critical target for photodynamic damage might be localized intracellularly.

In the present study, we hypothesized that more hydrophilic photosensitizers (compared with *m*THPC), which in general do not readily pass the cell membrane and therefore are ineffective in PDT, might become effective when coupled to internalizing MAbs. If this is true, hydrophilic photosensitizers might be ideal candidates for MAB targeting since their water solubility will facilitate the coupling to MAbs.

The porphyrin derivative 5-[4-[5-(carboxyl)-1-butoxy]phenyl]-10,15,20-tris-(4-methylpyridiniumyl)porphyrin iodide (TrisMPyP- Φ CO₂H) has an absorption maximum at 595 nm, which could be suitable for treatment of small tumors but not large tumors (light of a longer wavelength penetrates deeper into the tissue). This is an ideal model compound to test the feasibility of the above-mentioned approach because its 3 methyl-pyridinium moieties render it strongly hydrophilic.

Here, we describe a reproducible procedure for coupling TrisMPyP- Φ CO₂H to MAbs. The sensitizer was coupled to MAbs selectively reactive with squamous cell carcinoma (SCC). The *in vitro* photodynamic efficacy of the photosensitizer, both in free form and

coupled to internalizing and non-internalizing SCC-selective MAbs, was studied. Data on the biodistribution of the conjugates in SCC-bearing nude mice are provided.

MATERIAL AND METHODS

Sensitizer

TrisMPyP- Φ CO₂H (Fig. 1, *scheme* 1; M_r 1,159.64) was synthesized as described earlier (10).

Monoclonal antibodies

Selection and production of murine MAb (mMAb) U36 and its chimeric (mouse/human) IgG1 derivative (cMAb U36) have been described previously (11). MAb U36 recognizes the v6 domain of the 200 kDa CD44 splice variant epican, which is highly expressed in SCC of the head and neck (HNSCC), lung, skin, esophagus, and cervix, as well as in adenocarcinoma of breast and lung. Among normal tissues, expression was observed in only a subset of epithelial tissues: skin keratinocytes, breast and prostate myoepithelium, and bronchial epithelium (11).

mMAb 425 is an IgG2a MAb developed and characterized by Murthy *et al.* (12). It recognizes an epitope localized on the external domain of the EGF receptor (EGFR), which is highly expressed by various tumor types, including HNSCC, renal-cell cancer, gliomas, and carcinomas of the esophagus, bladder, cervix, stomach, lung, and breast (13). MAb 425 does not induce tyrosine kinase activity but inhibits the binding of EGF and TGF- α to EGFR.

Selection and production of mMAb E48 have been described previously (14). mMAb E48 is an IgG1 MAb which recognizes a 16 to 22 kDa glycosylphosphatidylinositol-anchored surface antigen. The antigen is expressed by 94% of primary HNSCCs. In 70% of these tumors, the antigen is expressed by the majority of cells. A comparable reactivity pattern was observed in 31 tumor-infiltrated lymph nodes from neck dissection specimens. In normal tissues, the antigen is expressed in stratified and transitional epithelium.

Cell lines

The HNSCC cell lines UM-SCC-11B and UM-SCC-22A (kindly provided by Dr. T.E. Carey, Ann Arbor, MI) and the vulvar cell line A431 were cultured in 5% CO₂ at 37°C in

DMEM (BioWhittaker, Alkmaar, the Netherlands) supplemented with 2 mM L-glutamine, 5% FCS (BioWhittaker), and 25 mM HEPES.

Analyses

¹H-NMR spectra of TrisMPyP- Φ CO₂H and TrisMPyP- Φ CO-TFP were recorded in a 4/1 (v/v) mixture of CD₃CN and D₂O on a Bruker AC 200 (200.13 MHz) spectrometer (Bruker, Rheinstetten, Germany). Chemical shifts are represented in δ (ppm) relative to δ (CD₂H₂CN) = 1.93.

Absorption of TrisMPyP- Φ CO₂H and TrisMPyP- Φ CONH-MAb conjugates was measured using an Ultrospec III spectrophotometer (Pharmacia Biotech, Roosendaal, the Netherlands). The sensitizer concentration in the conjugate preparations was assessed with the same apparatus at a wavelength of 424 nm. The absorption of a range of dilutions (1-9 μ g/ml) of TrisMPyP- Φ CO₂H in H₂O was measured and graphically depicted using the least-square method. The sensitizer concentration in the conjugate preparations was determined using this calibration curve.

For HPLC analysis of TrisMPyP- Φ CONH-¹²⁵I-MAb conjugates, an LKB (Bromma, Sweden) 2150 HPLC pump, an LKB 2152 LC controller, and a 10 x 300 mm Pharmacia Biotech Superdex 200 HR 10/30 column were used. The eluent consisted of 0.05 M sodium phosphate and 0.15 M sodium chloride (pH 6.8) and the flow rate was 0.5 ml/min. A Pharmacia LKB VWM 2141 UV detector was used at 424 nm for detection of the sensitizer, while radioactivity of the ¹²⁵I-labeled MAb was measured by an Ortec 406A single-channel analyzer connected to a Drew 3040 data collector (Betron Scientific, Rotterdam, the Netherlands).

The integrity of the TrisMPyP- Φ CONH-MAb conjugates was analyzed by electrophoresis on a Phastgel System (Pharmacia Biotech) using pre-formed 7.5% SDS-PAGE gels under non-reducing conditions. After running, gels were exposed to a Phosphor plate for 1 to 3 h and analyzed with a Phosphor Imager (B&L-Isogen Service Laboratory, Amsterdam, the Netherlands) for quantitation of the radiolabeled protein bands.

¹²⁵I-Labeling of MAbs

MAbs were labeled with ¹²⁵I using iodogen. One milligram of MAb dissolved in 500 μ l of PBS (pH 7.4) and 1 to 2 mCi ¹²⁵I (100 mCi/ml, Amersham, Aylesbury, UK) were mixed in a vial coated with 50 μ g of iodogen. After 5 min of incubation at room temperature, the reaction mixture was filtered through a 0.22 μ M Acrodisc filter (Gelman, Ann Arbor, MI)

and unbound ^{125}I was removed using a PD-10 column (Pharmacia Biotech) with 0.9% NaCl as eluent. After removal of unbound ^{125}I , the radiochemical purity always exceeded 98% (HPLC analysis).

Preparation of the TrisMPyP- $\Phi\text{CO-TFP}$ ester

The esterification of TrisMPyP- $\Phi\text{CO}_2\text{H}$ and subsequent reaction steps were carried out in the dark and under N_2 to prevent any unwanted photochemical reactions (9).

Fifty microliters of a 2,3,5,6-tetrafluorophenol solution (TFP; Janssen Chimica, Beerse, Belgium; 100 mg/ml in MeCN/ H_2O 9/1, v/v) were added to 500 μg of TrisMPyP- $\Phi\text{CO}_2\text{H}$, dissolved in 650 μl of an $\text{H}_2\text{O}/\text{MeCN}$ mixture (10/3, v/v). After addition of 165 μl of a 1-ethyl-3-(3-dimethylaminopropyl)-carbodiimide solution (EDC, Janssen Chimica; 5 mg/ml in H_2O), the pH was adjusted to 5.7 to 5.9 with 30 μl of 0.1 M Na_2CO_3 . During overnight stirring, the TrisMPyP- $\Phi\text{CO-TFP}$ (Fig. 1, *scheme 2*) precipitated. After centrifugation, the supernatant was removed and the product was washed with 2 ml H_2O at 4 $^\circ\text{C}$.

$^1\text{H-NMR}$ data of TrisMPyP- $\Phi\text{CO-TFP}$ in $\text{CD}_3\text{CN}/\text{D}_2\text{O}$ 4/1 (v/v): δ 9.16, 8.83 (12H, pyridinium), 9.04, 8.92 (8H, β -pyrroles), 8.14, 7.39 (4H, phenyl), 7.28 (1H, TFP), 4.68 (9H, $\text{N}^+\text{-Me}$), 4.35 (2H, OCH_2), 2.93 (2H, $\text{CH}_2\text{CO-TFP}$), 2.04 (4H, $(\text{CH}_2)_2$).

$^1\text{H-NMR}$ data of the starting compound TrisMPyP- $\Phi\text{CO}_2\text{H}$ in the same solvent mixture were as follows: δ 9.15, 8.82 (12H, pyridinium), 9.03, 8.90 (8H, β -pyrroles), 8.15, 7.38 (4H, phenyl), 4.68 (9H, $\text{N}^+\text{-Me}$), 4.30 (2H, OCH_2), 2.45 (2H, CH_2COOH), 2.02 (4H, $(\text{CH}_2)_2$).

Preparation of TrisMPyP- $\Phi\text{CONH-}^{125}\text{I-MAB}$ conjugates

For conjugation, the ester was dissolved in 500 μl MeCN and the concentration determined by absorption measurement. Chosen aliquots were added to 1 mg of ^{125}I -labeled MAb dissolved in 1 ml 0.9% NaCl at pH 9.5. After 30 min incubation, the TrisMPyP- $\Phi\text{CONH-}^{125}\text{I-MAB}$ conjugate (Fig. 1, *scheme 3*) was purified on a PD-10 column with 0.9% NaCl as the eluent. The integrity of the conjugate was analyzed by HPLC and gel electrophoresis as described above.

The sensitizer to the $^{125}\text{I-MAB}$ molar ratio was determined by measuring the absorbance at 424 nm to calculate the sensitizer concentration and by counting the ^{125}I activity for MAb quantitation.

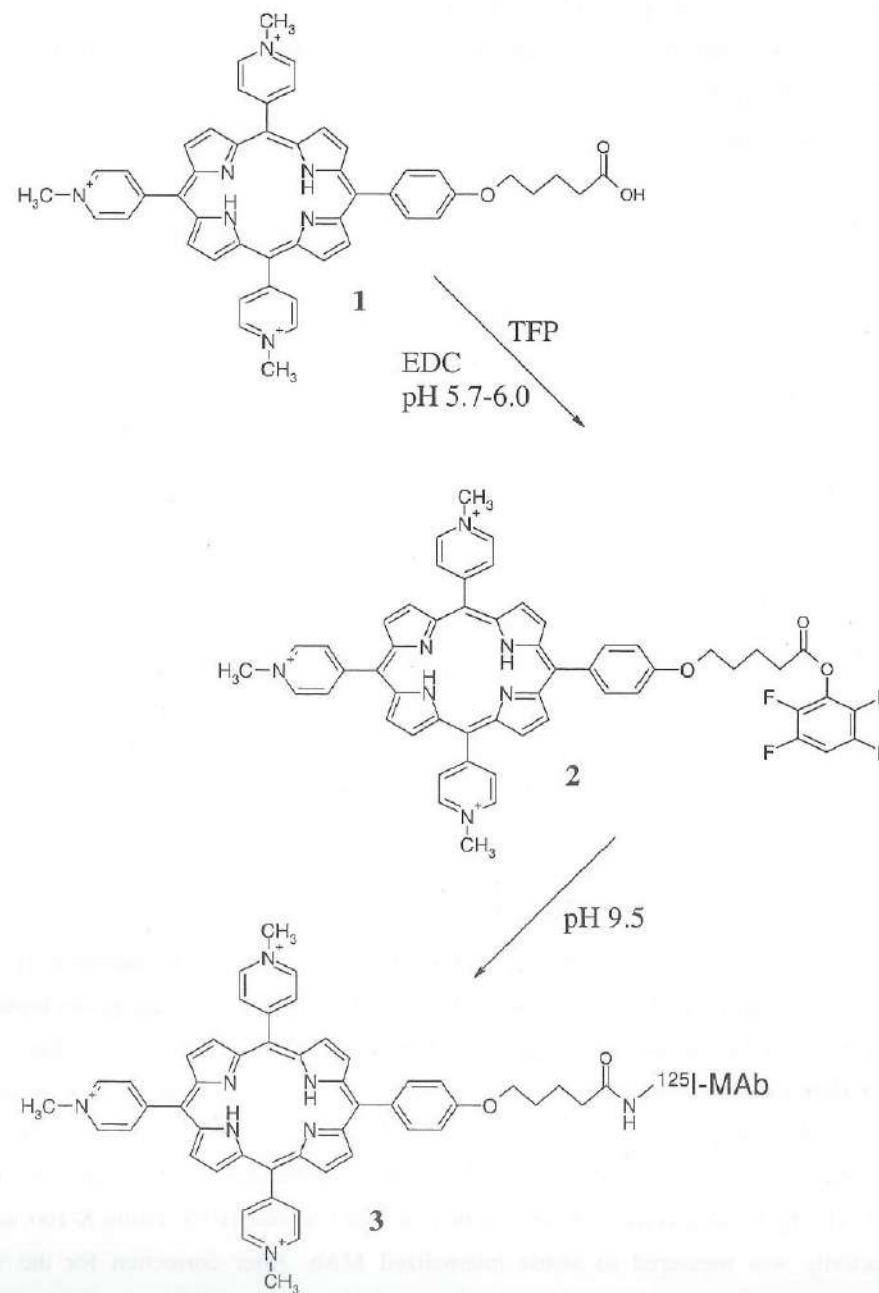


Figure 1. Schematic representation of the esterification of TrisMPyP- $\Phi\text{CO}_2\text{H}$, followed by conjugation to a ^{125}I -labeled MAb.

***In vitro* stability of TrisMPyP- Φ CONH- 125 I-MAb conjugates**

For measurement of the serum stability of the TrisMPyP- Φ CONH- 125 I-MAb conjugates, 15 μ g of conjugate in 25 μ l 0.9% NaCl were added to 25 μ l of human serum. After incubation for 24 h at 37°C, samples were analyzed by HPLC at 280 and 424 nm.

Immunoreactivity of TrisMPyP- Φ CONH- 125 I-MAb conjugates

In vitro binding characteristics of TrisMPyP- Φ CONH- 125 I-MAb conjugates were determined in an immunoreactivity assay essentially as described previously (9) and compared with those of the unconjugated 125 I-MAb. UM-SCC-11B cells were used for binding assays with 125 I-cMAB U36, A431 cells with 125 I-mMAB 425, and UM-SCC-22A cells with 125 I-mMAB E48.

Internalization of TrisMPyP- Φ CONH- 125 I-MAb conjugates

In vitro experiments were performed to determine the internalization capacity of TrisMPyP- Φ CONH- 125 I-cMAB U36, TrisMPyP- Φ CONH- 125 I-mMAB 425, and TrisMPyP- Φ CONH- 125 I-mMAB E48 conjugates. MABs were labeled with 2 mCi 125 I/mg MAB, and conjugates with a sensitizer:MAB ratio of 2:1 were synthesized.

A431 cells were plated in 6-well plates (10^4 cells/well) and grown for 5 days. After washing the cells with 3 ml PBS/0.5% BSA, conjugates (1×10^6 cpm) were added in 1 ml PBS/0.5% BSA. For each conjugate, the following conditions were tested in triplicate: (i) incubation at 0°C for 2 h to allow antibody binding, followed by incubation at 37°C for 2 h to allow internalization; (ii) incubation at 0°C for 4 h, for correction of acid-resistant surface binding at non-internalizing conditions; (iii) incubation for 2 h at 0°C, followed by 2 h at 37°C in the presence of 25 μ g naked MAB, for unspecific binding correction; (iv) incubation for 4 h at 0°C in the presence of 25 μ g naked MAB, for unspecific binding correction.

After incubation, cells were washed 3 times with 1 ml PBS/0.5% BSA to remove unbound MAB and incubated with 1 ml of 20 mM HCl/150 mM NaCl (pH 1.7) at 0°C for 15 min to release MAB bound to the surface of the cells. Supernatant was collected and counted for 125 I activity. Finally, cells were lysed with 1 ml of 0.1 M NaOH/1% Triton X-100, and the radioactivity was measured to assess internalized MAB. After correction for the values obtained for conditions ii-iv, the internalization at 37°C was calculated as the percentage of the total amount of radioactivity specifically bound to the cells (internalized and surface-bound).

Photoimmunotherapy *in vitro*

To determine the photodynamic efficacy of TrisMPyP- Φ CO₂H, *in vitro* PDT experiments were performed with free TrisMPyP- Φ CO₂H and cMAB U36-, mMAB 425-, and mMAB E48-conjugated TrisMPyP- Φ CO₂H. The efficacy was determined using the SRB (Sigma, St. Louis, MO) assay, for measurement of cellular protein content (15), as follows: A431 cells were plated in 96-well plates (750/well) and grown for 3 days before incubating with TrisMPyP- Φ CO₂H or TrisMPyP- Φ CONH-MAB conjugates (range 0.1 nM-1.0 μ M TrisMPyP- Φ CO₂H equivalents) in DMEM supplemented with 2 mM L-glutamine, 5% FCS, and 25 mM HEPES at 37°C. After 20 h, remaining unbound TrisMPyP- Φ CO₂H and TrisMPyP- Φ CONH-MAB conjugates were removed by washing twice with medium. Fresh medium was added, and cells were illuminated with a 150 W Scott KL 1500 lamp (Mainz, Germany) at a dose of 25 J/cm² (measured with an Ophir Laser Power Dosimeter; Optilas, Alphen a/d Rijn, the Netherlands). Three days after illumination, growth was assessed by staining cellular proteins with SRB and spectrophotometric measurement of the absorption at 540 nm with a microplate reader. As a control, cells were illuminated in the absence of TrisMPyP- Φ CO₂H or MAB-conjugated TrisMPyP- Φ CO₂H.

Biodistribution studies

The biodistribution characteristics of TrisMPyP- Φ CONH- 125 I-cMAB U36 conjugates with different sensitizer-to-MAB ratios were determined in nude mice bearing s.c. xenografts of the HNSCC cell line HNX-OE, tumor size ranging from 50 to 100 mm³. Conjugates were injected i.v. in 100 μ l of 0.9% NaCl. At 48 h p.i., mice were anesthetized, bled, killed, and dissected. Urine was collected, and organs were removed. After weighing, the amount of gamma-emitting radioactivity in organs, blood, and urine was measured in a gamma-counter (LKB-Wallac, 1282 CompuGamma; Pharmacia, Woerden, the Netherlands). Radioactivity uptake in the tissues was expressed as the percentage of the injected dose per gram of tissue (%ID/g). Besides that, tumor:non-tumor ratios were calculated.

RESULTS

Preparation of TrisMPyP- Φ CONH- 125 I-MAB conjugates

As a first step, TrisMPyP- Φ CO-TFP was prepared. Incubation of TrisMPyP- Φ CO₂H (Fig. 1, *scheme* 1) with a 70-fold excess of TFP using a 10-fold excess of EDC at pH 5.8

gave its corresponding TFP ester as a red/brown precipitate. After washing with H₂O, TrisMPyP- Φ CO-TFP (Fig. 1, *scheme 2*) was isolated in a yield of $75\% \pm 5\%$. ¹H-NMR analysis of the ester revealed the expected large downfield shift of the CH₂CO-TFP protons (from 2.45 to 2.93 ppm). Such a shift was also observed for biotin-TFP derivatives (16). ¹H-NMR analysis also revealed the presence of a small amount of residual TFP at δ 6.28 ppm. No effort was made to remove this free TFP because it did not interfere with the conjugation reaction with the MAb, a reaction that generates an additional portion of TFP.

For conjugation, TrisMPyP- Φ CO-TFP was dissolved in 500 μ l MeCN. When 35 nmol of this ester (generally in about 60 μ l MeCN) were added to 6.6 nmol (1.0 mg) of ¹²⁵I-MAb in 1 ml 0.9% NaCl, followed by incubation for 30 min at pH 9.5 and PD-10 column purification, a TrisMPyP- Φ CONH-¹²⁵I-MAb conjugate (Fig. 1, *scheme 3*) was obtained with a molar ratio of about 3.0, corresponding to a conjugation efficiency of about 60%. Purification of the conjugates on a PD-10 column also removed TFP and MeCN (17).

By adapting the amount of ester, conjugates with higher or lower ratios could be formed. For conjugates with a ratio ≤ 3 , recovery of the ¹²⁵I-MAb from the PD-10 column exceeded 95%. For conjugates with a higher ratio, this recovery dropped (*e.g.*, 70% recovery for a conjugate with a ratio of 5), indicating that the solubility of the MAb became impaired. Therefore, conjugates with a ratio >3 were not further evaluated.

Analyses and quality control

HPLC analysis of a TrisMPyP- Φ CONH-¹²⁵I-cMAb U36 conjugate, with absorption measurement at 424 nm for detection of the sensitizer and radioactivity measurement for detection of the ¹²⁵I-labeled MAb, revealed that the MAb was eluted as a monomeric peak and that the recovery of radioactivity from the column was $>95\%$. All of the sensitizer was confined to the MAb, indicating that any free sensitizer was effectively removed by PD-10 column purification.

Figure 2 shows the results of SDS-PAGE and subsequent Phosphor Imager analysis of a purified TrisMPyP- Φ CONH-¹²⁵I-cMAb U36 conjugate (Fig. 2, A and C) and unconjugated ¹²⁵I-cMAb U36 (Fig. 2, B and D) as a control. Both the TrisMPyP- Φ CO-conjugated and the unconjugated ¹²⁵I-MAb showed a single radiolabeled protein band with an apparent molecular weight of ± 150 kDa (deduced from SDS-PAGE analysis, data not shown).

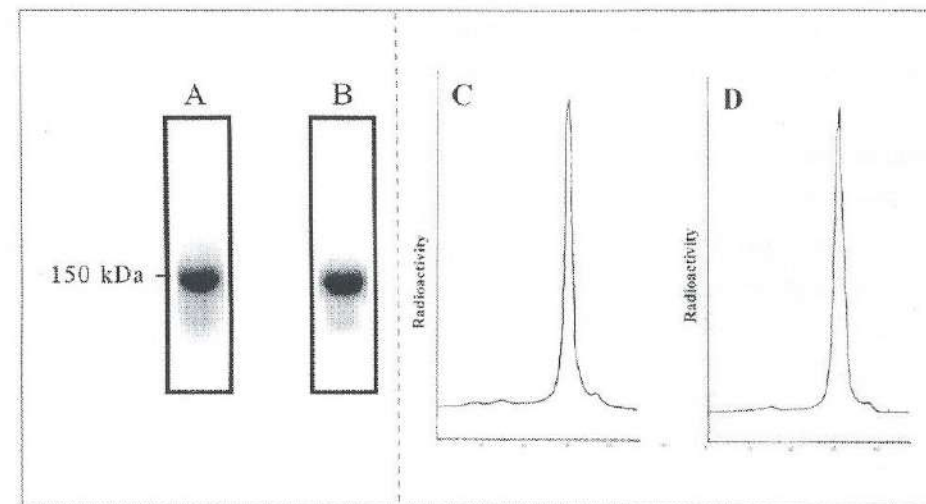


Figure 2. SDS-PAGE and Phosphor Imager analysis of a TrisMPyP- Φ CONH-¹²⁵I-cMAb U36 conjugate with ratio 2.5 (A and C) and unconjugated ¹²⁵I-cMAb U36 as a control (B and D).

For determination of serum stability, the TrisMPyP- Φ CONH-cMAb U36 conjugate was incubated in human serum for 24 h at 37°C. Subsequent HPLC analysis at 280 and 424 nm revealed that the HPLC profiles were identical to that at $t = 0$, showing that the conjugate was fully stable in human serum.

Cell-binding assays were performed to determine whether the coupling of TrisMPyP- Φ CO₂H influenced the immunoreactivity of cMAb U36, mMAB 425, or mMAB E48. For the conjugates studied (sensitizer:MAb ratios of 1:1 to 3:1), the immunoreactivity was, in all cases, the same as for their corresponding ¹²⁵I-MAbs (85-90%).

Internalization of TrisMPyP- Φ CONH-¹²⁵I-MAb conjugates

Before starting PDT experiments, TrisMPyP- Φ CONH-¹²⁵I-cMAb U36, TrisMPyP- Φ CONH-¹²⁵I-mMAb 425, and TrisMPyP- Φ CONH-¹²⁵I-mMAb E48 conjugates were characterized for their internalizing capacity with A431 cells. The ¹²⁵I-cMAb U36 and ¹²⁵I-mMAb 425 conjugates were internalized by the cells. Within our experimental set-up, $18.3 \pm 6.3\%$ and $12.4 \pm 1.8\%$ internalization values (mean \pm SD) were observed for ¹²⁵I-cMAb U36 and ¹²⁵I-mMAb 425 conjugates, respectively. Addition of excess naked MAb totally blocked

binding. The ^{125}I -mMAB E48 conjugates, while bound to a similar extent to A431 cells as the ^{125}I -cMAB U36- and ^{125}I -mMAB 425 conjugates (binding ratios E48:U36:425 were 1:0.6:1.1), were not internalized by the cells under these conditions.

Photoimmunotherapy *in vitro*

The phototoxicity of free TrisMPyP- $\Phi\text{CO}_2\text{H}$ and cMAB U36-, mMAB 425-, and mMAB E48-conjugated TrisMPyP- $\Phi\text{CO}_2\text{H}$ was assessed in A431 cells using the SRB assay. The results are depicted in Figure 3. Neither the free sensitizer nor the non-internalizing mMAB E48-conjugated sensitizer resulted in growth inhibition after PDT with sensitizer concentrations up to $1\ \mu\text{M}$.

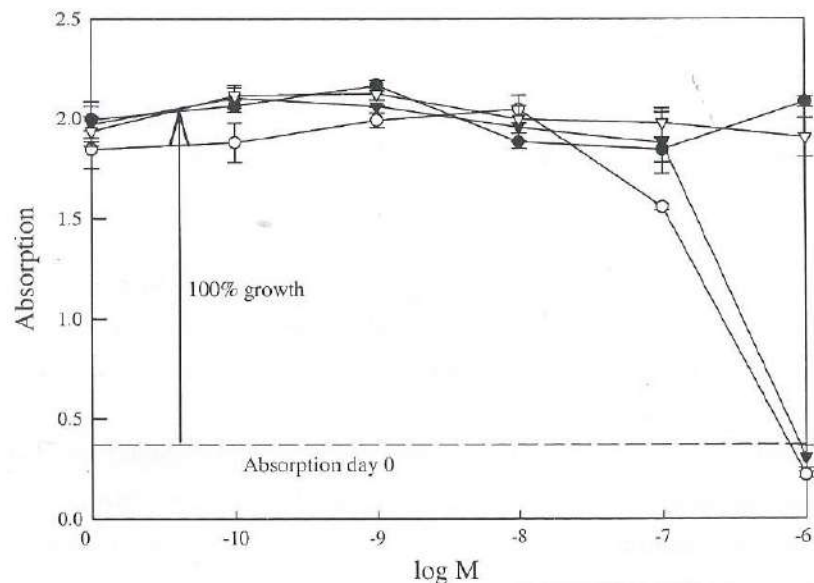


Figure 3. Anti-proliferative effect of TrisMPyP- $\Phi\text{CO}_2\text{H}$ and TrisMPyP- ΦCONH -MAB conjugates with a ratio of 2 on A431 cells upon illumination with $25\ \text{J}/\text{cm}^2$ (SRB assay). TrisMPyP- $\Phi\text{CO}_2\text{H}$ (\bullet), TrisMPyP- ΦCONH -cMAB U36 (\blacktriangledown), TrisMPyP- ΦCONH -mMAB 425 (\circ), and TrisMPyP- ΦCONH -mMAB E48 (∇). Results of triplicate experiments are indicated (means \pm SD). The molarity (M, x-axis) of the free or conjugated TrisMPyP- $\Phi\text{CO}_2\text{H}$ is indicated logarithmically.

When coupled to the internalizing mMAB 425 and cMAB U36, TrisMPyP- $\Phi\text{CO}_2\text{H}$ showed photodynamic efficacy. At $0.1\ \mu\text{M}$, mMAB 425-conjugated TrisMPyP- $\Phi\text{CO}_2\text{H}$ showed growth inhibition of about 25%. At $1\ \mu\text{M}$, PDT was much more effective and resulted in cell killing since the absorption was lower than that at the day of illumination (day 0). The efficacy of PDT with cMAB U36-conjugated TrisMPyP- $\Phi\text{CO}_2\text{H}$ was similar to that of PDT with the mMAB 425-conjugated sensitizer.

Conjugated and free TrisMPyP- $\Phi\text{CO}_2\text{H}$ appeared to be non-toxic without illumination. Unconjugated mMAB 425 did not result in growth inhibition with or without illumination (data not shown).

Biodistribution studies

As a first approach to test the *in vivo* behavior of the conjugates, TrisMPyP- ΦCONH - ^{125}I -cMAB U36 conjugates with different sensitizer-to-MAB ratios were evaluated for their biodistribution characteristics in HNX-OE xenograft-bearing nude mice. Figure 4 shows the biodistribution (Fig. 4A) and tumor:non-tumor ratios (Fig. 4B) of ^{125}I -cMAB U36 and TrisMPyP- ΦCONH - ^{125}I -cMAB U36 conjugates with ratios of 1.2, 2.1, and 3.0. The unconjugated ^{125}I -MAB and the conjugates ($100\ \mu\text{g}$; $10\ \mu\text{Ci}\ ^{125}\text{I}$) were injected in 4 groups of 6 mice, and mice were killed 48 h after injection.

The results depicted in Figure 4A show that the conjugates accumulate selectively in the tumor but uptake is lower than for the unconjugated ^{125}I -MAB. The conjugates with an increased ratio show a lower tumor uptake. Tumor uptake was 15.5, 8.6, 6.5, and 4.0 %ID/g for the unconjugated ^{125}I -cMAB U36 and the conjugates, with ratios of 1.2, 2.1, and 3.0, respectively. A similar pattern was observed for the blood values. Apparently, coupling of TrisMPyP- $\Phi\text{CO}_2\text{H}$ decreases the half-life of the ^{125}I -MAB in blood, resulting in a lower tumor accumulation.

Tumor-to-blood ratios 2 days p.i were 1.1 for the unconjugated ^{125}I -cMAB U36 as well as for the 3 conjugates (Fig. 4B). In general, tumor-to-normal tissue ratios slightly decreased for conjugates with increasing sensitizer:MAB ratio.

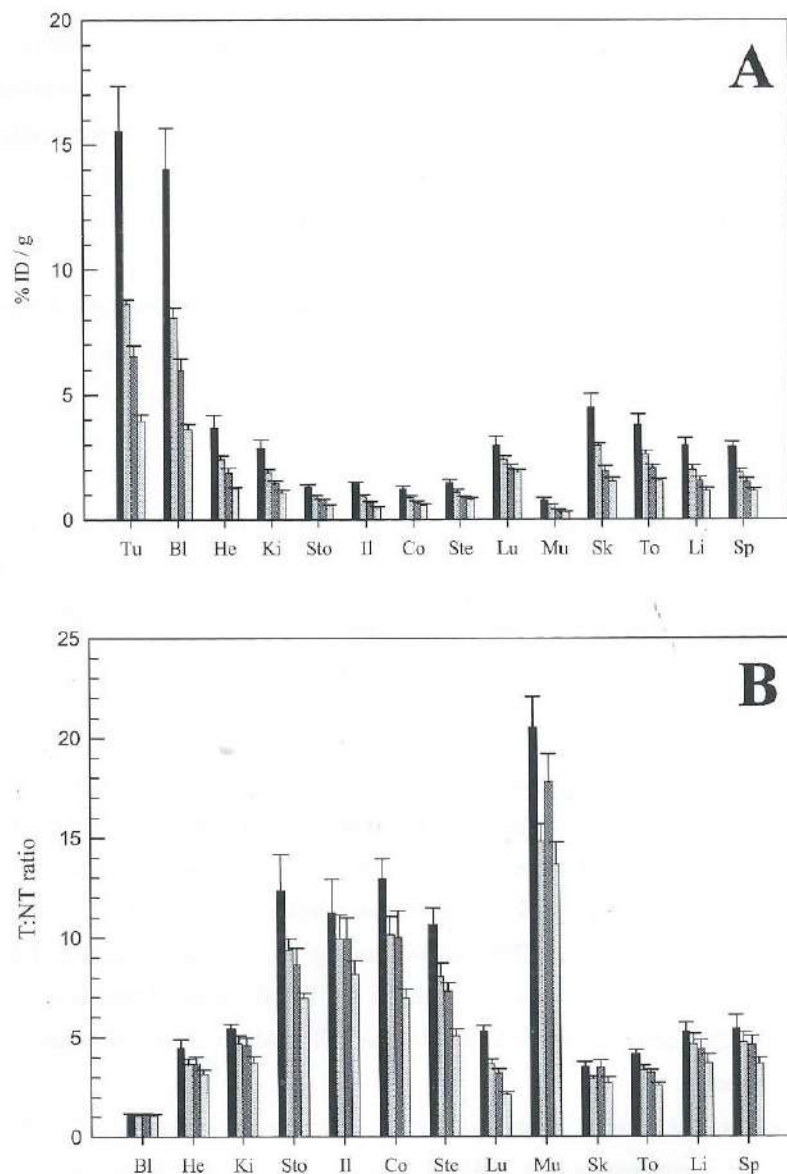


Figure 4. Biodistribution (A) and tumor to non-tumor ratios (B) of (for each set of four bars from left to right): unconjugated ^{125}I -cMab U36 and three TrisMPyP- ΦCONH - ^{125}I -cMab U36 conjugates with a ratio of 1.2, 2.1, and 3.0. Each preparation (100 μg MAb, 10 μCi ^{125}I) was injected i.v. in 6 HNX-OE bearing nude mice; 48 h p.i. mice were bled, killed, and dissected and radioactivity levels (%ID/g + SE) of blood, tumor and several organs were assessed. Tu: tumor, Bl: blood, He: heart, Ki: kidney, Sto: stomach, Il: ileum, Co: colon, Ste: sternum, Lu: lung, Mu: muscle, Sk: skin, To: tongue, Li: liver, Sp: spleen.

DISCUSSION

The critical target for photodynamic damage is most probably localized intracellularly (9). Therefore, the capacity of photosensitizers to enter the target cell is an important parameter in PDT efficacy. Hydrophilic photosensitizers do not readily pass the cell membrane; therefore, they are not ideal sensitizers for therapeutic use. In the present study, we tested the hypothesis that hydrophilic photosensitizers would become of therapeutic value when directed into the tumor cell by internalizing, tumor-selective MAbs. If successful, this approach could reduce normal tissue toxicity induced by PDT while retaining anti-tumor effects.

We determined the photodynamic efficacy of MAb-conjugated TrisMPyP- $\Phi\text{CO}_2\text{H}$ as a model. TrisMPyP- $\Phi\text{CO}_2\text{H}$ is a hydrophilic porphyrin derivative with optimal chemical properties for coupling to MAbs. The 3 methyl-pyridinium moieties in the molecule strongly enhance the water solubility of the porphyrin, while the presence of only 1 carboxyl group makes its conjugation to MAbs by means of the TFP ester method straightforward because no chemical cross-linking can occur. The TFP ester method was previously used for *m*THPC-MAb and ^{186}Re -MAb conjugates (9, 17). For the present study, TrisMPyP- ΦCO -NH- ^{125}I -MAb conjugates were reproducibly produced *via* the synthesis of the TFP-esterified compound, followed by addition of this ester to the ^{125}I -MAb at pH 9.5. The yield of both reaction steps was satisfactory: about 75% for the esterification and about 60% for the conjugation, which is optimal for this kind of methodology. Therefore, overall, 45% of the porphyrin was conjugated to the MAb.

It appeared possible to couple 3 TrisMPyP- $\Phi\text{CO}_2\text{H}$ molecules to 1 MAb molecule without impairment of MAb solubility. When conjugates with a higher porphyrin:MAb ratio were synthesized, MAb solubility was impaired. In these cases, the MAbs precipitated during the conjugation. Precipitation was also observed when making *m*THPC-MAb conjugates with *m*THPC:MAb ratios >4. Folli *et al.* (18) observed the same phenomenon when making photoimmunoconjugates with the photosensitizer indocyanin. After synthesis of indocyanin-MAb conjugates at a ratio of 2, a small proportion of the MAbs precipitated during a subsequent 24 h storage period.

In vitro PDT studies were performed to verify the hypothesis that conjugation to an internalizing MAb increases the phototoxicity of TrisMPyP- $\Phi\text{CO}_2\text{H}$ (Fig. 3). Unconjugated TrisMPyP- $\Phi\text{CO}_2\text{H}$ and the TrisMPyP- ΦCO -NH-mMAb E48 conjugate, which was not internalized by the cell, exhibited no phototoxicity. When coupled to cMAb U36 or mMAb

425, which were internalized by the cell after conjugation, phototoxicity was observed. These results clearly demonstrate the potency of internalizing photosensitizer-MAb conjugates and at the same time open new avenues for the therapeutic application of hydrophilic photosensitizers.

TrisMPyP- Φ CO-NH- 125 I-MAb conjugates with a molar ratio of ≤ 3 remained fully immunoreactive, while SDS-PAGE indicated that there was no aggregate formation (Fig. 2). However, the radiopharmacokinetic behavior of TrisMPyP- Φ CO-NH- 125 I-MAb conjugates in xenograft-bearing nude mice differed from that of unconjugated 125 I-MAb (Fig. 4A). For conjugates with a mean ratio of 1.2, 2.1, or 3.0, the 125 I levels in the blood at 48 h p.i. were 58%, 42%, and 26%, respectively, of that of the unconjugated 125 I-MAb. Thus, there was a strong correlation between the porphyrin:MAb ratio and blood clearance. Apparently, conjugates with a higher ratio are more susceptible to removal from the blood, which probably occurs due to hepatic extraction. We previously described similar pharmacokinetic profiles for *m*THPC-MAb conjugates with different ratios (9). Other groups have also observed a ratio-dependent blood clearance of conjugated MAbs (19-21). Tumor-to-blood ratios were the same irrespective of the sensitizer-to-MAb ratios of the different conjugates (Fig. 4B).

In our study, TrisMPyP- Φ CO $_2$ H was used as a model compound. This compound showed remarkable phototoxicity after transportation into the cell. Therefore, an interesting optimization would be to synthesize the corresponding chlorin (1 double bond in the porphyrin ring reduced) or the bacteriochlorin derivative (2 double bonds in the porphyrin ring reduced) of TrisMPyP- Φ CO $_2$ H. Reduction of a double bond shifts the absorption maximum to a longer wavelength, making the sensitizer also suitable for treatment of larger tumors. Another possibility is to use sensitizers with optimal photochemical characteristics that are readily available at the moment but, due to their hydrophilic nature, demonstrate limited therapeutic efficacy when applied as free agents in PDT. In this respect, one of the most promising candidate sensitizers is phthalocyanine tetrasulphonate. Studies on coupling of this photosensitizer to internalizing tumor-selective MAbs and therapeutic evaluation of these conjugates are ongoing in our laboratories.

REFERENCES

1. Weishaupt, K. R., Gomer, C. J., and Dougherty, T. J. Identification of singlet oxygen as the cytotoxic agent in photoinactivation of a murine tumor. *Cancer Res.*, *36*: 2326-2329, 1976.
2. Penning, L. C., Tijssen, K., Boegheim, J. P. J., van Steveninck, J., and Dubbelman, T. M. A. R. Relationship between photodynamically induced damage to various cellular parameters and loss of clonogenicity in different cell types with hematoporphyrin derivative as sensitizer. *Biochim. Biophys. Acta*, *1221*: 250-258, 1994.
3. Henderson, B. W., Waldow, S. M., Mang, T. S., Potter, W. R., Malone, P. B., and Dougherty, T. J. Tumor destruction and kinetics of tumor cell death in two experimental mouse tumors following photodynamic therapy. *Cancer Res.*, *45*: 572-576, 1985.
4. Kros, G., Korbek, M., and Dougherty, G. J. Induction of immune cell infiltration into murine SCCVII tumour by Photofrin-based photodynamic therapy. *Br. J. Cancer*, *71*: 549-555, 1995.
5. Fromm, D., Kessel, D., and Webber, J. Feasibility of photodynamic therapy using endogenous photosensitization for colon cancer. *Arch. Surg.*, *131*: 667-669, 1996.
6. Nseyo, U. O., and Lamm, D. L. Therapy of superficial bladder cancer. *Sem. Oncol.*, *23*: 598-604, 1996.
7. Furuse, K., Fukuoka, M., Kato, H., Horai, T., Kubota, K., Kodama, N., Kusunoki, Y., Takifuji, N., Okunaka, T., Konaka, C., Wada, H., and Hayata, Y. A prospective phase II study on photodynamic therapy with Photofrin II for centrally located early-stage lung cancer. *J. Clin. Oncol.*, *11*: 1852-1857, 1993.
8. Savary, J-F., Monnier, P., Fontollet, C., Mizeret, J., Wagnières, G., Braichotte, D., and van den Bergh, H. Photodynamic therapy for early squamous cell carcinomas of the esophagus, bronchi, and mouth with *meta*-tetrahydroxyphenylchlorin. *Arch. Otolaryngol. Head Neck Surg.*, *123*: 162-168, 1997.
9. Vrouenraets, M. B., Visser, G. W. M., Stewart, F. A., Stigter, M., Oppelaar, H., Postmus, P. E., Snow, G. B., and van Dongen, G. A. M. S. Development of *meta*-tetrahydroxyphenylchlorin-mono-clonal antibody conjugates for photoimmunotherapy. *Cancer Res.*, *59*: 1505-1513, 1999.
10. Casas, C., Saint-Jalmes, B., Loup, C., Lacey, C. J., and Meunier, B. Synthesis of cationic metalloporphyrin precursors related to the design of DNA cleavers. *J. Org. Chem.*, *58*: 2913-2917, 1993.
11. Schrijvers, A. H. G. J., Quak, J. J., Uytendinck, A. M., van Walsum, M., Meijer, C. J. L. M., Snow, G. B., and van Dongen, G. A. M. S. MAb U36, a novel monoclonal antibody successful in immunotargeting of squamous cell carcinoma of the head and neck. *Cancer Res.*, *53*: 4383-4390, 1993.
12. Murthy, U., Basu, A., Rodeck, U., Herlyn, M., Ross, A. H., and Das, M. Binding of an antagonistic monoclonal antibody to an intact and fragmented EGR-receptor polypeptide. *Arch. Biochem. Biophys.*, *252*: 549-560, 1987.
13. Stanton, P., Richards, S., Reeves, J., Nikolic, M., Edington, K., Clark, L., Robertson, G., Souter, D., Mitchell, R., Hendler, F. J., Cooke, T., Parkinson, E. K., and Ozanne, B. W. Epidermal growth factor

- receptor expression by human squamous cell carcinomas of the head and neck, cell lines and xenografts. *Br. J. Cancer*, 70: 427-433, 1994.
14. Quak, J. J., van Dongen, G. A. M. S., Balm, A. J. M., Brakkee, J. P. G., Scheper, R. J., Snow, G. B., and Meijer, C. J. L. M. A 22-kDa surface antigen detected by monoclonal antibody E48 is exclusively expressed in stratified squamous and transitional epithelia. *Am. J. Pathol.*, 136: 191-197, 1990.
 15. Skehan, P., Storeng, R., Scudiero, D., Monks, A., McMahon, J., Vistica, D., Warren, J. T., Bokesch, H., Kenney, S., and Boyd, M. R. New colorimetric cytotoxicity assay for anticancer-drug screening. *J. Natl. Cancer Inst.*, 82: 1107-1112, 1990.
 16. Van Gog, F. B., Visser, G. W. M., Gowrising, R. W., Snow, G. B., and van Dongen, G. A. M. S. Synthesis and evaluation of ^{99m}Tc/⁹⁹Tc-MAG3-biotin conjugates for antibody pretargeting strategies. *Nucl. Med. Biol.*, 25: 611-619, 1998.
 17. Van Gog, F. B., Visser, G. W. M., Stroomer, J. W., Roos, J. C., Snow, G. B., and van Dongen, G. A. M. S. High dose rhenium-186-labeling of monoclonal antibodies for clinical application: pitfalls and solutions. *Cancer*, 80: 2360-2370, 1997.
 18. Folli, S., Westermann, P., Braichotte, D., Pèlerin, A., Wagnières, G., van den Bergh, H., and Mach, J.-P. Antibody-indocyanin conjugates for immunodetection of human squamous cell carcinoma in nude mice. *Cancer Res.*, 54: 2643-2649, 1994.
 19. Boniface, G. R., Izard, M. E., Walker, K. Z., McKay, D. R., Soby, P. J., Turner, J. H., and Morris, J. G. Labeling of monoclonal antibodies with Samarium-153 for combined radioimmunoscintigraphy and radioimmunotherapy. *J. Nucl. Med.*, 30: 683-691, 1989.
 20. Smith, A., Zangemeister-Wittke, U., Waibel, R., Schenker, T., Schubiger, P. A., and Stahel, R. A. A comparison of ⁶⁷Cu- and ¹³¹I-labeled forms of monoclonal antibodies SEN7 and SWA20 directed against small-cell lung cancer. *Int. J. Cancer*, 8: 43-48, 1994.
 21. Van Gog, F. B., Visser, G. W. M., Klok, R., van der Schors, R., Snow, G. B., and van Dongen, G. A. M. S. Monoclonal antibodies labeled with Rhenium-186 using the MAG3 chelate: relationship between the number of chelated groups and biodistribution characteristics. *J. Nucl. Med.*, 37: 352-362, 1996.

Chapter 4

**TARGETING OF ALUMINIUM (III) PHTHALOCYANINE
TETRASULFONATE BY USE OF
INTERNALIZING MONOCLONAL ANTIBODIES:
IMPROVED EFFICACY IN PHOTODYNAMIC THERAPY**

Maarten B. Vrouenraets, Gerard W.M. Visser, Marijke Stigter,
Hugo Oppelaar, Gordon B. Snow and Guus A.M.S. van Dongen

Cancer Research, 61: 1970-1975, 2001

ABSTRACT

The use of monoclonal antibodies (MAbs) directed against tumor-associated antigens for targeting of photosensitizers is an interesting option to improve the selectivity of photodynamic therapy (PDT). Hydrophilic photosensitizers are most suitable for conjugation to MAbs because of their water solubility. The photosensitizer aluminium (III) phthalocyanine tetrasulfonate (AlPc(SO₃H)₄) has many ideal photochemical properties; however, because of its hydrophilicity, the free form of this sensitizer does not readily reach the critical intracellular target and, therefore, is ineffective in PDT. On the basis of our previous studies, we hypothesized that AlPc(SO₃H)₄ might be suitable for PDT when coupled to internalizing tumor-selective MAbs.

In this study, a reproducible procedure is presented for coupling of AlPc(SO₃H)₄ to MAbs via the tetra-glycine derivative AlPc(SO₂N_{gly})₄. Conjugation was performed to chimeric MAb U36 and murine MAbs E48 and 425 using a labile ester. Conjugates showed preservation of integrity and immunoreactivity and full stability in serum *in vitro*. At molar ratios >4, the solubility of the conjugates decreased. Data on the *in vitro* efficacy of PDT showed that in the chosen experimental setup the internalizing AlPc(SO₂N_{gly})₄-mMAb 425 conjugate was about 7500 times more toxic to A431 cells than the free sensitizer (IC₅₀s, 0.12 nM *versus* 900 nM). The AlPc(SO₂N_{gly})₄-mMAb 425 conjugate was also more toxic than *meta*-tetrahydroxyphenylchlorin (*m*THPC)-mMAb 425 conjugates and free *m*THPC that had been tested previously (Chapter 2) in the same system (IC₅₀s, 7.3 nM and 2.0 nM, respectively). Biodistribution analysis of AlPc(SO₂N_{gly})₄-¹²⁵I-cMAb U36 conjugates with different sensitizer:MAb ratios in squamous cell carcinoma-bearing nude mice revealed selective accumulation in the tumor, although to a lesser extent than for the unconjugated ¹²⁵I-cMAb U36, whereas tumor:blood ratios were similar. These findings indicate that AlPc(SO₃H)₄ has high potential for use in PDT when coupled to internalizing tumor-selective MAbs.

INTRODUCTION

The use of monoclonal antibodies (MAbs) directed against tumor-associated antigens for selective targeting of photosensitizers is an interesting option. This approach should selectively increase the photosensitizer concentration in tumors. If this also translates to an

increased photodynamic effect, this could be a major advantage for photodynamic therapy (PDT) of large surface areas where normal tissue toxicity becomes dose limiting. Expression of tumor-associated antigens on normal tissues is limited; therefore, it can be anticipated that these tissues will be spared when using MAb-conjugated photosensitizers.

In a series of studies on photoimmunoconjugates, we started with the development of *meta*-tetrahydroxyphenylchlorin (*m*THPC)-MAb conjugates for PDT of squamous cell carcinoma (SCC) (1). *m*THPC was selected because in free form it is considered to be one of the most potent and promising photosensitizers for clinical use. Biodistribution analysis in tumor-bearing nude mice showed that the tumor selectivity of *m*THPC was improved by coupling to tumor-selective MAbs. Furthermore, *m*THPC-MAb conjugates were effective in *in vitro* photoimmunotherapy of A431 cells, although less effective than the free sensitizer (IC₅₀s, 7.3 *versus* 2 nM). Importantly, efficacy was only observed when *m*THPC-MAb conjugates were internalized, which was a strong indication that the critical target for photodynamic damage is localized intracellularly. A serious problem in the development of these conjugates was the poor water solubility of *m*THPC.

For coupling to MAbs, photosensitizers more hydrophilic than *m*THPC would be much more suitable. As free compounds, such photosensitizers are ineffective because of their inability to enter the tumor cell, but, coupled to internalizing MAbs, phototoxicity can be enhanced, as we recently described in our study on the hydrophilic sensitizer 5-[4-[5-(carboxyl)-1-butoxy]phenyl]-10,15,20-tris-(4-methylpyridiniumyl)porphyrin Iodide (2). This sensitizer was selected as a conceptual model compound because of its hydrophilicity. Its photochemical properties make the photosensitizer of limited value for clinical photoimmunotherapy. It is excited with light of 595 nm (with a very low ϵ of $7.0 \times 10^3 \text{ M}^{-1} \text{ cm}^{-1}$), and light of this short wavelength is not suitable for treatment of larger tumors because it hardly penetrates into tissue.

In the present study, the concept of using internalizing MAbs for photoimmunotherapy with hydrophilic sensitizers is further investigated by using a more suitable photosensitizer, aluminium (III) phthalocyanine tetrasulfonate (AlPc(SO₃H)₄). Within the family of sulfonated phthalocyanines, which can have a sulfonation degree from 0 up to 4, this compound is the most hydrophilic member. Because phthalocyanines have a strong absorption maximum at about 675 nm ($\epsilon = 1.7 \times 10^5 \text{ M}^{-1} \text{ cm}^{-1}$), they can be used for treatment of larger tumors.

Several conjugation procedures for phthalocyanine-MAb conjugates have been described previously. In 1994, Morgan *et al.* described the coupling of AlPc(SO₃H)₄ to MAb

E7 via $\text{AlPc}(\text{SO}_2\text{Cl})_4$ (3). Very recently, Carcenac *et al.* reported on the preparation of $\text{AlPc}(\text{SO}_3\text{H})_4$ -MAB 35A7 conjugates via a mono five-carbon spacer chain (4). Both groups observed limited phototoxicity of their conjugates in PDT *in vitro*.

In this study, we describe a reproducible procedure for conjugation of $\text{AlPc}(\text{SO}_3\text{H})_4$ as the tetra-glycine derivative. The modified sensitizer was coupled to MABs selectively reactive with SCC. The *in vitro* photodynamic efficacy of the photosensitizer, both in free form and coupled to internalizing SCC-selective MABs, was studied. Biodistribution analysis of the conjugates was performed in SCC-bearing nude mice.

MATERIALS AND METHODS

Sensitizer

Aluminium (III) phthalocyanine tetrasulfonate chloride ($\text{AlPc}(\text{SO}_3\text{H})_4$; Fig. 1, *scheme 1*; M_r 895.19) was obtained from Porphyrin Products (Logan, UT).

Monoclonal antibodies

Selection, production, and characterization of murine MAB (mMAB) U36 directed against CD44v6 (5), its chimeric (mouse/human) IgG1 derivative (cMAB U36), the IgG2a mMAB 425 directed against the epidermal growth factor receptor (EGFR) (6,7), and the IgG1 mMAB E48 directed against a M_r 16,000-22,000 glycosylphosphatidylinositol-anchored surface antigen (8) have been described before.

Cell lines

The HNSCC cell lines UM-SCC-11B and UM-SCC-22A (kindly provided by Dr. T.E. Carey, University of Michigan, Ann Arbor, MI) were cultured under 5% CO_2 at 37°C in Dulbecco's modified Eagle's medium (DMEM; BioWhittaker, Alkmaar, the Netherlands) supplemented with 2 mM L-glutamine, 5% FCS (BioWhittaker), and 25 mM HEPES. The vulvar SCC cell line A431 was cultured under the same conditions.

Analyses

The absorption of free and MAB-conjugated $\text{AlPc}(\text{SO}_3\text{H})_4$ was measured using an Ultrospec III spectrophotometer (Pharmacia Biotech, Roosendaal, the Netherlands). The sensitizer concentration in the conjugate preparations was assessed with the same apparatus at

a wavelength of 351 nm. The absorption of a range of dilutions (1-9 $\mu\text{g}/\text{ml}$) of $\text{AlPc}(\text{SO}_3\text{H})_4$ in H_2O was measured and graphically depicted using the least square method. The sensitizer concentration in the conjugate preparations was determined using this calibration curve.

HPLC analysis during the several modification reactions of the starting compound $\text{AlPc}(\text{SO}_3\text{H})_4$ was performed using an LKB 2150 HPLC-pump (Pharmacia Biotech), an LKB 2152 LC controller (Pharmacia Biotech) and a 25-cm Lichrosorb 10 RP 18 column (Chrompack, Middelburg, The Netherlands). Two eluentia were used: eluent A, consisting of a 5:95 (v/v) mixture of ethanol and 0.01 M sodium phosphate buffer (pH 6), and eluent B, consisting of a 9:1 (v/v) mixture of methanol and H_2O . A gradient was used in which eluent A was gradually replaced by eluent B. The gradient (flow rate, 1 ml/min) was as follows: 5 min, 100% eluent A; linear increase of eluent B to 100% during 10 min; 10 min, 100% eluent B. Absorption was measured at 210 and 351 nm by a Pharmacia LKB VWM 2141 UV detector.

For HPLC analysis of phthalocyanine- ^{125}I -MAB conjugates, an LKB 2150 HPLC-pump, an LKB 2152 LC controller, and a 10 x 300-mm Superdex 200 HR 10/30 column (Pharmacia Biotech) were used. The eluent consisted of 0.05 M sodium phosphate/0.15 M sodium chloride (pH 6.8), and the flow rate was 0.5 ml/min. A Pharmacia LKB VWM 2141 UV detector was used at 351 nm for detection of the sensitizer, whereas radioactivity of the ^{125}I -labeled MAB was measured by an Ortec 406A single-channel analyzer connected to a Merck-Hitachi D2000 integrator (Merck, Darmstadt, Germany).

The integrity of the phthalocyanine- ^{125}I -MAB conjugates was analyzed by electrophoresis on a Phastgel System (Pharmacia Biotech) using preformed 7.5% SDS-PAGE gels under nonreducing conditions. After running, gels were exposed to a Phosphor plate for 1-3 h and analyzed with a Phosphor Imager (B&L-Isogen Service Laboratory, Amsterdam, the Netherlands) for quantitation of the radiolabeled protein bands.

^{125}I -Labeling of MABs

Labeling of MABs with ^{125}I was performed under mild conditions using Iodogen (9). One mg of MAB dissolved in 500 μl of PBS (pH 7.4) and 1-2 mCi ^{125}I (100 mCi/ml; Amersham, Aylesbury, England) were mixed in a vial coated with 50 μg of Iodogen. After 5-min incubation at room temperature, the reaction mixture was filtered through a 0.22 μM Acrodisc filter (Gelman Sciences, Inc., Ann Arbor, MI) and unbound ^{125}I was removed using a PD-10 column (Pharmacia Biotech) with 0.9% NaCl as eluent. After removal of unbound ^{125}I , the radiochemical purity always exceeded 98% (HPLC analysis).

Preparation of $\text{AlPc}(\text{SO}_2\text{NHCH}_2\text{CO-TFP})_4$ ester

The synthesis of the phthalocyanine derivatives and subsequent conjugation reaction were carried out in the dark and under N_2 to prevent any unwanted photochemical reactions.

Preparation of the ester was performed in three steps. The first step was the synthesis of the tetrasulfonylchloride $\text{AlPc}(\text{SO}_2\text{Cl})_4$ (Fig. 1, *scheme 2*; Ref. 10). For this, 250 mg (0.28 mmol) of $\text{AlPc}(\text{SO}_3\text{H})_4$ were stirred together with 3.0 ml (41 mmol) of thionylchloride (SOCl_2 ; Sigma-Aldrich, Zwijndrecht, the Netherlands) and 100 μl of DMF for 2 h at 80°C . The solution was then cooled to 0°C and added to 7 ml of ice water (3.8% NaCl). The temperature was kept at 0°C . The precipitated $\text{AlPc}(\text{SO}_2\text{Cl})_4$ was filtered off and washed with ice water. The product was dried *in vacuo* over P_2O_5 at room temperature.

In the next step, the tetracarboxylic acid $\text{AlPc}(\text{SO}_2\text{NHCH}_2\text{COOH})_4$ (Fig. 1, *scheme 3*) was prepared *in situ* as follows. To 7.0 mg (7.2 μmol) of $\text{AlPc}(\text{SO}_2\text{Cl})_4$, dissolved in 1 ml of DMF, 14.4 mg (0.19 mmol) of glycine and 65 μl (0.26 mmol) of N,O-bis(trimethylsilyl)acetamide (BTA; Sigma-Aldrich) were added (11). The mixture was stirred at room temperature for 48 h before adding 500 μl of water to quench all of the reactive intermediates and stop the reaction.

Hereafter, the four carboxylic acid groups were esterified using an excess of 2,3,5,6-tetrafluorophenol (TFP; Janssen Chimica, Beerse, Belgium). To 100 μl of the crude $\text{AlPc}(\text{SO}_2\text{NHCH}_2\text{COOH})_4$ solution (containing 460 nmol), 700 μl of water, 200 μl (0.12 mmol) of a TFP solution (100 mg/ml in MeCN/ H_2O 9/1, v/v), and 50 mg (0.26 mmol) of solid 1-ethyl-3-(3-dimethylaminopropyl)-carbodiimide solution (EDC; Janssen Chimica) were added. During 30 min stirring, the $\text{AlPc}(\text{SO}_2\text{NHCH}_2\text{CO-TFP})_4$ ester (Fig. 1, *scheme 4*) precipitated. After centrifugation, the supernatant was removed, and the product was washed twice with 5 ml H_2O at 4°C , followed by drying *in vacuo* over P_2O_5 . The ester was dissolved in 250 μl MeCN, analyzed by HPLC, and the concentration was determined by absorption measurement.

Preparation of $\text{AlPc}(\text{SO}_2\text{NHCH}_2\text{COOH})_3\text{SO}_2\text{NHCH}_2\text{CONH-}^{125}\text{I-MAb}$ conjugates

For conjugation, chosen ester aliquots (containing 10 to 45 nmol ester) in MeCN were added to 1 mg of ^{125}I -labeled MAb dissolved in 1 ml 0.9% NaCl (pH 9.5). After 30 min-incubation, the $\text{AlPc}(\text{SO}_2\text{NHCH}_2\text{COOH})_3\text{SO}_2\text{NHCH}_2\text{CONH-}^{125}\text{I-MAb}$ conjugate (Fig. 1, *scheme 5*) was purified on a PD-10 column with 0.9% NaCl as the eluent. The integrity of the conjugate was analyzed by HPLC and gel electrophoresis as described above.

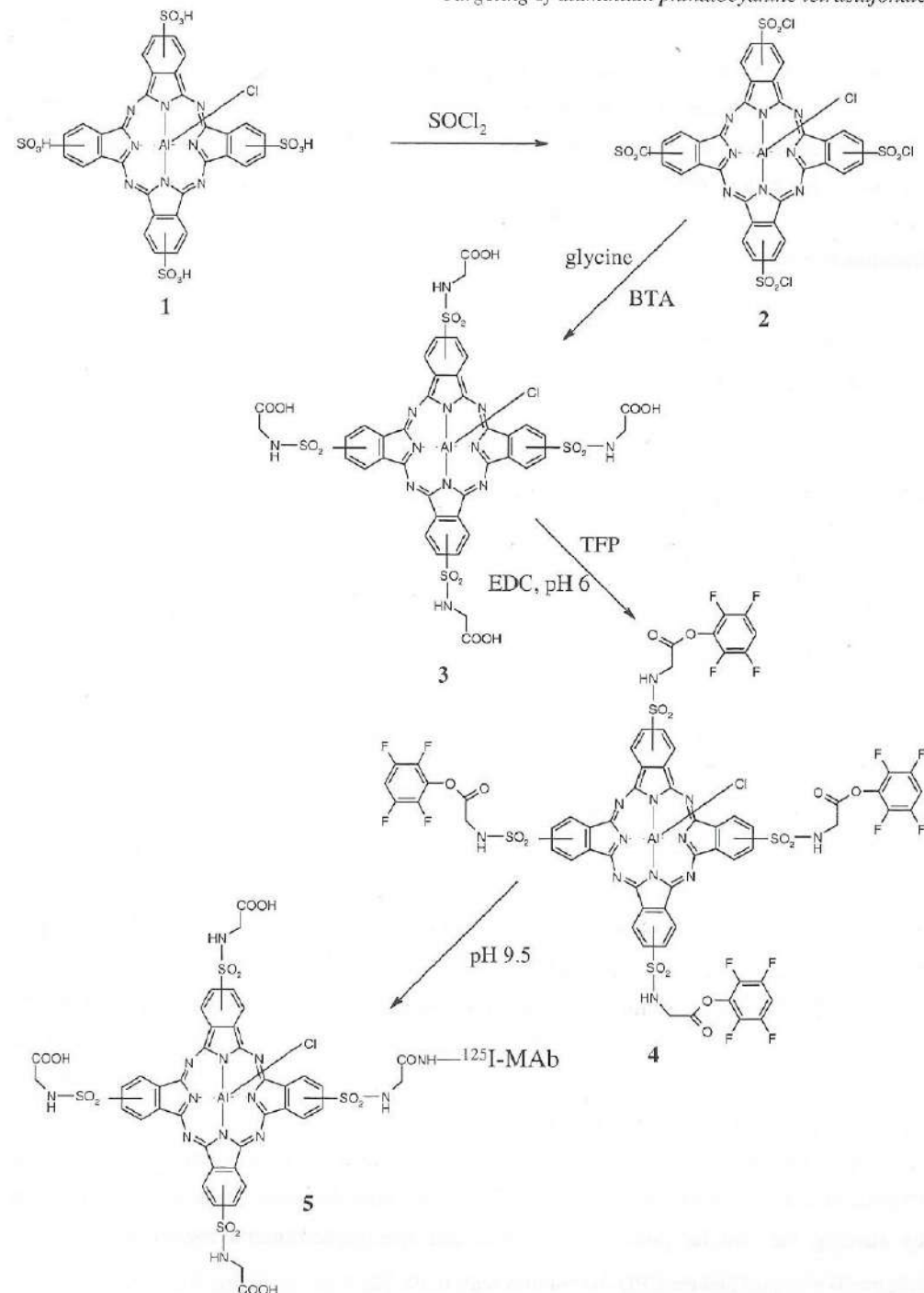


Figure 1. Schematic representation of the synthesis of $\text{AlPc}(\text{SO}_2\text{NHCH}_2\text{COOH})_4$ via $\text{AlPc}(\text{SO}_2\text{Cl})_4$, its esterification, and conjugation to a ^{125}I -labeled MAb.

In vitro stability of $\text{AlPc}(\text{SO}_2\text{N}_{\text{gly}})_4$ - ^{125}I -MAB conjugates¹

For measurement of the serum stability of the $\text{AlPc}(\text{SO}_2\text{N}_{\text{gly}})_4$ - ^{125}I -MAB conjugates, 15 μg of conjugate in 25 μl 0.9% NaCl were added to 25 μl of human serum. After incubation for 24 h at 37°C, samples were analyzed with HPLC at 280 and 351 nm.

Immunoreactivity of $\text{AlPc}(\text{SO}_2\text{N}_{\text{gly}})_4$ - ^{125}I -MAB conjugates

In vitro binding characteristics of $\text{AlPc}(\text{SO}_2\text{N}_{\text{gly}})_4$ - ^{125}I -MAB conjugates were determined in an immunoreactivity assay as described previously (1) and compared with those of the unconjugated ^{125}I -MAB. UM-SCC-11B cells were used for binding assays with cMAB U36, A431 cells for mMAB 425, and UM-SCC-22A cells for mMAB E48.

Internalization of $\text{AlPc}(\text{SO}_2\text{N}_{\text{gly}})_4$ - ^{125}I -MAB conjugates

In vitro experiments to determine the internalization of $\text{AlPc}(\text{SO}_2\text{N}_{\text{gly}})_4$ - ^{125}I -cMAB U36, $\text{AlPc}(\text{SO}_2\text{N}_{\text{gly}})_4$ - ^{125}I -mMAB 425, and $\text{AlPc}(\text{SO}_2\text{N}_{\text{gly}})_4$ - ^{125}I -mMAB E48 conjugates by A431 cells were performed exactly as described previously (2). For this purpose, the MABs were labeled with 2 mCi ^{125}I /mg MAB, and conjugates with a sensitizer:MAB ratio of 2:1 were synthesized.

Photoimmunotherapy *in vitro*

In vitro PDT experiments were performed to determine the phototoxicity of free $\text{AlPc}(\text{SO}_3\text{H})_4$ and cMAB U36-conjugated, mMAB 425-conjugated, and mMAB E48-conjugated $\text{AlPc}(\text{SO}_3\text{H})_4$. The toxicity was determined using the SRB (Sigma Chemical Co.) assay, which measures the cellular protein content, as follows (12). A431 cells were plated in 96-well plates (750 cells/well) and grown for 3 days before incubating with $\text{AlPc}(\text{SO}_3\text{H})_4$ or $\text{AlPc}(\text{SO}_2\text{N}_{\text{gly}})_4$ -MAB conjugates (range, 0.1 nM-1.0 μM $\text{AlPc}(\text{SO}_3\text{H})_4$ equivalents) in DMEM supplemented with 2 mM L-glutamine, 5% FCS, and 25 mM HEPES at 37°C. After 20 h, remaining unbound $\text{AlPc}(\text{SO}_3\text{H})_4$ and $\text{AlPc}(\text{SO}_2\text{N}_{\text{gly}})_4$ -MAB conjugates were removed by washing twice with medium. Fresh medium was added, and cells were illuminated at 675 nm with a Spectra Physics dye laser (model 373) pumped by a 12-W argon laser (Spectra Physics model 171) at a dose of 25 J/cm^2 . Three days after illumination, growth was assessed by staining the cellular proteins with SRB and spectrophotometric measurement of the

absorption at 540 nm with a microplate reader. As a control, cells were illuminated in the absence of $\text{AlPc}(\text{SO}_3\text{H})_4$ or MAB-conjugated $\text{AlPc}(\text{SO}_3\text{H})_4$.

Biodistribution studies

The biodistribution of unconjugated ^{125}I -cMAB U36 and $\text{AlPc}(\text{SO}_2\text{N}_{\text{gly}})_4$ - ^{125}I -cMAB U36 conjugates with different sensitizer:MAB ratios was determined in nude mice bearing s.c. xenografts of the HNSCC cell line HNX-OE. Tumor size ranged from 50 to 100 mm^3 . The ^{125}I -MAB preparations were injected i.v. in 100 μl of 0.9% NaCl. At 48 h p.i., mice were anesthetized, bled, killed, and dissected. The organs were removed and weighed. The amount of γ -emitting radioactivity in organs and blood was measured in a gamma counter (LKB-Wallac, 1282 CompuGamma; Pharmacia, Woerden, the Netherlands). Radioactivity uptake in the tissues was expressed as the %ID/g of tissue. Tumor:nontumor ratios were also calculated.

RESULTS

Preparation of $\text{AlPc}(\text{SO}_2\text{NHCH}_2\text{CO-TFP})_4$ ester

The first step in the synthesis of the ester was the preparation of the tetrasulfonylchloride $\text{AlPc}(\text{SO}_2\text{Cl})_4$ (Fig. 1, *scheme 2*) by stirring the starting compound $\text{AlPc}(\text{SO}_3\text{H})_4$ (Fig. 1, *scheme 1*) in ~150-fold excess of liquid SOCl_2 for 2 h at 80°C. After work-up, the product was isolated in a yield of about 80%.

In the next step, the $\text{AlPc}(\text{SO}_2\text{Cl})_4$ was converted to its tetra-glycine derivative $\text{AlPc}(\text{SO}_2\text{NHCH}_2\text{COOH})_4$ (Fig. 1, *scheme 3*) in DMF using a large excess of glycine and N,O-bis(trimethylsilyl)acetamide (BTA). The use of BTA to dissolve glycine in DMF by means of conversion into the corresponding disilylated intermediate has been described by Dressman *et al.* (11). After addition of water, the crude reaction mixture was esterified during 30 min using a large excess of TFP and EDC at pH 5.8. After thorough washing of the resulting precipitate with H_2O (which removed acetamide, trimethylsilylhydroxide, EDC, TFP, glycine-TFP ester, and the partially hydrolyzed sensitizer derivatives), the $\text{AlPc}(\text{SO}_2\text{NHCH}_2\text{CO-TFP})_4$ ester (Fig. 1, *scheme 4*) was isolated in a yield of 45% \pm 5%. This tetra-ester was found to hydrolyze relatively easily. HPLC analysis at 351 nm (Fig. 2) revealed that hydrolysis had occurred during the washing step, resulting in a product mixture consisting of 80% $\text{AlPc}(\text{SO}_2\text{NHCH}_2\text{CO-TFP})_4$ (HPLC retention time, 16.3 min), 20%

¹ $\text{AlPc}(\text{SO}_2\text{NHCH}_2\text{COOH})_3\text{SO}_2\text{NHCH}_2\text{CONH-MAB}$ conjugates are designated as $\text{AlPc}(\text{SO}_2\text{N}_{\text{gly}})_4$ -MAB conjugates if the modification of $\text{AlPc}(\text{SO}_3\text{H})_4$ is not relevant for understanding.

AlPc(SO₂NHCH₂CO-TFP)₃SO₂NHCH₂COOH (retention time, 14.4 min), and the presence of a small amount of TFP, detected at 210 nm (retention time, 5.4 min).

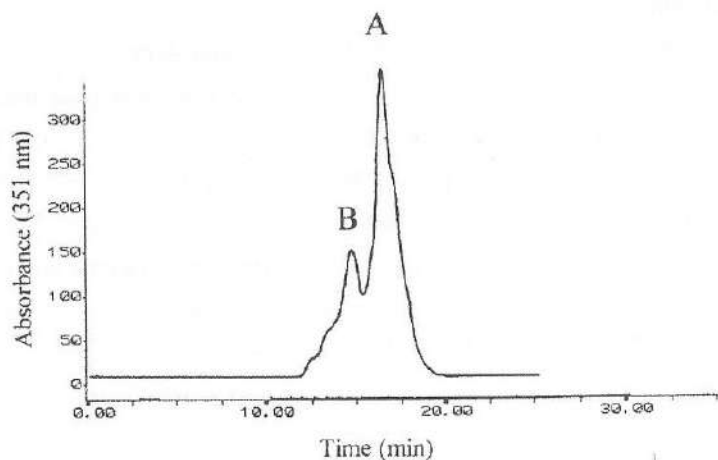


Figure 2. Hydrolysis profile of the TFP-ester of the modified tetrasulfonate phthalocyanine in MeCN/H₂O by HPLC analysis (absorbance measurement at 351 nm): AlPc(SO₂NHCH₂CO-TFP)₄ (peak A) and AlPc(SO₂NHCH₂CO-TFP)₃SO₂NHCH₂COOH (peak B).

Conjugation

The AlPc(SO₂NHCH₂CO-TFP)₄ ester was dissolved in 250 μ l of MeCN before conjugation. When 35 nmol of ester (in about 50 μ l of MeCN) were added to 6.6 nmol (1.0 mg) of ¹²⁵I-MAb in 1 ml of 0.9% NaCl, followed by incubation for 30 min at pH 9.5 and PD-10 column purification, an AlPc(SO₂NHCH₂COOH)₃SO₂NHCH₂CONH-¹²⁵I-MAb conjugate (Fig. 1, *scheme 5*) was obtained with a molar ratio of about 3.0, corresponding with a conjugation efficiency of about 55%. Purification of the conjugates on a PD-10 column also removed MeCN and TFP (13).

Under the conditions that would lead to conjugates with a ratio >4, the recovery of the ¹²⁵I-MAb from the PD-10 column dropped significantly, because the solubility of the MAb became impaired. Therefore, conjugates with a ratio above 4 were not further evaluated.

Analyses and quality control of the conjugates

The quality of the AlPc(SO₂N_{gly})₄-MAb conjugates was analyzed by HPLC and SDS-PAGE analysis. HPLC analysis of a AlPc(SO₂N_{gly})₄-¹²⁵I-cMAb U36 conjugate, with UV

detection at 351 nm for detection of the sensitizer and radioactivity measurement for detection of the ¹²⁵I-labeled MAb, showed the conjugate to be eluted as a monomeric peak. All of the sensitizer was confined to the MAb, whereas the recovery of the radioactivity from the column was >95%.

Figure 3 shows the results of the SDS-PAGE and subsequent Phosphor Imager quantitation of an AlPc(SO₂N_{gly})₄-¹²⁵I-cMAb U36 conjugate (Fig. 3, A and C) with unconjugated ¹²⁵I-cMAb U36 (Fig. 3, B and D) as a control. In both cases, a single radiolabeled protein band was observed with an apparent molecular weight of \pm 150,000 (deduced from SDS-PAGE analysis; data not shown).

The AlPc(SO₂N_{gly})₄-cMAb U36 conjugate was incubated in human serum for 24 h at 37°C for determination of the serum stability of the SO₂-N_{gly} bond. HPLC analysis at 280 and 351 nm revealed that the HPLC profiles were identical to that at the start of the incubation, indicating that the conjugate was fully stable in human serum.

Cell-binding assays were performed to determine whether the coupling of AlPc(SO₃H)₄ influenced the immunoreactivity of cMAb U36, mMAb 425, or mMAb E48. For all of the conjugates studied (sensitizer:MAb ratios of 1:1 to 4:1), the immunoreactivity was the same as for their corresponding ¹²⁵I-MAbs (85-90%).

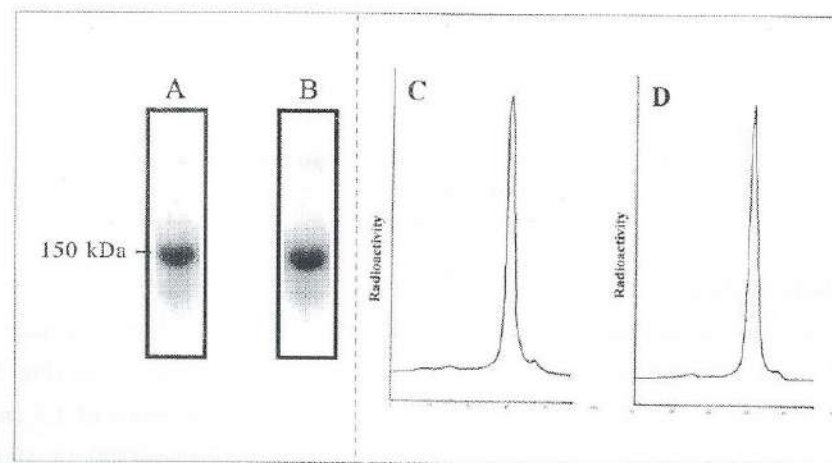


Figure 3. SDS-PAGE and Phosphor Imager analysis of a AlPc(SO₂N_{gly})₄-¹²⁵I-cMAb U36 conjugate with sensitizer:MAb ratio 2 (A and C) and unconjugated ¹²⁵I-cMAb U36 as a control (B and D). The 150 kDa-band contained 93% (C) and 94% (D) of the total amount of radioactivity.

Internalization of $\text{AlPc}(\text{SO}_2\text{N}_{\text{gly}})_4$ - ^{125}I -MAB conjugates

Internalization experiments were performed to determine whether the $\text{AlPc}(\text{SO}_2\text{N}_{\text{gly}})_4$ - ^{125}I -cMAB U36, $\text{AlPc}(\text{SO}_2\text{N}_{\text{gly}})_4$ - ^{125}I -mMAB 425, and $\text{AlPc}(\text{SO}_2\text{N}_{\text{gly}})_4$ - ^{125}I -mMAB E48 conjugates were internalized by the A431 cells. Within our experimental setup, $54.3 \pm 2.3\%$ (1.0×10^6 sensitizer molecules/cell), $36.6 \pm 0.9\%$ (1.1×10^6 sensitizer molecules/cell), and $31.6 \pm 0.5\%$ (mean \pm SD) internalization (0.65×10^6 sensitizer molecules/cell) was observed for ^{125}I -cMAB U36, ^{125}I -mMAB 425, and ^{125}I -mMAB E48 conjugates, respectively. The addition of excess naked MAB totally blocked binding.

Photoimmunotherapy *in vitro*

The phototoxicity of unconjugated $\text{AlPc}(\text{SO}_3\text{H})_4$ and cMAB U36-conjugated, mMAB 425-conjugated, and mMAB E48-conjugated $\text{AlPc}(\text{SO}_3\text{H})_4$, with a molar ratio of 2, was assessed in A431 cells using the SRB assay. The results are depicted in Figure 4. The IC_{50} of the free sensitizer was 900 nM. When coupled to the MABs U36, 425, or E48, the sensitizer showed an increased photodynamic efficacy. The mMAB 425-conjugated $\text{AlPc}(\text{SO}_2\text{N}_{\text{gly}})_4$ showed the highest phototoxicity with an IC_{50} of 0.12 nM. At sensitizer concentrations from 1 nM up to 1 μM , PDT resulted in cell killing [lower absorption than at the day of illumination (day 0)]. The efficacies of PDT with cMAB U36-conjugated (IC_{50} , 1.6 nM) and mMAB E48-conjugated (IC_{50} , 32 nM) $\text{AlPc}(\text{SO}_3\text{H})_4$ were less than with mMAB 425-conjugated $\text{AlPc}(\text{SO}_3\text{H})_4$, but were still much greater than for the free sensitizer.

Conjugated and free $\text{AlPc}(\text{SO}_3\text{H})_4$ appeared to be nontoxic without illumination. The unconjugated MABs did not result in growth inhibition with or without illumination (data not shown).

Biodistribution studies

Biodistribution analysis was performed in HNX-OE xenograft-bearing nude mice. Figure 5 shows the biodistribution data (Fig. 5A) and tumor to nontumor values (Fig. 5B) of ^{125}I -cMAB U36 and $\text{AlPc}(\text{SO}_2\text{N}_{\text{gly}})_4$ - ^{125}I -cMAB U36 conjugates with ratios of 1.2 and 2.4. The unconjugated ^{125}I -MAB (100 μg ; 10 μCi of ^{125}I) and both conjugates (100 μg ; 10 μCi of ^{125}I) were injected in three groups of six mice, and the mice were killed 48 h after injection.

The results depicted in Figure 5A show that the $\text{AlPc}(\text{SO}_2\text{N}_{\text{gly}})_4$ -conjugated ^{125}I -MABs accumulate selectively in the tumor, but the uptake is lower than for the unconjugated ^{125}I -MAB. The conjugate with the highest ratio shows the lowest tumor accumulation. The tumor

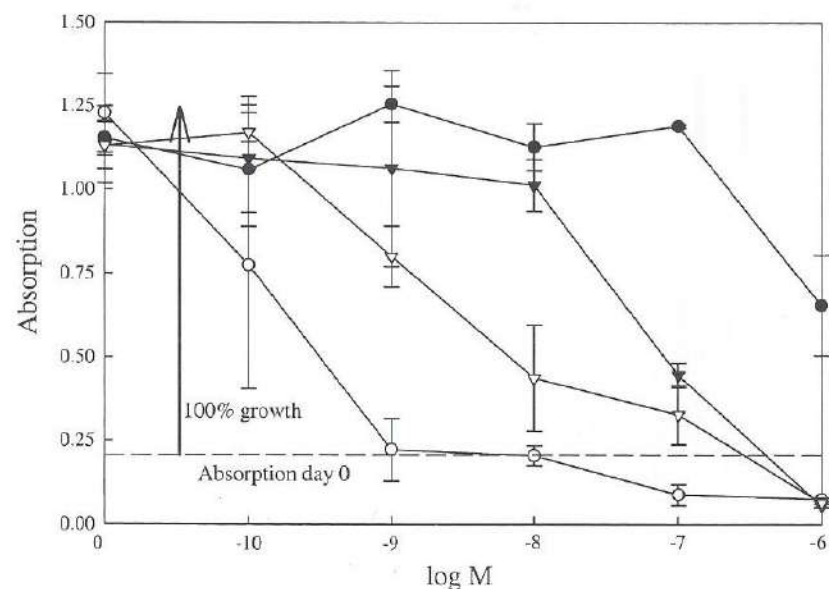


Figure 4. The antiproliferative effect of $\text{AlPc}(\text{SO}_3\text{H})_4$ and $\text{AlPc}(\text{SO}_2\text{N}_{\text{gly}})_4$ -MAB conjugates with sensitizer:MAB ratio 2 on A431 cells upon illumination with 25 J/cm^2 (SRB assay). $\text{AlPc}(\text{SO}_3\text{H})_4$ (●), $\text{AlPc}(\text{SO}_2\text{N}_{\text{gly}})_4$ -cMAB U36 (▽), $\text{AlPc}(\text{SO}_2\text{N}_{\text{gly}})_4$ -mMAB 425 (○), and $\text{AlPc}(\text{SO}_2\text{N}_{\text{gly}})_4$ -mMAB E48 (▼). Results of triplicate experiments are indicated (means \pm SD). The molarity (M; x-axis) of the free or conjugated $\text{AlPc}(\text{SO}_3\text{H})_4$ is indicated logarithmically.

uptake was 12.6, 9.6, and 6.8 %ID/g for the unconjugated ^{125}I -cMAB U36 and the conjugates with a ratio of 1.2 and 2.4, respectively. The blood values were 13.1, 10.3, and 7.7 %ID/g, respectively. Therefore, coupling of $\text{AlPc}(\text{SO}_2\text{N}_{\text{gly}})_4$ decreases the half-life of the ^{125}I -MAB in blood, resulting in a lower tumor accumulation.

Tumor:blood ratios 2 days p.i were about 0.9 for both the unconjugated ^{125}I -cMAB U36 and for the conjugates (Fig. 5B). For most organs, tumor:normal tissue ratios slightly decreased for conjugates with increasing sensitizer:MAB ratio.

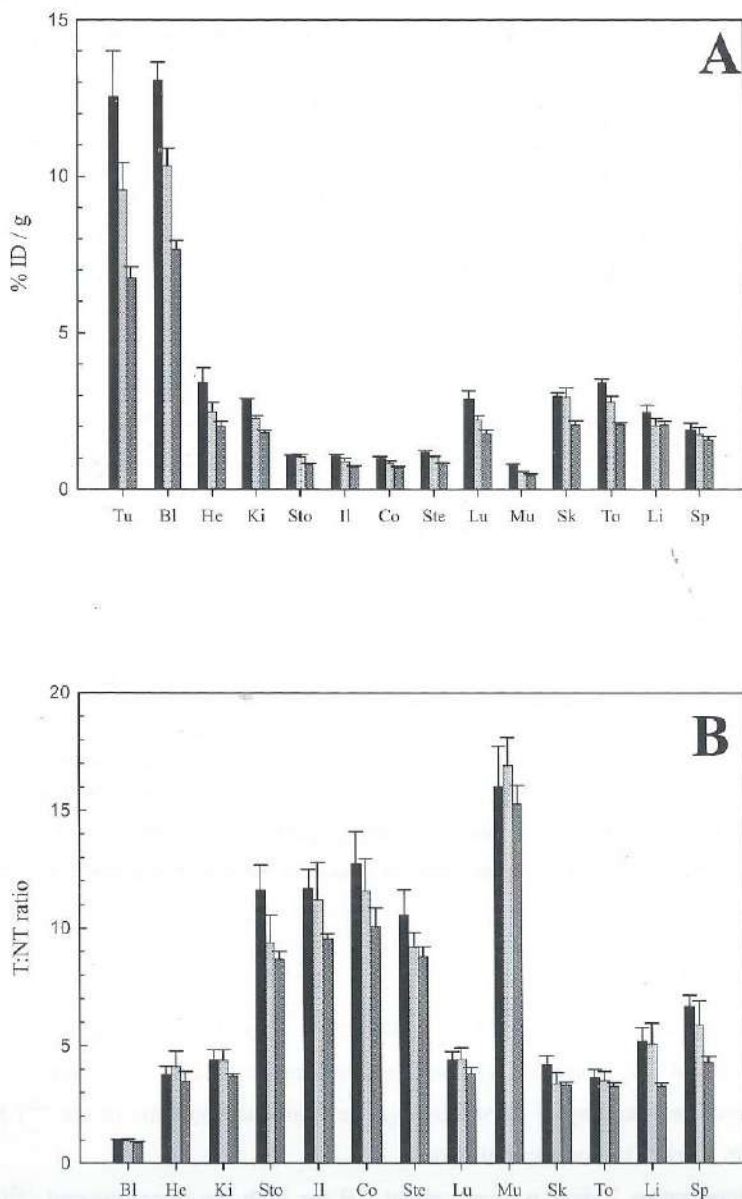


Figure 5. Biodistribution (A) and tumor to non-tumor ratios (B) of (for each set of three bars from left to right): unconjugated ^{125}I -cMab U36 and two $\text{AIPc}(\text{SO}_2\text{N}_{\text{gly}})_4$ - ^{125}I -cMab U36 conjugates with a sensitizer:MAB ratio of 1.2 and 2.4. Each preparation ($100\ \mu\text{g}$ of MAB; $10\ \mu\text{Ci}$ of ^{125}I) was intravenously injected in six HNX-OE bearing nude mice; 48 h p.i. mice were bled, sacrificed, and dissected, and the radioactivity levels (%ID/g + SE) of blood, tumor, and several organs were assessed. Tu: tumor, Bl: blood, He: heart, Ki: kidney, Sto: stomach, Il: ileum, Co: colon, Ste: sternum, Lu: lung, Mu: muscle, Sk: skin, To: tongue, Li: liver, Sp: spleen.

DISCUSSION

The photosensitizer $\text{AIPc}(\text{SO}_3\text{H})_4$ in its free form is not clinically effective because of its hydrophilicity, which hampers uptake in the tumor cells. In the present study, we showed that, because of its water solubility, $\text{AIPc}(\text{SO}_3\text{H})_4$ could easily be coupled to MABs. When coupled to internalizing MABs, conjugates were obtained that were highly effective for *in vitro* photoimmunotherapy and that resulted in selective tumor targeting in nude mice. mMAB 425-conjugated $\text{AIPc}(\text{SO}_2\text{N}_{\text{gly}})_4$ was about 7500 times more effective than the free sensitizer *in vitro* (IC_{50}s , 0.12 nM versus 900 nM). These data indicate that the sensitizer $\text{AIPc}(\text{SO}_3\text{H})_4$, although ineffective in free form, becomes highly effective in photoimmunotherapy when coupled to an internalizing tumor-selective MAB. Ineffectiveness of $\text{AIPc}(\text{SO}_3\text{H})_4$ in free form can be explained by its limited capacity to enter the cell and by the chosen experimental setup in which a washing step was performed just before illumination. In the same system, we previously tested *m*THPC-mMAB 425 conjugates and free *m*THPC. IC_{50}s for these compounds were 7.3 nM and 2.0 nM, respectively (1). In this case, the free sensitizer was more effective than the conjugate.

Although several attempts have been described to develop photosensitizer-MAB conjugates, clinically effective conjugates have not been produced thus far. The group of Hasan developed several conjugation procedures for the photosensitizer chlorin $_{66}$. Conjugates produced with poly-L-lysine as a linker appeared to be most promising. Biodistribution data (14) and phototoxicity studies (15) after i.p. administration of chlorin $_{66}$ -mMAB OC125 F(ab') $_2$ in a xenograft nude mouse model of ovarian cancer revealed that the conjugate was more tumor selective and phototoxic than the free sensitizer. Because complete eradication of tumor cells was not consistently found, additional refinement investigations are ongoing.

$\text{AIPc}(\text{SO}_3\text{H})_4$ lacks a functional moiety suitable for direct conjugation to MABs; therefore, the sensitizer required prior modification. To obtain a good yield (80%), the tetrasulfonylchloride $\text{AIPc}(\text{SO}_2\text{Cl})_4$ was precipitated in ice water. The water temperature was a critical parameter in this process because sulfonylchlorides are labile in water, and hydrolysis of the $\text{SO}_2\text{-Cl}$ bond readily takes place at higher temperatures. Morgan *et al.* reported on the synthesis of conjugates by direct addition of $\text{AIPc}(\text{SO}_2\text{Cl})_4$ to MABs (3). In our hands, this approach resulted in the formation of unstable conjugates.

In the second step, therefore, the SO_2Cl group was converted to $\text{SO}_2\text{NHCH}_2\text{COOH}$ so that the carboxylic acid moiety could be converted into the active TFP-ester. This TFP-ester approach was used previously for *m*THPC-MAB (1) and TrisMPyP- $\Phi\text{CO-NH-MAB}$

photoimmunoconjugates (2), and it is routinely applied in ongoing clinical radioimmunotherapy studies with ^{186}Re -MAG3-MAb conjugates. The chemistry was most straightforward when all of the four SO_2Cl groups were converted. Because glycine did not dissolve in DMF, BTA was used. The two $(\text{CH}_3)_3\text{Si}$ -groups of BTA bind to the NH_2 and COOH group of glycine (to form $\text{NHSi}(\text{CH}_3)_3$ and $\text{COOSi}(\text{CH}_3)_3$, respectively), which renders the compound soluble in DMF, whereas the silylated nitrogen is more nucleophilic, increasing the product yield.

After this reaction, the resulting product was esterified with TFP in a one-pot reaction. $\text{AlPc}(\text{SO}_2\text{NHCH}_2\text{CO-TFP})_4$ precipitated, thus providing an easy and convenient purification and isolation. This tetra-ester was found to be susceptible to hydrolysis, even under neutral conditions, but for conjugation this hydrolysis was not a problem (see below). The overall yield of these two subsequent reaction steps (45%) was reasonable.

In a previous study on the development of *m*THPC-MAb conjugates (1), we analyzed conjugate formation as a function of the number of ester groups/sensitizer molecule. When tetra-esterified *m*THPC-(TFP) $_4$ was used for conjugation, the sensitizer immediately adhered to the MAb because of its poor water solubility without forming covalent bonds. To deal with this problem, before conjugation *m*THPC-(TFP) $_4$ was partially hydrolyzed to leave a conjugation mixture mainly consisting of mono-ester and completely hydrolyzed sensitizer. In the present study, we intended to follow the same strategy for conjugation with the tetra-ester $\text{AlPc}(\text{SO}_2\text{N}_{\text{gly}}\text{-TFP})_4$, also because di-, tri-, and tetra-esters are theoretically able to cross-link MAbs. Partial hydrolysis of the $\text{AlPc}(\text{SO}_2\text{N}_{\text{gly}}\text{-TFP})_4$ ester before conjugation resulted in phthalocyanine-MAb conjugates with a conjugation efficiency of only 20%. When the more polar $\text{AlPc}(\text{SO}_2\text{N}_{\text{gly}}\text{-TFP})_4$ tetra-ester [compared with *m*THPC-(TFP) $_4$] was used without prior hydrolysis, an immediate noncovalent adherence to MAbs did not take place. Moreover, cross-linking of the MAbs did not occur as assessed by SDS-PAGE and HPLC analysis, whereas the conjugation efficiency was 55%. Apparently, with the MAb concentration used (1 mg/ml), the remaining ester groups were hydrolyzed before a second MAb molecule could bind to the sensitizer. On the basis of these results, partial hydrolysis of the ester before conjugation to the MAb was not performed.

It was possible to couple four $\text{AlPc}(\text{SO}_2\text{N}_{\text{gly}})_4$ molecules to one MAb molecule without impairment of the solubility of the resulting MAbs. Under the chemical conditions that would lead to conjugates with a higher phthalocyanine:MAb ratio, the MAbs precipitated during the conjugation. This precipitation of MAbs after conjugation of photosensitizers to lysine residues is consistent with previous observations. *m*THPC-MAb conjugates with a

ratio >4 , TrisMPyP- $\Phi\text{CO-NH-MAb}$ conjugates with a ratio >3 , and indocyanin-MAb conjugates with a ratio >2 showed the same phenomenon (1,2,16).

Although $\text{AlPc}(\text{SO}_2\text{N}_{\text{gly}})_4$ -MAb conjugates with a molar ratio of ≤ 4 showed preservation of immunoreactivity, and HPLC and SDS-PAGE analysis indicated that there was no aggregate formation, the radiopharmacokinetic behavior of these conjugates in xenograft-bearing nude mice differed from that of unconjugated ^{125}I -MAb. For conjugates with a mean ratio of 1.2 and 2.4, the ^{125}I levels in the blood at 48 h p.i. were 79 and 59%, respectively, of that of the unconjugated ^{125}I -MAb. We observed a similar ratio-dependent blood clearance for *m*THPC-MAb, TrisMPyP- $\Phi\text{CO-NH-MAb}$, $^{99\text{m}}\text{Tc}/^{99}\text{Tc}$ -MAG3-labeled and ^{186}Re -MAG3-MAb conjugates (1,2,17). Other groups have also described this phenomenon (18, 19). In view of these data, the recent results of Carcenac *et al.*, published during our ongoing studies, are remarkable (4). They reported on the coupling of $\text{AlPc}(\text{SO}_3\text{H})_4$ to MAb 35A7 via a mono five-carbon spacer chain and produced conjugates with a ratio as high as 16 in this way. These conjugates had neither impaired solubility nor impaired biodistribution characteristics.

Our data on the photodynamic efficacy of MAb- and unconjugated $\text{AlPc}(\text{SO}_3\text{H})_4$, assessed by using the SRB assay, confirmed the hypothesis that the phototoxicity of the sensitizer was increased by coupling to internalizing MAbs. The mMAb 425-conjugated compound, in particular, showed a superior phototoxicity (IC_{50} , 0.12 nM). For $(\text{AlPcS}_4\text{A}_1)_{12}$ -MAb 35A7 conjugates, Carcenac *et al.* used the MTT assay for phototoxicity measurement and found, while using a double light dose, an IC_{50} of about 350 nM (4). The low toxicity might be attributable to the fact that their conjugate did not internalize, which might also explain why the conjugate was only about five times more effective than the free sensitizer.

In conclusion, our data show that hydrophilic photosensitizers, although ineffective in free form, can be transformed into very potent antitumor agents when coupled to internalizing MAbs.

REFERENCES

1. Vrouenraets, M. B., Visser, G. W. M., Stewart, F. A., Stigter, M., Oppelaar, H., Postmus, P. E., Snow, G. B., and van Dongen, G. A. M. S. Development of *meta*-tetrahydroxyphenylchlorin-monoclonal antibody conjugates for photoimmunotherapy. *Cancer Res.*, *59*: 1505-1513, 1999.
2. Vrouenraets, M. B., Visser, G. W. M., Stigter, M., Oppelaar, H., Stewart, F. A., Snow, G. B., and van Dongen, G. A. M. S. Targeting of a hydrophylic photosensitizer by use of internalizing monoclonal antibodies: a new possibility for use in photodynamic therapy. *Int. J. Cancer*, in press, 2000.
3. Morgan, J., Lottman, H., Abbou, C. C., and Chopin, D. K. A comparison of direct and liposomal antibody conjugates of sulfonated aluminum phthalocyanines for selective photoimmunotherapy of human bladder carcinoma. *Photochem. Photobiol.*, *60*: 486-496, 1994.
4. Carcenac, M., Larroque, C., Langlois, R., van Lier, J. E., Artus, J.-C., and Pèlerin, A. Preparation, phototoxicity and biodistribution studies of anti-carcinoembryonic antigen monoclonal antibody-phthalocyanine conjugates. *Photochem. Photobiol.*, *70*: 930-936, 1999.
5. Schrijvers, A. H. G. J., Quak, J. J., Uytendinck, A. M., van Walsum, M., Meijer, C. J. L. M., Snow, G. B., and van Dongen, G. A. M. S. MAb U36, a novel monoclonal antibody successful in immunotargeting of squamous cell carcinoma of the head and neck. *Cancer Res.*, *53*: 4383-4390, 1993.
6. Murthy, U., Basu, A., Rodeck, U., Herlyn, M., Ross, A. H., and Das, M. Binding of an antagonistic monoclonal antibody to an intact and fragmented EGR-receptor polypeptide. *Arch. Biochem. Biophys.*, *252*: 549-560, 1987.
7. Rodeck, U., Herlyn, M., Herlyn, D., Molthoff, C., Atkinson, B., Varello, M., Steplewski, Z., and Koprowski, H. Tumor growth modulation by an antibody to the epidermal growth factor receptor: immunologically mediated and effector cell-independent effects. *Cancer Res.*, *47*: 3692-3696, 1987.
8. Quak, J. J., van Dongen, G. A. M. S., Balm, A. J. M., Brakkee, J. P. G., Scheper, R. J., Snow, G. B., and Meijer, C. J. L. M. A 22-kDa surface antigen detected by monoclonal antibody E48 is exclusively expressed in stratified squamous and transitional epithelia. *Am. J. Pathol.*, *136*: 191-197, 1990.
9. Haisma, H. J., Hilgers, J., and Zurawski, V. R. Iodination of monoclonal antibodies for diagnosis and therapy using a convenient one-vial method. *J. Nucl. Med.*, *27*: 1890-1895, 1986.
10. Clark, P. F., Howard, H. T., Wardleworth, J. New phthalocyanine dyestuffs. U.K. Patent 952606, 1964.
11. Dressman, B. A., Spangle, L. A., and Kaldor, S. W. Solid phase synthesis of hydantoins using a carbamate linker and a novel cyclization/cleavage step. *Tetrahedron Lett.*, *37*: 937-940, 1996.
12. Skehan, P., Storeng, R., Scudiero, D., Monks, A., McMahon, J., Vistica, D., Warren, J. T., Bokesch, H., Kenney, S., and Boyd, M. R. New colorimetric cytotoxicity assay for anticancer-drug screening. *J. Natl. Cancer Inst.*, *82*: 1107-1112, 1990.
13. Van Gog F. B., Visser G. W. M., Stroomer J. W., Roos J. C., Snow G. B., and van Dongen, G. A. M. S. High dose rhenium-186-labeling of monoclonal antibodies for clinical application: pitfalls and solutions. *Cancer* *80*: 2360-2370, 1997.
14. Duska, L. R., Hamblin, M. R., Bamberg, M. P., and Hasan, T. Biodistribution of charged F(ab')₂ photoimmunoconjugates in a xenograft model of ovarian cancer. *Br. J. Cancer*, *75*: 837-844, 1997.
15. Molpus, K. L., Hamblin, M. R., Rizvi, I., and Hasan, T. Intraperitoneal photoimmunotherapy of ovarian carcinoma xenografts in nude mice using charged photoimmunoconjugates. *Gynecol. Oncol.*, *76*: 397-404, 2000.
16. Folli, S., Westermann, P., Braichotte, D., Pèlerin, A., Wagnières, G., Van den Bergh, H., and Mach, J.-P. Antibody-indocyanin conjugates for immunodetection of human squamous cell carcinoma in nude mice. *Cancer Res.*, *54*: 2643-2649, 1994.
17. Van Gog, F. B., Visser, G. W. M., Klok, R., van der Schors, R., Snow, G. B., and van Dongen, G. A. M. S. Monoclonal antibodies labeled with Rhenium-186 using the MAG3 chelate: relationship between the number of chelated groups and biodistribution characteristics. *J. Nucl. Med.*, *37*: 352-362, 1996.
18. Boniface, G. R., Izard, M. E., Walker, K. Z., McKay, D. R., Soby, P. J., Turner, J. H., and Morris, J. G. Labeling of monoclonal antibodies with Samarium-153 for combined radioimmunoscinigraphy and radioimmunotherapy. *J. Nucl. Med.*, *30*: 683-691, 1989.
19. Smith, A., Zangemeister-Wittke, U., Waibel, R., Schenker, T., Schubiger, P. A., and Stahel, R. A. A comparison of ⁶⁷Cu- and ¹³¹I-labeled forms of monoclonal antibodies SEN7 and SWA20 directed against small-cell lung cancer. *Int. J. Cancer*, *8*: 43-48, 1994.

Chapter 5

**COMPARISON OF ALUMINIUM (III) PHTHALOCYANINE
TETRASULFONATE- AND *META*-
TETRAHYDROXYPHENYLCHLORIN-MONOCLONAL ANTIBODY
CONJUGATES FOR THEIR EFFICACY IN PHOTODYNAMIC
THERAPY *IN VITRO***

Maarten B. Vrouenraets, Gerard W.M. Visser, Marijke Stigter,
Hugo Oppelaar, Gordon B. Snow and Guus A.M.S. van Dongen

International Journal of Cancer, 98: 793-798, 2002

ABSTRACT

A challenge in photodynamic therapy (PDT) is to improve the tumor selectivity of the photosensitizers by using monoclonal antibodies (MAbs). With this aim, we developed MAb-conjugates with the hydrophobic photosensitizer *meta*-tetrahydroxyphenylchlorin (*m*THPC) and with the hydrophilic sensitizer aluminium (III) phthalocyanine tetrasulfonate (AlPcS₄). The capacity of these photoimmunoconjugates for selective targeting of squamous cell carcinoma (SCC) *in vivo* was demonstrated previously in SCC-bearing nude mice. Preliminary *in vitro* PDT studies with the vulvar SCC cell line A431 showed promising phototoxicity with both sensitizers when coupled to the internalizing MAb 425.

To rank the photosensitizers for their potential in photoimmunotherapy, we herein describe an extensive *in vitro* evaluation of *m*THPC-MAb and AlPcS₄-MAb conjugates. Both classes of conjugates were directly compared using 5 different SCC cell lines as target and 3 different MAbs (BIWA 4, E48 and 425) for tumor cell targeting. In contrast to free AlPcS₄ (IC₅₀ ≥ 700 nM), MAb-conjugated AlPcS₄ was found to be highly phototoxic in PDT in all 5 cell lines. AlPcS₄-BIWA 4 was most consistently effective with IC₅₀ values ranging from 0.06–5.4 nM. *m*THPC-MAb conjugates were in general hardly effective. Phototoxicity (log IC₅₀) of the AlPcS₄-MAb conjugates was found to be strongly correlated with their total cell binding capacity (internalized and surface bound) and to be less correlated with their internalization capacity. In conclusion, these data show a high potential of AlPcS₄-MAb conjugates in comparison to *m*THPC-MAb conjugates for use in PDT.

INTRODUCTION

A challenge in photodynamic therapy (PDT) is to improve the tumor selectivity of the photosensitizers. Photoimmunotherapy, which combines phototoxicity of the sensitizers with the selectivity of monoclonal antibodies (MAbs) directed against tumor-associated antigens, could lead to this improvement. This approach would be very suitable, especially for the treatment of large surface areas, where normal tissue toxicity becomes dose-limiting. Recently, interest in photoimmunotherapy has grown. Soukos *et al.* (1) conjugated the sensitizer chlorin_{e6} to the anti-EGFR MAb C225 for treatment of oral precancer, whereas by the same group chlorin_{e6}-MAb 17.1A conjugates (an anti-EpCAM MAb) were developed for intraperitoneal photoimmunotherapy (2). Carcenac *et al.* (3) used the anti-CEA MAb 35A7

for targeting of the sensitizer AlPcS₄. All these photoimmunoconjugates await more extensive *in vitro* and *in vivo* evaluation before their potential for use in PDT becomes clear.

During the past few years, we have been focusing on the use of photoimmunoconjugates for PDT of squamous cell carcinoma (SCC). To this end, we developed MAb-conjugates with the hydrophobic photosensitizer *meta*-tetrahydroxyphenylchlorin (*m*THPC; Ref. 4) and the hydrophilic sensitizers 5-[4-[5-(carboxyl)-1-butoxy]phenyl]-10,15,20-tris-(4-methylpyridiniumyl)porphyrin Iodide (TrisMPyP-ΦCO₂H; Ref. 5) and aluminium (III) phthalocyanine tetrasulfonate (AlPcS₄; Ref. 6).

The sensitizer *m*THPC ($\epsilon_{652} = 2.2 \times 10^4 \text{ M}^{-1}\text{cm}^{-1}$), one of the most frequently used sensitizers in the clinic, was chosen initially. Its hydrophobicity, however, was found to be a serious chemical obstacle for efficient conjugation, which requires aqueous solutions. Pilot *in vitro* PDT studies indicated that *m*THPC-conjugates are effective, although to a variable extent. The internalizing conjugate *m*THPC-MAb 425 was highly effective in PDT of cell line A431, but the non-internalizing conjugate *m*THPC-MAb U36 was hardly effective in UM-SCC-22A cells. These observations led us to postulate that the critical target for photodynamic damage might be localized intracellularly and led us to focus on the internalization aspect and hydrophilic sensitizers.

Hydrophilic sensitizers in free form do not easily enter cells. Such sensitizers, however, might exhibit an increased phototoxicity when coupled to internalizing MAbs. In line with this, we demonstrated that the hydrophilic model compound TrisMPyP-ΦCO₂H shows phototoxicity when coupled to such MAbs. Subsequently, the tetrasulfonated derivative of aluminium (III) phthalocyanine (AlPcS₄) was used for coupling, because this sensitizer has much better photochemical characteristics for use in PDT than TrisMPyP-ΦCO₂H ($\epsilon_{675} = 1.7 \times 10^5$ vs $\epsilon_{595} = 7.0 \times 10^3 \text{ M}^{-1}\text{cm}^{-1}$). Furthermore, within the family of sulfonated phthalocyanines (with a sulfonation degree from 0 up to 4), this is the most hydrophilic member. Due to this good water solubility its coupling to MAbs is relatively easy. Pilot *in vitro* PDT studies using the A431 cell line revealed a remarkable phototoxicity of AlPcS₄-MAb 425. The conjugate seemed also more toxic than the *m*THPC-MAb 425 conjugate and free *m*THPC that had been tested before in the same system.

The aim of the present study was to get detailed insight in the activity profiles of *m*THPC-MAb versus AlPcS₄-MAb conjugates. To this end, both classes of sensitizer-MAb conjugates were compared in extensive *in vitro* PDT studies using 5 different SCC cell lines as target and 3 different MAbs (BIWA 4, E48 and 425) as the targeting vehicle. The

phototoxicity of the conjugates was related to their cell binding and internalization characteristics.

MATERIAL AND METHODS

Sensitizers

Meta-tetrahydroxyphenylchlorin (*m*THPC; $M_r = 680.76$) was obtained from Scotia Pharmaceuticals (Surrey, UK) as a pure solid. Aluminium (III) phthalocyanine tetrasulfonate chloride (AlPcS₄; $M_r = 895.19$) was obtained from Porphyrin Products (Logan, UT). *m*THPC has a strong absorption maximum at 652 nm ($\epsilon = 2.2 \times 10^4 \text{ M}^{-1}\text{cm}^{-1}$), AlPcS₄ at 675 nm ($\epsilon = 1.7 \times 10^5 \text{ M}^{-1}\text{cm}^{-1}$).

Monoclonal antibodies

Photoimmunoconjugates were produced with the following SCC-selective MABs: (i) BIWA 4, a humanized MAB (hMAB) derived from the murine MAB (mMAB) BIWA 1, which recognizes the v6 domain of CD44 splice variants (Boehringer Ingelheim, Austria (7)); (ii) the IgG1 mMAB E48 recognizing a 16-22 kDa glycosylphosphatidylinositol (GPI)-anchored surface antigen (8); and (iii) the IgG2a mMAB 425 recognizing an epitope localized on the external domain of the epidermal growth factor receptor (EGFR (9)).

Cell lines

The HNSCC cell lines UM-SCC-22A, UM-SCC-22B (kindly provided by Dr. T.E. Carey, Ann Arbor, MI) and OE were cultured under 5% CO₂ at 37°C in Dulbecco's modified Eagle's medium (DMEM; BioWhittaker, Alkmaar, the Netherlands) supplemented with 2 mM L-glutamine, 5% FCS (BioWhittaker) and 25 mM HEPES. The vulvar cell lines A431 and SCV-7 were cultured under the same conditions.

Preparation of AlPcS₄-MAB and *m*THPC-MAB conjugates

The sensitizer conjugates of either ¹²⁵I-labeled or unlabeled BIWA 4, E48 or 425, were prepared according to the multistep procedures as previously described (4,6). All reaction steps were carried out in the dark and under N₂ to prevent any unwanted photochemical reactions during the preparation of the photoimmunoconjugates (4).

In short, AlPcS₄-MAB conjugates (Fig. 1) were produced by conversion of AlPc(SO₃H)₄ into the tetra-glycine derivative, followed by tetra-esterification with 2,3,5,6-tetrafluorophenol (TFP) and direct conjugation of this tetra-ester with the MABs. Cross-linking of MABs did not occur as assessed by SDS-PAGE and HPLC analysis. *m*THPC-MAB conjugates (Fig. 2) were prepared by tetracarboxymethylation of *m*THPC, followed by tetra-esterification with TFP. In this case, before conjugation partial hydrolysis of the ester was performed to leave a conjugation mixture mainly consisting of mono-ester and completely hydrolyzed sensitizer. After the conjugation reaction, the AlPcS₄- and *m*THPC-MAB conjugates were purified on a PD-10 column with 0.9% NaCl as the eluent.

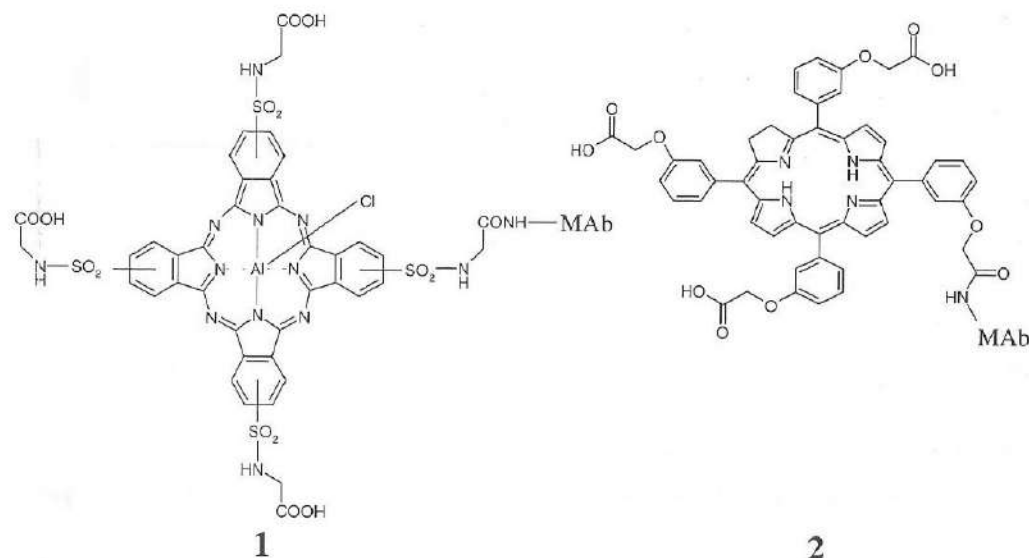


Figure 1. Chemical structure of MAB-conjugated aluminium (III) phthalocyanine tetrasulfonate chloride.

Figure 2. Chemical structure of MAB-conjugated *meta*-tetrahydroxyphenylchlorin.

¹⁴⁵I-Labeling of MABs

Labeling of the native MABs with ¹²⁵I was performed under mild conditions using Iodogen (10). One mg of MAB dissolved in 500 μ l of PBS (pH 7.4) and 2 mCi ¹²⁵I (100 mCi/ml, Amersham, Aylesbury, England) were mixed in a vial coated with 50 μ g of Iodogen.

After 5 min incubation at room temperature, the reaction mixture was filtered through a 0.22 μm Acrodisc filter (Gelman Sciences Inc., Ann Arbor, MI) and unbound ^{125}I was removed using a PD-10 column (Pharmacia Biotech, Roosendaal, the Netherlands) with 0.9% NaCl as eluent. After removal of unbound ^{125}I , the radiochemical purity always exceeded 98% (HPLC analysis).

Analyses

Absorption of free and MAb-conjugated sensitizers was measured using an Ultrospec III spectrophotometer (Pharmacia Biotech). The amount of sensitizer bound to the MAb was assessed with the same apparatus at a wavelength of 351 nm (AlPcS₄) or 415 nm (*m*THPC). To this end, the absorption of a range of dilutions (1-9 $\mu\text{g}/\text{ml}$) of AlPcS₄ in H₂O or *m*THPC in MeCN was measured and graphically depicted using the least square method. The sensitizer concentration in the conjugate preparations was determined using the corresponding calibration curve.

For HPLC analysis of AlPcS₄- ^{125}I -MAb and *m*THPC- ^{125}I -MAb conjugates, an LKB 2150 HPLC-pump, an LKB 2152 LC controller and a 10 x 300 mm Superdex 200 HR 10/30 column (Pharmacia Biotech) were used. The eluent consisted of 0.05 M sodium phosphate/0.15 M sodium chloride (pH 6.8) and the flow-rate was 0.5 ml/min. A Pharmacia LKB VWM 2141 UV detector was used at 351 nm (AlPcS₄) or 415 nm (*m*THPC) for detection of the sensitizer, whereas radioactivity of the ^{125}I -labeled MAb was measured by an Ortec 406A single channel analyzer connected to a Merck-Hitachi D2000 integrator (Merck, Darmstadt, Germany). HPLC analysis showed the conjugates to be eluted as a monomeric peak. All sensitizer was confined to the MAbs, whereas the recovery of the radioactivity from the column was >95%.

Additional analysis of the integrity of the sensitizer- ^{125}I -MAb conjugates was performed by electrophoresis on a Phastgel System (Pharmacia Biotech) using preformed 7.5% SDS-PAGE gels under nonreducing conditions. After running, gels were exposed to a Phosphor plate for 1-3 h and analyzed with a Phosphor Imager (B&L-Isogen Service Laboratory, Amsterdam, the Netherlands) for quantitation of the radiolabeled protein bands. For all 6 conjugates (2 sensitizers x 3 MAbs) a single radiolabeled protein band was observed with an apparent molecular weight of ± 150 kDa, comprising more than 95% of the radioactivity.

Immunoreactivity of AlPcS₄- ^{125}I -MAb and *m*THPC- ^{125}I -MAb conjugates

In vitro binding characteristics of the conjugates were determined in an immunoreactivity assay using 0.1% paraformaldehyde-fixed cells essentially as described previously (4), and compared to those of the unconjugated ^{125}I -MAb. UM-SCC-22A cells were used for binding assays with BIWA 4 and E48, and A431 cells for 425. For all 6 conjugates the immunoreactivity was the same as for their corresponding ^{125}I -MAbs (85-90%), whereas binding of the conjugates was totally blocked by addition of excess corresponding unconjugated cold MAb.

PDT *in vitro*

In vitro PDT experiments were performed to determine the phototoxicity of AlPcS₄ and *m*THPC in free form as well as conjugated to the MAbs BIWA 4, E48 and 425. The toxicity to the cell lines 22A, 22B, A431, SCV-7 and OE was determined using the sulforhodamine B (SRB, Sigma, St. Louis, MO) assay (that measures the cellular protein content) as follows (11): cells were plated in 96-well plates (750 cells/well) and grown for 3 days before incubation with free AlPcS₄/*m*THPC or AlPcS₄/*m*THPC-MAb conjugates (range 0.1 nM-1.0 μM AlPcS₄/*m*THPC equivalents) in DMEM supplemented with 2 mM L-glutamine, 5% FCS and 25 mM HEPES at 37°C. After 20 h, remaining unbound AlPcS₄/*m*THPC and AlPcS₄/*m*THPC-MAb conjugates were removed by washing twice with medium. Fresh medium was added and cells were illuminated at 675 nm (for AlPcS₄) with a Spectra Physics dye laser (model 373) pumped by a 12 Watt Argon Laser (Spectra Physics model 171) and at 652 nm (for *m*THPC) with a 6 W Diode Laser (AOC Medical Systems) at a dose of 25 J/cm² (fluence rate 47 mW/cm²). Three days after illumination, growth was assessed by staining the cellular proteins with SRB and spectrophotometric measurement of the absorption at 540 nm with a microplate reader. As a control, cells were illuminated in the absence of AlPcS₄/*m*THPC or MAb-conjugated AlPcS₄/*m*THPC.

Cell binding and internalization

In vitro experiments were performed essentially as described before (6) to rank the binding and internalizing capacity of AlPcS₄- ^{125}I -BIWA 4, AlPcS₄- ^{125}I -E48 and AlPcS₄- ^{125}I -425 conjugates, the corresponding *m*THPC- ^{125}I -MAb conjugates and the unconjugated ^{125}I -MAbs. The MAbs were labeled with 2 mCi $^{125}\text{I}/\text{mg}$ MAb and conjugates with a sensitizer:MAb ratio of 2:1 were used.

Cells were plated in 6-well plates and grown for 5 days. As each cell line had a different growth rate and because it was crucial that the number of cells was equal at the moment of conjugate addition (3.2×10^5 cells), different amounts of cells were plated (22A: 8.3×10^4 , 22B: 8.3×10^4 , A431: 1.0×10^4 , SCV-7: 5×10^4 and OE: 7.5×10^4 cells/well). After washing the cells with 3 ml PBS/0.5% BSA, conjugates (1×10^6 cpm, corresponding with 9×10^{11} MAb molecules) were added in 1 ml PBS/0.5% BSA. For each conjugate, the following conditions were tested in triplicate: (A) Incubation at 0°C for 2 h to allow antibody binding, followed by incubation at 37°C for 2 h to allow internalization; (B) Incubation at 0°C for 4 h, as a control for possible acid resistant surface binding at non-internalizing conditions; (C) Incubation for 2 h at 0°C followed by 2 h at 37°C in the presence of $25 \mu\text{g}$ naked MAb, for unspecific binding correction; and (D) Incubation for 4 h at 0°C in the presence of $25 \mu\text{g}$ naked MAb, for unspecific binding correction.

After the incubation, cells were washed 3 times with 1 ml PBS/0.5% BSA to remove unbound MAb. The ^{125}I activity in the washing solution was counted. The cells were incubated with 1 ml 20 mM HCl/150 mM NaCl (pH 1.7) at 0°C for 15 min to release MAb bound to the surface of the cells. The supernatant was collected and counted for ^{125}I activity. Finally, cells were lysed with 1 ml 0.1 M NaOH/1% Triton X-100 and the radioactivity was measured to assess the percentage of internalized MAb.

The amount of radioactivity internalized at 37°C was expressed as the percentage of the total amount of radioactivity added to the cells (%Int). The amount of radioactivity specifically bound to the cells (internally + externally) was calculated in the same way (%Int + Ext).

Statistics

All given values represent arithmetic means with a corresponding standard deviation. Associations between the phototoxicity of the conjugates and the capacity of total cell binding (%Int + Ext) and internalization (%Int) were calculated with SPSS 10.0 software (SPSS Inc., Chicago, IL) using Pearson and Spearman Rank correlation analyses. Two-sided significance levels were calculated and p-values < 0.05 were considered statistically significant.

RESULTS

Preparation of AlPcS₄-MAB and mTHPC-MAB conjugates

For conjugation, amounts of sensitizer solution were added to the MABs (either unlabeled or labeled with ^{125}I) that reproducibly resulted in conjugates with a mean sensitizer:MAB molar ratio of 2. The conjugation efficiency for the AlPcS₄-MAB conjugates was about 55%, for the mTHPC-MAB conjugates about 60% (corrected for completely hydrolyzed ester, which is unable to couple).

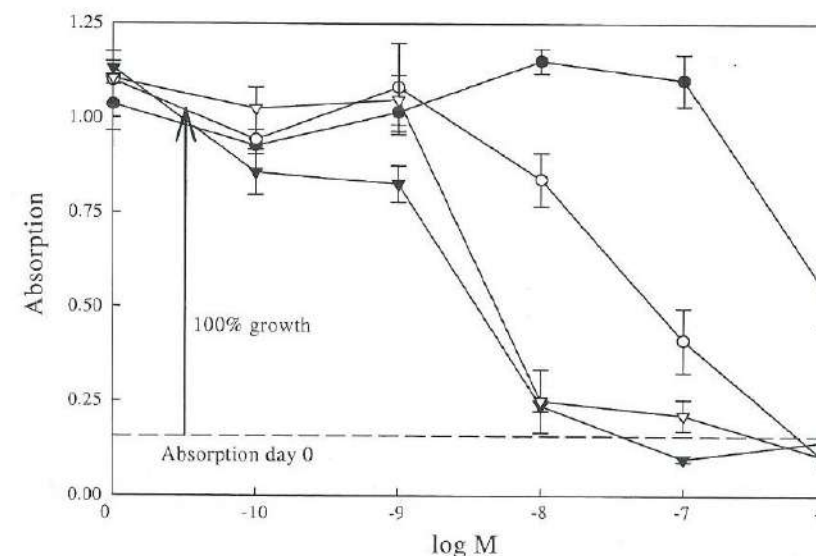


Figure 3. Anti-proliferative effect of AlPcS₄ and AlPcS₄-MAB conjugates with sensitizer:MAB molar ratio 2 on 22A cells upon illumination with 25 J/cm^2 (SRB assay). AlPcS₄ (●), AlPcS₄-BIWA 4 (▽), AlPcS₄-425 (○), and AlPcS₄-E48 (▼). Results of triplicate experiments are indicated (means \pm SD). The molarity (M; x-axis) of the free or conjugated AlPcS₄ is indicated logarithmically.

PDT *in vitro*

The phototoxicity of the BIWA 4-, E48- and 425-conjugated AlPcS₄ and *m*THPC (sensitizer:MAB molar ratio 2) and the corresponding free sensitizers, was assessed in 22A, 22B, A431, SCV-7 and OE cells using the SRB assay. The results of free and MAb-conjugated AlPcS₄ in 22A cells are graphically depicted in Figure 3 as a representative example. Coupled to the MABs BIWA, E48 or 425, the AlPcS₄ sensitizer showed an increased photodynamic efficacy, compared to the free compound. The E48-conjugated AlPcS₄ showed the highest phototoxicity with an IC₅₀ value of 2.4 nM. At sensitizer concentrations from 100 nM up to 1 μM, PDT resulted in 22A cell killing (lower absorption than at the day of illumination [day 0]). The efficacy's of PDT with BIWA 4 and 425-conjugated AlPcS₄ (IC₅₀ values of 3.5 and 33 nM, respectively) were slightly less than with E48-conjugated AlPcS₄, but were much better than that of the free sensitizer (IC₅₀ 700 nM).

Table 1 summarizes the *in vitro* PDT IC₅₀ results for free and MAB-conjugated AlPcS₄ and *m*THPC obtained in all 5 cell lines. It shows that the AlPcS₄-MAB conjugates were highly phototoxic in 11 out of 15 cases (IC₅₀ values ≤ 100 nM). With the exception of AlPcS₄-E48 in the OE cell line, the AlPcS₄-conjugates were more effective than the free sensitizer for all conjugate/cell line combinations. This was most obvious for AlPcS₄-BIWA 4 conjugates in cell lines 22B and OE (IC₅₀ 0.07 and 0.06 nM, respectively) and for AlPcS₄-425 conjugates in cell lines A431 and SCV-7 (IC₅₀ 0.12 and 0.10 nM, respectively).

	22A	22B	A431	SCV-7	OE
AlPcS ₄ -BIWA 4	3.5 ± 0.7	0.07 ± 0.01	5.4 ± 0.9	0.90 ± 0.02	0.06 ± 0.007
AlPcS ₄ -E48	2.4 ± 0.1	600 ± 125	32 ± 3	500 ± 80	>1000
AlPcS ₄ -425	33 ± 3	100 ± 20	0.12 ± 0.05	0.10 ± 0.02	500 ± 70
AlPcS ₄	700 ± 75	>1000	900 ± 130	>1000	900 ± 70
<i>m</i> THPC-BIWA 4	>1000	>1000	>1000	200 ± 20	300 ± 20
<i>m</i> THPC-E48	300 ± 25	1000	600 ± 80	>1000	>1000
<i>m</i> THPC-425	>1000	>1000	7.3 ± 0.7	>1000	>1000
<i>m</i> THPC	1·10 ¹	0.8 ± 0.3	1·10 ¹	3.4 ± 0.4	0.3 ± 0.02

¹ At a *m*THPC concentration of 1 nM, growth was >50%. At concentrations ≥10 nM, PDT resulted in cell killing (lower absorption than at the day of illumination). Therefore, in these two cases the IC₅₀ could not be calculated exactly.

Table 1. *In vitro* PDT efficacy (IC₅₀) of free and MAB-conjugated AlPcS₄ and *m*THPC.

Table 1 also shows that the phototoxicity of the *m*THPC-MAB conjugates to the same set of cell lines was low. The only exception was the combination *m*THPC-425/cell line A431, with an IC₅₀ of 7.3 nM. For each cell line, the free sensitizer was more effective than the *m*THPC-conjugate.

Conjugated and free AlPcS₄ or *m*THPC appeared to be non-toxic without illumination. The unconjugated MABs did not result in growth inhibition with or without illumination (data not shown).

Cell binding and internalization

In vitro experiments were performed to rank the total cell binding and internalization capacity of the AlPcS₄-¹²⁵I-MAB conjugates (sensitizer:MAB molar ratio 2), the corresponding *m*THPC-¹²⁵I-MAB conjugates and the unconjugated ¹²⁵I-MABs, using the cell lines 22A, 22B, A431, SCV-7 and OE. For the unconjugated and conjugated MABs, the addition of excess naked MAB totally blocked binding (conditions C and D, Material and Methods). Acid washing of cells, which had been cultured for 4 h at 0°C, showed that acid resistant surface binding was negligible under these non-internalizing conditions (condition B, Material and Methods). The resulting percentages internalization (% Int) and total binding (% Int + Ext) are graphically depicted in Figure 4.

These data showed that for 12 out of 15 cases, the AlPcS₄-¹²⁵I-MAB conjugates bound to the cells to a larger extent than the unconjugated ¹²⁵I-MABs, whereas the binding of the *m*THPC-¹²⁵I-MAB conjugates was lower than for the unconjugated ¹²⁵I-MABs in 9 out of 15 cases.

Statistics

The efficacy of PDT with AlPcS₄-MAB and *m*THPC-MAB conjugates appeared to be variable among different cell lines (Table 1). We tested whether the efficacy might be related to the extent of total cell binding or to the extent of internalization of the sensitizer-MAB conjugate. The Pearson as well as the Spearman Rank correlation test showed a significant correlation (R = -0.70; p = 0.004, respectively, R = -0.74; p = 0.002) between the total cell binding (% Int + Ext) of the AlPcS₄-MAB conjugates and the log IC₅₀. These correlations remained similar when the data on *m*THPC-conjugates were included in the analyses (R = -0.75; p < 0.001, respectively, R = -0.79; p < 0.001). (For this purpose IC₅₀ values > 1,000 nM were set at 1,000 nM). Figure 5 shows a scatter plot of this relationship.

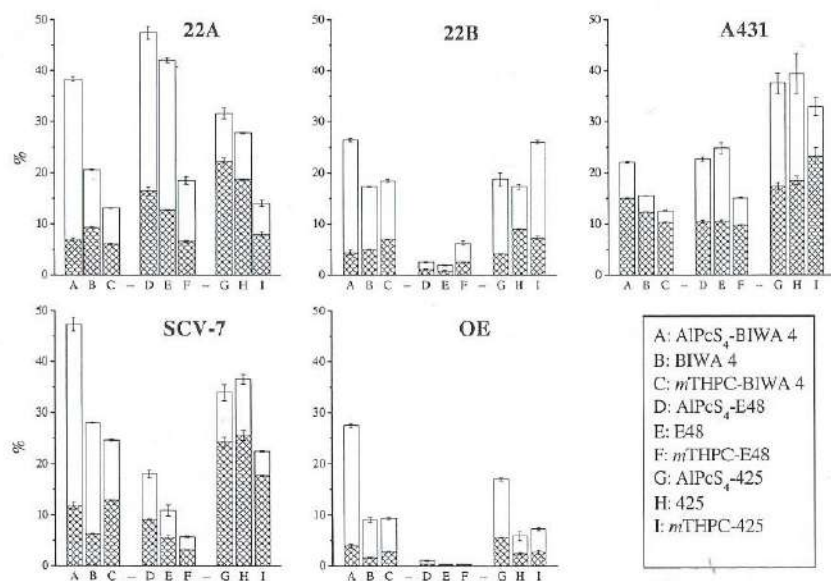


Figure 4. Percentages internalization (mean \pm SD; hatched bars) and total cell binding (mean \pm SD; hatched + blank bars) of the AlPcS₄-¹²⁵I-MAb conjugates (sensitizer:MAB molar ratio 2), the corresponding mTHPC-¹²⁵I-MAB conjugates, and the unconjugated ¹²⁵I-MABs.

The correlations between the log IC₅₀ of the AlPcS₄-conjugates and the internalization (% Int) were not significant (Pearson: R = -0.41; p = 0.13; Spearman: R = -0.39; p = 0.15). When data on mTHPC were included in the analyses these figures were R = -0.46; p = 0.012, respectively R = -0.44; p = 0.016).

DISCUSSION

We recently described the coupling of mTHPC and AlPcS₄ to MABs for use in PDT (4,6). In contrast to unconjugated mTHPC, free AlPcS₄ is known to be clinically ineffective because its hydrophilicity hampers uptake in the tumor cells. The water solubility of AlPcS₄, however, enabled a relatively simple coupling to MABs. Pilot *in vitro* PDT studies showed that mTHPC-MAB as well as AlPcS₄-MAB might be promising compounds (4,6).

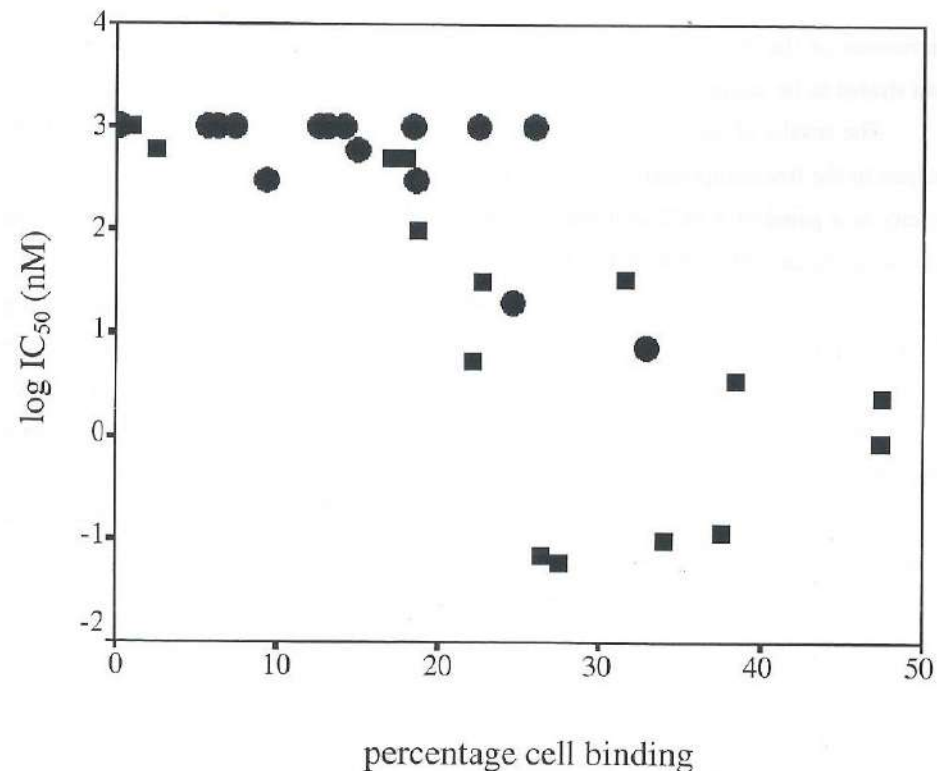


Figure 5. Scatter plot of the relationship between the percentage total cell binding (% Int + Ext) of AlPcS₄-MAB (■) and mTHPC-MAB (●) conjugates (x-axis) and the log IC₅₀ of these conjugates (y-axis). Log IC₅₀ values > 3 were set at 3. Error bars have been omitted and were \leq 15% in case of percentage cell binding and \leq 20% in case of log IC₅₀.

In our study, we describe an extensive *in vitro* evaluation of mTHPC-MAB and AlPcS₄-MAB conjugates. For this purpose, we used 5 cell lines randomly selected from a panel of well-characterized SCC cell lines available at our laboratory. With respect to the choice of the MABs we selected MAB-antigen combinations that are highly realistic for application in clinical PDT of SCC of the head and neck (HNSCC). Immunohistochemical studies had shown that BIWA 4, directed against the CD44v6 antigen, homogeneously binds to SCC of the head and neck, lung, skin, esophagus and cervix (12). mMAb E48, directed against a GPI-anchored surface antigen, binds to 94% of primary HNSCC. In 70% of these tumors, binding with the majority of cells was observed (13). mMAb 425, directed against EGFR, binds to various tumor types including HNSCC (14), renal cell cancer, gliomas and

carcinomas of the esophagus, bladder, cervix, stomach, lung and breast. The 3 MABs have been shown to be capable for selective tumor targeting in HNSCC patients (13,15,16).

The results of our study emphasize the high potential of MAB-conjugated AlPcS₄. In contrast to the free compound (IC₅₀ ≥ 700 nM), the MAB-conjugated sensitizer showed a high toxicity to a panel of 5 SCC cell lines. Especially the AlPcS₄-BIWA 4 conjugates showed a promising efficacy (IC₅₀ 0.06-5.4 nM).

The toxicity of the AlPcS₄-MAB conjugates was compared to that of analogous *m*THPC-MAB conjugates in the same setting. The data show that *m*THPC-MAB conjugates are generally ineffective. Only the combination *m*THPC-425/A431 cells revealed significant toxicity (IC₅₀ 7.3 nM), the combination that was earlier found to be effective (4). In line with other reports, free *m*THPC was consistently highly phototoxic (IC₅₀ 0.3-10 nM).

Earlier results suggested the critical target for PDT to be localized intracellularly, because internalizing sensitizer-MAB conjugates were more effective in PDT than non-internalizing conjugates (5,6). Attempting to substantiate this observation, *in vitro* cell binding experiments were extended in the current study. For this purpose, calculation methods for assessment of the internalization capacity of sensitizer-MAB conjugates were modified. Formerly, the internalization was calculated as the percentage of the total amount of radioactivity bound to the cells (internalized and surface bound). In our present study, however, total cell binding and internalization were calculated as the percentage of the total amount of radioactivity added to the cells. By doing so the absolute amount of bound/internalized conjugate is taken into account, which enables a more adequate comparison between the different sensitizer-¹²⁵I-MAB/cell line combinations. To illustrate the difference between the old and the new calculation method we can consider a situation in which 10⁶ cpm of conjugate are added to a cell culture, resulting in 2x10⁵ cpm total cell binding (Int + Ext) and 10⁵ cpm internalization (Int). With the old calculation method the percentage internalization would be established at 50%, whereas with the calculation performed in our study this would be 10%. Essential in this new approach is that the total amount of radioactivity added to the cells, the specific activity of the ¹²⁵I-MAB in the sensitizer-MAB conjugate and the number of cells used in the *in vitro* assay, must be the same for each sensitizer-¹²⁵I-MAB/cell line combination.

The thus obtained results of the *in vitro* cell binding experiments were revealing. Despite the fact that the immunoreactivity (*i.e.* immunoreactive fraction) of the ¹²⁵I-MABs was not influenced by coupling of AlPcS₄ or *m*THPC, the binding characteristics of the conjugates differed from that of the unconjugated ¹²⁵I-MABs. The total level of AlPcS₄-¹²⁵I-

MAB binding was in 12 out of 15 conjugate/cell line combinations higher than for the unconjugated ¹²⁵I-MABs, whereas that of *m*THPC-¹²⁵I-MAB conjugates was in general lower. *m*THPC and AlPcS₄ seem to exert these opposite effects by influencing antibody-antigen interaction as (1) binding of the photoimmunoconjugates was in all cases totally blocked by the addition of cold antibody and (2) binding of photoimmunoconjugates to cells with minimal antigen expression was near zero (like for the combination MAB E48/cell line OE). The origin of these opposite effects might be the difference in polarity between AlPcS₄ and *m*THPC.

In our present study, only a strong correlation was observed between the phototoxicity (log IC₅₀) of AlPcS₄-MAB conjugates and the total binding capacity of these conjugates to the cells (% Int + Ext), not with their internalization capacity (% Int). With regard to this, new insights due to the analysis of more cell lines and conjugates have modified our interpretation in comparison to previous studies that were based on a more restricted variety of experimental settings (4,5,6). The variation in phototoxicity seems much larger than the variation in total cell binding capacity, however, which might be explained by kinetic differences in both assays (20 h incubation in the PDT experiments and 2 + 2 h incubation in the cell binding experiments). To substantiate these findings cellular uptake studies have to be performed in which intra- and extracellular sensitizer concentrations are measured by fluorescence measurement after 20 h incubation.

*m*THPC-MAB conjugates were in general ineffective and therefore the relationship between phototoxicity and cell binding/internalization could not be evaluated separately. With this respect it is of note that *m*THPC-MAB conjugates were most phototoxic in case of *m*THPC-425 and A431 cells, a combination that showed the highest level of total conjugate binding.

In conclusion, our results demonstrate the high potential of AlPcS₄-MAB conjugates in comparison to *m*THPC-MAB conjugates for use in PDT. Whereas AlPcS₄ in free form is not effective in PDT, as was confirmed herein, it becomes highly effective when coupled to tumor-specific MABs.

REFERENCES

1. Soukos, N. S., Hamblin, M. R., Keel, S., Fabian, R. L., Deutsch, T. F., and Hasan, T. Epidermal growth factor receptor-targeted immunophotodiagnosis and photoimmunotherapy of oral precancer *in vivo*. *Cancer Res.*, *61*: 4490-4496, 2001.
2. Molpus, K. L., Hamblin, M. R., Rizvi, I., and Hasan, T. Intraperitoneal photoimmunotherapy of ovarian carcinoma xenografts in nude mice using charged photoimmunoconjugates. *Gynecol. oncol.*, *76*: 397-404, 2000.
3. Carcenac, M., Larroque, C., Langlois, R., van Lier, J. E., Artus, J.-C., and Pèlegri, A. Preparation, phototoxicity and biodistribution studies of anti-carcinoembryonic antigen monoclonal antibody-phthalocyanine conjugates. *Photochem. Photobiol.*, *70*: 930-936, 1999.
4. Vrouenraets, M. B., Visser, G. W. M., Stewart, F. A., Stigter, M., Oppelaar, H., Postmus, P. E., Snow, G. B., and van Dongen, G. A. M. S. Development of *meta*-tetrahydroxyphenylchlorin-monoclonal antibody conjugates for photoimmunotherapy. *Cancer Res.*, *59*: 1505-1513, 1999.
5. Vrouenraets, M. B., Visser, G. W. M., Stigter, M., Oppelaar, H., Stewart, F. A., Snow, G. B., and van Dongen, G. A. M. S. Targeting of a hydrophilic photosensitizer by use of internalizing monoclonal antibodies: a new possibility for use in photodynamic therapy. *Int. J. Cancer*, *88*: 108-114, 2000.
6. Vrouenraets, M. B., Visser, G. W. M., Stigter, M., Oppelaar, H., Stewart, F. A., Snow, G. B., and van Dongen, G. A. M. S. Targeting of aluminum (III) phthalocyanine tetrasulfonate by use of internalizing monoclonal antibodies: improved efficacy in photodynamic therapy. *Cancer Res.*, *61*: 1970-1975, 2001.
7. Heider, K. H., Sproll, M., Susani, S., Patzelt, E., Baumier, P., Ostermann, E., Ahorn, H., and Adolf, G. R. Characterization of a high-affinity monoclonal antibody specific for CD44v6 as candidate for immunotherapy of squamous cell carcinomas. *Cancer Immunol. Immunother.*, *43*: 245-253, 1996.
8. Quak, J. J., van Dongen, G. A. M. S., Balm, A. J. M., Brakkee, J. P. G., Scheper, R. J., Snow, G. B., and Meijer, C. J. L. M. A 22-kDa surface antigen detected by monoclonal antibody E48 is exclusively expressed in stratified squamous and transitional epithelia. *Am. J. Pathol.*, *136*: 191-197, 1990.
9. Murthy, U., Basu, A., Rodeck, U., Herlyn, M., Ross, A. H., and Das, M. Binding of an antagonistic monoclonal antibody to an intact and fragmented EGF-receptor polypeptide. *Arch. Biochem. Biophys.*, *252*: 549-560, 1987.
10. Haisma, H. J., Hilgers, J., and Zurawski, V. R. Iodination of monoclonal antibodies for diagnosis and therapy using a convenient one-vial method. *J. Nucl. Med.*, *27*: 1890-1895, 1986.
11. Skehan, P., Storeng, R., Scudiero, D., Monks, A., McMahon, J., Vistica, D., Warren, J. T., Bokesch, H., Kenney, S., and Boyd, M. R. New colorimetric cytotoxicity assay for anticancer-drug screening. *J. Natl. Cancer Inst.*, *82*: 1107-1112, 1990.
12. Heider, K. H., Mulder, J. W. R., Ostermann, E., Susani, S., Patzelt, E., Pals, S. T., and Adolf, G. R. Splice variants of the cell surface glycoprotein CD44 associated with metastatic tumor cells are expressed in normal tissues of humans and cynomolgus monkeys. *Eur. J. Cancer*, *31A*: 2385-2391, 1995.
13. De Bree, R., Roos, J. C., Quak, J. J., den Hollander, W., Wilhelm, A. J., van Lingen, A., Snow, G. B., and van Dongen, G. A. M. S. Biodistribution of radiolabeled monoclonal antibody E48 IgG and F(ab')₂ in patients with head and neck cancer. *Clin. Cancer Res.*, *1*: 277-286, 1995.
14. Stanton, P., Richards, S., Reeves, J., Nikolic, M., Edington, K., Clark, L., Robertson, G., Souter, D., Mitchell, R., Hendler, F. J., Cooke, T., Parkinson, E. K., and Ozanne, B. W. Epidermal growth factor receptor expression by human squamous cell carcinomas of the head and neck, cell lines and xenografts. *Br. J. Cancer*, *70*: 427-433, 1994.
15. Stroomer, J. W. G., Roos, J. C., Sproll, M., Quak, J. J., Heider, K. H., Wilhelm, A. J., Castelijns, J. A., Meyer, R., Kwakkelstein, M. O., Snow, G. B., Adolf, G. A., and van Dongen, G. A. M. S. Safety and biodistribution of 99mTechnetium-labeled anti-CD44v6 monoclonal antibody BIWA 1, in head and neck cancer patients. *Clin. Cancer Res.*, *6*: 3046-3055, 2000.
16. Bier, H., Reiffen, K. H., Haas, I., and Stasiecki, P. Dose-dependent access of murine anti-epidermal growth factor receptor monoclonal antibody to tumor cells in patients with advanced laryngeal and hypopharyngeal carcinoma. *Eur. Arch. Otorhinolaryngol.*, *7*: 433-439, 1995.

Chapter 6

SUMMARY AND CONCLUSIONS

SUMMARY AND CONCLUSIONS

Photodynamic therapy (PDT), a method for the treatment of superficially localized tumors (**Chapter 1**), uses light sensitive molecules (photosensitizers) and light. After injection, the photosensitizer accumulates more or less selectively in the tumor, which makes visualization of the tumor possible due to the fluorescent properties of the sensitizer. Subsequently the tumor area is irradiated with laser light with a wavelength between 600 and 800 nm, depending on the sensitizer used. This light excites the sensitizer in the tumor. In this excited state the sensitizer reacts with oxygen, resulting in the formation of singlet oxygen, a cytotoxic form of oxygen.

PDT is a developing technique and its ultimate clinical potential has yet to be established. An important aspect of PDT, hampering its clinical success, is the lack of tumor selectivity of the photosensitizers. Especially PDT of large surface areas can therefore result in severe normal tissue damage. Furthermore, PDT can result in skin photosensitivity, which means that patients must stay out of bright light following the administration of the photosensitizer. Therefore the improvement of tumor selectivity of photosensitizers is a major issue in PDT.

The use of monoclonal antibodies directed against tumor-associated antigens for selective targeting of photosensitizers is a realistic option as was shown by Pèlegri *et al.* (1) with fluorescein-anti-CEA MAb conjugates. These conjugates were more effective in tumor detection in nude mice than the free photosensitizer Photofrin[®]. Because no therapeutically effective photoimmunoconjugates have been reported until now, the aim of the studies described in this thesis was the development of such conjugates.

This study was started with the photosensitizer *m*THPC, being one of the most promising sensitizers available. **Chapter 2** describes a protocol for the reproducible synthesis of *m*THPC-MAB conjugates. Before conjugation, the sensitizer was radiolabeled with ¹³¹I to facilitate the assessment of the *in vitro* and *in vivo* behavior, and was modified to *m*THPC-(CH₂COOH)₄. This latter modification was performed to make it water soluble and to create a functional moiety suitable for coupling.

Biodistribution data in the HNSCC xenograft line HNX-OE bearing nude mice showed that the tumor selectivity of cMAb U36-conjugated *m*THPC was strongly improved in comparison with free *m*THPC. Since the improved selectivity of sensitizers by MAbs does not guarantee improved efficacy, *in vitro* studies were performed to assess the phototoxicity of the newly developed *m*THPC-MAB conjugates. Preliminary results suggested that *m*THPC

when coupled to the internalizing anti-EGFR MAb 425 was more toxic (A431 cells; IC₅₀ of 7.3 nM) than when coupled to a non-internalizing MAb (UM-SCC-22A cells; IC₅₀ > 1 μM).

Because this chapter was the first report on the covalent coupling of *m*THPC to MAbs, as well as on the selective tumor targeting of *m*THPC *in vivo*, the data presented herein were patented by the producer of this photosensitizer (patent application WO 01/74398 A1).

As described in the discussion section of this chapter, about 150 ng *m*THPC per g of tumor could be delivered with *m*THPC-cMAb U36 conjugates, using a MAb dose of 400 μg/mouse. This tumor uptake seems to be comparable to that obtained with free *m*THPC: Using a similar *in vivo* model, *e.g.* nude mice bearing a HNSCC xenograft, Ris *et al.* (2) measured a tumor uptake of 160 ng/g tumor 4 days after injection of a relatively high dose of 0.3 mg/kg. PDT at that time with 20 J/cm² resulted in extensive tumor necrosis. These data suggest that the MAb-conjugates are able to target suitable amounts of *m*THPC to the tumor to obtain tumor necrosis with PDT.

In comparison with the data obtained by Westermann *et al.* (3), who studied the biodistribution of *m*THPC-PEG in colon carcinoma xenograft bearing nude mice, the *m*THPC-cMAb U36 conjugates performed comparable: 48 h after *i.v.* injection the %ID/g were 7.5% for *m*THPC-PEG and 5.7% for *m*THPC-cMAb U36 (conjugate with a molar ratio of 0.9), respectively. The tumor to skeletal muscle ratio, which is commonly used as a reference in experimental studies of PDT, was at this time point 18.6 for *m*THPC-PEG and 19 for *m*THPC-cMAb U36. However, as there are indications that the ability of *m*THPC to generate singlet oxygen becomes less upon pegylation (4), the suitability of this compound for PDT remains questionable.

Also the *m*THPC-MAB conjugates we developed were not optimal for *in vivo* use. First, the biodistribution of conjugates with a *m*THPC:MAB molar ratio as low as 0.9 was impaired, compared to the unconjugated MAB. Second, preliminary *in vitro* PDT experiments revealed that *m*THPC-cMAb U36 conjugates hardly exhibited phototoxicity to UM-SCC-22A cells, despite the fact that the CD44v6 target antigen is abundantly expressed on these cells.

Because the hydrophobicity of *m*THPC was probably one of the main causes for these problems, the use of water soluble sensitizers would be much more attractive. Moreover, a better water solubility facilitates the coupling to MAbs. With this respect, the previously described observation that an internalizing *m*THPC-MAB conjugate was more toxic than a non-internalizing conjugate was of major importance. This observation led us to hypothesize that more hydrophilic sensitizers (compared to *m*THPC), which in free form do not readily

pass the cell membrane and are therefore ineffective in PDT, would become effective when coupled to internalizing MABs.

In **Chapter 3**, this hypothesis was confirmed with the compound 5-[4-[5-(carboxyl)-1-butoxy]phenyl]-10,15,20-tris-(4-methylpyridiniumyl)porphyrin iodide (TrisMPyP- Φ CO₂H). This hydrophilic porphyrin derivative just served as a model compound, as its weak absorption ($\epsilon = 7.0 \times 10^3 \text{ M}^{-1}\text{cm}^{-1}$) at an absorption maximum of 595 nm makes it of limited value for photoimmunotherapy. *In vitro* efficacy data showed that the internalizing MAB U36 and MAB 425 conjugates were phototoxic to A431 cells, while the non-internalizing E48 conjugate and the unconjugated compound were not.

Remarkably, despite the better water solubility of the sensitizer (compared to *m*THPC), also these conjugates showed some intrinsic limitations for tumor targeting. A decreased solubility of the conjugates was observed at a sensitizer:MAB molar ratio >3. Furthermore, as for the *m*THPC-MAB conjugates, also upon coupling of this hydrophilic sensitizer the biodistribution of the MAB became impaired. The conjugates with a higher ratio were increasingly susceptible to removal from the blood, which probably occurs due to hepatic extraction. Other groups have also observed ratio-dependent blood clearance when coupling photosensitizers or radionuclide-binding chelates to MABs (1,5-8).

During the course of this project several papers from other research groups appeared on tumor targeting of therapeutic photosensitizers by MABs. Most of these studies were performed by the group of Dr. T. Hasan of the Wellman Laboratories of Photomedicine, Harvard Medical School in Boston, USA, using chlorin₆₆ monoethylenediamine monoamide as the photosensitizer. In initial experiments they coupled chlorin₆₆ via polyglutamic acid to MAB OC125. These conjugates only have been tested in a murine model for peritoneal dissemination of ovarian cancer after i.p. injection, not after i.v. administration (9). In later studies, this group used poly-L-lysine for linking of the sensitizer to MABs, and polysuccinylation for charge modification, resulting in cationic- and anionic chlorin₆₆-MAB conjugates. Conjugates were prepared with MAB 17-1A for targeting of hepatic metastases of colorectal cancer in nude mice upon i.v. injection (10). The major challenge was to obtain high uptake of sensitizer in the tumor and high tumor:normal liver ratios. Tumor uptake of the anionic chlorin₆₆-MAB 17-1A conjugate appeared 7-fold higher than of the cationic one at 24 h p.i. However, tumor uptake as well as tumor:normal liver ratio of the anionic photoimmunoconjugate were not better than for the unconjugated anionic chlorin₆₆, indicating that the use of the tumor-targeting 17-1A MAB in their hands did not lead to increased tumor specificity.

The best targeting results thusfar were obtained by the group of Carcenac and Pèlegri, Montpellier, France (11). They coupled AlPcS₄ to a 35A7 MAB directed against carcinoembryonic antigen (CEA) via a five-carbon spacer chain to yield conjugates with a molar ratio ranging from 5 to 16 mol of AlPcS₄ per mol of MAB. Even conjugates containing 16 AlPcS₄ molecules remained fully soluble and showed a similar tumor selectivity in nude mice bearing colon carcinoma xenografts as the unconjugated MAB. Authors attributed this to the unchanged hydrophilic properties of the MABs after conjugation. As will become clear from the next paragraph we were not able to obtain such ideal targeting results with the same sensitizer. However, the efficacy of the conjugates made by this group was initially disappointing.

In **Chapter 4**, the concept of using internalizing MABs for photoimmunotherapy was further investigated by using the therapeutically better suited hydrophilic sensitizer aluminium phthalocyanine tetrasulfonate (AlPc(SO₃H)₄, $\epsilon = 1.7 \times 10^5 \text{ M}^{-1}\text{cm}^{-1}$ at 675 nm). The AlPcS₄-MAB conjugates showed several similarities with the *m*THPC-MAB conjugates. As AlPc(SO₃H)₄ also lacks a functional moiety suitable for direct conjugation, conjugation was performed via its tetra-glycine derivative. At molar ratios >4 the solubility of the MABs decreased, as for the previously described conjugates. Finally, biodistribution data in HNX-OE bearing nude mice were similar to those obtained with *m*THPC-MAB conjugates: AlPcS₄-cMAB U36 accumulated selectively in the tumor, although to a lesser extent than for the unconjugated MAB. Conjugates with a higher sensitizer:MAB ratio were cleared more rapidly from the blood than the unconjugated MAB. These data form an interesting contrast with those obtained by Carcenac *et al.* (11). A possible explanation for the much more rapid clearance of our conjugates is that the modification of all four SO₃H groups in AlPcS₄ to form its tetra-glycine derivative has decreased its hydrophilicity in such a way that the biodistribution of the MAB becomes affected.

Preliminary *in vitro* data suggested that AlPcS₄-MAB conjugates were much more phototoxic than the *m*THPC-MAB conjugates. The internalizing AlPcS₄-MAB 425 conjugate was about 7500 times more toxic to A431 cells (25 J/cm² at 675 nm) than the free compound (IC₅₀s, 0.12 nM *versus* 900 nM), and about 60 times more toxic than *m*THPC-MAB 425 in the same model.

In **Chapter 5** an extensive *in vitro* evaluation of *m*THPC- and AlPcS₄-MAB conjugates is described. The phototoxicity of both classes of conjugates was directly compared using five different SCC cell lines as target and three MABs (BIWA 4, E48 and 425) for targeting (25 J/cm² at 652 nm for *m*THPC and 675 nm for AlPcS₄). With respect to

the choice of the MABs we selected MAB-antigen combinations that are highly realistic for clinical application in PDT of squamous cell carcinoma. *m*THPC-MAB conjugates were in general hardly effective (in contrast to free *m*THPC), while AlPcS₄-MAB conjugates were highly phototoxic to all five cell lines. Especially AlPcS₄-BIWA 4 conjugates, directed against the tumor-associated antigen CD44v6, were effective with IC₅₀ values ranging from 0.06-5.4 nM.

Furthermore, the phototoxicity of the conjugates was related to their cell binding and internalization characteristics. A strong correlation was observed between the phototoxicity of AlPcS₄-MAB conjugates and the total binding capacity (internalized and surface bound) of these conjugates. In contrast to our previous findings, these more extensive studies revealed that efficacy was not correlated with internalization capacity only.

Recently, our promising findings with AlPc(SO₃H)₄-MAB conjugates were confirmed by Carcenac *et al.* (12). In an *in vitro* study, they observed a clear advantage of an internalizing over a non-internalizing dye-MAB conjugate.

In conclusion, the results presented in this thesis show that *m*THPC in its free form is a much more phototoxic compound than when conjugated to a MAB, and this sensitizer is therefore not optimal for use in photoimmunotherapy. In contrast to these data, very promising results were obtained with AlPcS₄. *In vitro*, this sensitizer appeared to be a potent antitumor agent, especially when coupled to the anti-CD44v6 MAB BIWA 4. However, in view of the data of Carcenac (11), further improvement of this conjugate for *in vivo* application seems possible.

REFERENCES

1. Pèlerin, A., Folli, S., Buchegger, F., Mach, J-P., Wagnières, G., and van den Bergh, H. Antibody-fluorescein conjugates for photoimmunodiagnosis of human colon carcinoma in nude mice. *Cancer*, *67*: 2529-2537, 1991.
2. Ris, H.-B., Li, Q., Krueger, T., Lim, C. K., Reynolds, B., Althaus, U., and Altermatt, H. J. Photosensitizing effects of *m*-tetrahydroxyphenylchlorin on human tumor xenografts: correlation with sensitizer uptake, tumor doubling time and tumor histology. *Int. J. Cancer*, *76*: 872-874, 1998.
3. Westermann, P., Glanzmann, T., Andrejevic, S., Braichotte, D. R., Forrer, M., Wagnières, G. A., Monnier, P., van den Bergh, H., Mach, J. P., and Folli, S. Long circulating half-life and high tumor selectivity of the photosensitizer *meta*-tetrahydroxyphenylchlorin conjugated to polyethylene glycol in nude mice grafted with a human colon carcinoma. *Int. J. Cancer*, *76*: 842-850, 1998.
4. Reuther, T., Kübler, A. C., Zillmann, U., Flechtenmacher, C., and Sinn, H. Comparison of the *in vivo* efficiency of Photofrin II-, *m*THPC-, *m*THPC-PEG- and *m*THPCnPEG-mediated PDT in a human xenografted head and neck carcinoma. *Lasers Surg. Med.*, *29*: 314-322, 2001.
5. Folli, S., Westermann, P., Braichotte, D., Pèlerin, A., Wagnières, G., van den Bergh, H., and Mach, J.P. Antibody-indocyanin conjugates for immunodetection of human squamous cell carcinoma in nude mice. *Cancer Res.*, *54*: 2643-2649, 1994.
6. Boniface, G. R., Izard, M. E., Walker, K. Z., McKay, D. R., Soby, P. J., Turner, J. H., and Morris, J. G. Labeling of monoclonal antibodies with Samarium-153 for combined radioimmunoscintigraphy and radioimmunotherapy. *J. Nucl. Med.*, *30*: 683-691, 1989.
7. Smith, A., Zangemeister-Wittke, U., Waibel, R., Schenker, T., Schubiger, P. A., and Stahel, R. A. A comparison of ⁶⁷Cu- and ¹³¹I-labeled forms of monoclonal antibodies SEN7 and SWA20 directed against small-cell lung cancer. *Int. J. Cancer*, *8*: 43-48, 1994.
8. Van Gog, F. B., Visser, G. W. M., Klok, R., van der Schors, R., Snow, G. B., and van Dongen, G. A. M. S. Monoclonal antibodies labeled with Rhenium-186 using the MAG3 chelate: relationship between the number of chelated groups and biodistribution characteristics. *J. Nucl. Med.*, *37*: 352-362, 1996.
9. Goff, B. A., Blake, J., Bamberg, M. P., and Hasan, T. Treatment of ovarian cancer with photodynamic therapy and immunoconjugates in a murine ovarian cancer model. *Br. J. Cancer*, *74*: 1194-1198, 1996.
10. Hamblin, M. R., Del Governatore, M., Rizvi, I., and Hasan, T. Biodistribution of charged 17.1A photoimmunoconjugates in a murine model of hepatic metastasis of colorectal cancer. *Br. J. Cancer*, *83*: 1544-1551, 2000.
11. Carcenac, M., Larroque, C., Langlois, R., van Lier, J. E., Artus, J.-C., and Pèlerin, A. Preparation, phototoxicity and biodistribution studies of anti-carcinoembryonic antigen monoclonal antibody-phthalocyanine conjugates. *Photochem. Photobiol.*, *70*: 930-936, 1999.
12. Carcenac, M., Dorvillius, M., Garambois, V., Glaussel, F., Larroque, C., Langlois, R., Hynes, N. E., van Lier, J. E., and Pèlerin A. Internalisation enhances photo-induced cytotoxicity of monoclonal antibody-phthalocyanine conjugates. *Br. J. Cancer*, *85*: 1787-1793, 2001.

SAMENVATTING EN CONCLUSIES

SAMENVATTING EN CONCLUSIES

Fotodynamische therapie (PDT), een methode voor de behandeling van oppervlakkig gelegen tumoren (**Hoofdstuk 1**), maakt gebruik van lichtgevoelige moleculen (fotosensitizers) en licht. Na injectie hoopt de fotosensitizer met een beperkte selectiviteit in de tumor op, en kan deze eventueel gevisualiseerd worden door gebruik te maken van de fluorescerende eigenschappen van de sensitizer. Vervolgens wordt de tumor belicht met laserlicht met een golflengte tussen 600 en 800 nm, afhankelijk van de gebruikte sensitizer. Dit licht brengt de sensitizer in de tumor in een aangeslagen toestand. In deze toestand reageert de sensitizer met zuurstof, resulterend in de vorming van singlet zuurstof, een cytotoxische vorm van zuurstof.

PDT bevindt zich in de ontwikkelingsfase en de klinische mogelijkheden van deze therapie moeten nog grotendeels worden vastgesteld. Een belangrijk aspect van PDT dat klinisch succes in de weg staat, is het gebrek aan tumorselectiviteit van de fotosensitizers. Vooral PDT van grote oppervlakten kan daardoor leiden tot grote schade aan het normale gezonde weefsel. PDT kan bovendien lichtgevoeligheid van de huid veroorzaken, waardoor patiënten na toediening van de sensitizer blootstelling aan zonlicht moeten vermijden. De verbetering van de tumorselectiviteit van fotosensitizers is daarom een belangrijk aandachtspunt in PDT.

Dat het gebruik van monoclonale antilichamen (MAbs) gericht tegen tumor-geassocieerde antigenen een realistische optie is voor selectieve targetering van fotosensitizers, werd eerder aangetoond door Pèlegriin *et al.* (1) met fluoresceïn-anti-CEA MAb conjugaten. In naakte muizen waren deze conjugaten effectiever voor tumordetectie dan de vrije sensitizer Photofrin®. Omdat er nog niet eerder therapeutisch effectieve fotoimmunoconjugaten ontwikkeld waren, was het doel van de in dit proefschrift beschreven studies de ontwikkeling van dergelijke conjugaten.

Het onderzoek werd begonnen met *m*THPC, één van de meest veelbelovende beschikbare sensitizers. **Hoofdstuk 2** beschrijft een protocol voor de reproduceerbare synthese van *m*THPC-MAb conjugaten. Vóór conjugatie werd de sensitizer radioactief gelabeld met ¹³¹I om de bepaling van het *in vitro* en *in vivo* gedrag te vergemakkelijken, en gemodificeerd tot *m*THPC-(CH₂COOH)₄. Laatstgenoemde modificatie werd uitgevoerd om *m*THPC wateroplosbaar te maken en tevens om een functionele groep te creëren die gebruikt kan worden voor conjugatie.

Biodistributieresultaten in naakte muizen met hoofd/hals-plaveiselcelcarcinoom HNX-OE xenografts lieten zien dat de tumorselectiviteit van cMAb U36-geconjugerd *m*THPC sterk verbeterd was ten opzichte van vrij *m*THPC. Omdat de door MAbs verbeterde selectiviteit van sensitizers geen verbeterde effectiviteit garandeert, werden *in vitro* studies uitgevoerd om de fototoxiciteit van de ontwikkelde *m*THPC-MAb conjugaten te bepalen. Preliminair resultaten suggereerden dat *m*THPC, gekoppeld aan het internaliserende anti-EGFR MAb 425, toxischer was (A431 cellen; IC₅₀ 7.3 nM) dan wanneer gekoppeld aan een niet-internaliserend MAb (UM-SCC-22A cellen; IC₅₀ > 1 µM).

Omdat de covalente koppeling van *m*THPC aan MAbs niet eerder beschreven was, en bovendien sprake was van selectieve tumortargeting van *m*THPC *in vivo*, werden de data gepatenteerd door de producent van deze sensitizer (patent applicatie WO 01/74398 A1).

Zoals beschreven in de discussieparagraaf van dit hoofdstuk, kon ongeveer 150 ng *m*THPC per gram tumor worden afgegeven met *m*THPC-cMAb U36 conjugaten, indien een MAb-dosis van 400 µg per muis gebruikt werd. Deze tumoropname lijkt vergelijkbaar met die beschreven voor vrij *m*THPC: in een vergelijkbaar *in vivo* model, d.w.z. naakte muizen met een HHPCC-xenograft, vonden Ris *et al.* (2) een tumoropname van 160 ng/g tumor, 4 dagen na injectie van een relatief hoge dosis van 0.3 mg/kg. PDT op dat tijdstip met 20 J/cm² resulteerde in aanzienlijke tumornecrose. Deze data suggereren dat de *m*THPC-MAb conjugaten voldoende *m*THPC naar de tumor kunnen targeten om bij PDT tot tumornecrose te kunnen leiden.

In vergelijking met de data van Westermann *et al.* (3), die de biodistributie van *m*THPC-PEG bestudeerde in naakte muizen met geïmplanteerde darmkanker xenografts, gedroegen de *m*THPC-cMAb U36 conjugaten zich vergelijkbaar: 48 uur na i.v. injectie waren de %ID/g respectievelijk 7.5% voor *m*THPC-PEG en 5.7% voor *m*THPC-cMAb U36 (conjugaat met een molaire ratio van 0.9). De tumor:spier ratio, een veelgebruikte parameter in experimentele PDT studies, was op dat tijdstip 18.6 voor *m*THPC-PEG en 19 voor *m*THPC-cMAb U36. Aangezien er echter aanwijzingen zijn dat het vermogen van *m*THPC om singlet zuurstof te produceren afneemt door koppeling van PEG (4), blijft de geschiktheid van deze verbinding voor PDT twijfelachtig.

Ook de door ons ontwikkelde *m*THPC-MAb conjugaten waren niet optimaal voor *in vivo* gebruik. Ten eerste was de biodistributie van de conjugaten, zelfs bij een lage *m*THPC:MAb molaire ratio van 0.9, afwijkend ten opzichte van die van het ongeconjugeerde MAb. Ten tweede lieten preliminair *in vitro* PDT experimenten zien dat *m*THPC-cMAb

U36 conjugaten nauwelijks fototoxisch waren voor UM-SCC-22A cellen, ondanks het feit dat het CD44v6 target-antigeen zeer hoog tot expressie komt op deze cellen.

Omdat de hydrofobiciteit van *m*THPC waarschijnlijk één van de hoofdoorzaken was voor deze problemen, zou het gebruik van wateroplosbare sensitizers veel aantrekkelijker kunnen zijn. Een betere wateroplosbaarheid vergemakkelijkt bovendien de koppeling aan MAbs. De hiervoor beschreven waarneming dat een internaliserend *m*THPC-MAb conjugaat toxischer was dan een niet-internaliserend conjugaat, was in dit verband zeer belangrijk. Uit deze observatie vloeide onze hypothese voort dat hydrofielere sensitizers (ten opzichte van *m*THPC), die in vrije vorm de celmembranen niet gemakkelijk passeren en daardoor niet effectief zijn in PDT, effectief zouden kunnen worden indien gekoppeld aan internaliserende MAbs.

In **Hoofdstuk 3** werd deze hypothese bevestigd met de verbinding 5-[4-[5-(carboxyl)-1-butoxy]phenyl]-10,15,20-tris-(4-methylpyridiniumyl)porphyrine iodide (TrisMPyP- Φ CO₂H). Dit hydrofiële porphyrine derivaat fungeerde als een modelverbinding, omdat het door zijn lage absorptie ($\epsilon = 7.0 \times 10^3 \text{ M}^{-1}\text{cm}^{-1}$) bij een absorptiemaximum van 595 nm van zeer beperkte waarde is voor fotoimmunotherapie. *In vitro* effectiviteit-resultaten lieten zien dat de internaliserende MAbs U36 en 425 conjugaten fototoxisch waren voor A431 cellen, terwijl het niet-internaliserende E48 conjugaat en de ongeconjugeerde verbinding dat niet waren.

Ondanks de betere wateroplosbaarheid van de sensitizer (in vergelijking met *m*THPC), hadden ook deze conjugaten enkele beperkingen voor wat betreft tumortargeting. Conjugaten met een sensitizer:MAB molaire ratio >3 lieten een verminderde oplosbaarheid zien. Bovendien resulteerde de koppeling van deze hydrofiële sensitizer ook in een afwijkende biodistributie van het MAb, net zoals in het geval van *m*THPC-MAB conjugaten. De conjugaten met een hogere ratio vertoonden de neiging tot snelle klaring uit het bloed, wat waarschijnlijk gebeurt door opname door de lever. Andere onderzoeksgroepen hebben deze ratio-afhankelijke klaring uit het bloed ook waargenomen na het koppelen van fotosensitizers of radionuclide-bindende chelatoren aan MAbs (1,5-8).

Gedurende de loop van dit project verschenen enkele artikelen van andere onderzoeksgroepen over tumortargeting van therapeutische sensitizers met behulp van MAbs. De meeste van deze studies werden uitgevoerd door de groep van Dr. T. Hasan van de Wellman Laboratories of Photomedicine, Harvard Medical School in Boston (VS), die chlorin₆₆ monoethylenediamine monoamide als fotosensitizer gebruikte. In eerste instantie koppelden ze chlorin₆₆ via polyglutaminezuur aan MAb OC125. Deze conjugaten zijn getest

in een muizenmodel van peritoneaal verspreid ovariumcarcinoom, alleen na i.p. injectie, en niet na i.v. injectie (9). In latere studies gebruikten deze onderzoekers poly-L-lysine voor het koppelen van de sensitizer aan MAbs. Bovendien werd polysuccinylering gebruikt als methode voor het modificeren van de lading, wat resulteerde in kationische en anionische chlorin₆₆-MAB conjugaten. Conjugaten werden gemaakt met MAb 17-1A voor het targeten van levermetastasen van darmkanker in naakte muizen (10). De grootste uitdaging was om een hoge sensitizer-opname in de tumor te verkrijgen, naast een hoge tumor:normale-lever ratio. De opname in de tumor van het anionische chlorin₆₆-MAB 17-1A conjugaat bleek 7-maal hoger dan die van het kationische, 24 uur na i.v. injectie. Zowel de tumoropname als de tumor:normale-lever ratio van het anionische fotoimmunoconjugaat waren echter niet beter dan die van het ongeconjugeerde anionische chlorin₆₆, hetgeen duidelijk maakt dat het gebruik van het 17-1A MAB in hun geval niet leidde tot een betere tumorspecificiteit.

De tot dusver beste targeting resultaten werden behaald door de groep van Carcenac en Pèlerin, Montpellier, Frankrijk (11). Zij koppelden aluminium phthalocyanine tetrasulfaat (AlPc(SO₃H)₄) aan MAb 35A7, gericht tegen het carcinoembryonisch antigeen (CEA), via een spacer bestaande uit 5 CH₂-eenheden, resulterend in conjugaten met een molaire ratio van 5 tot 16 mol AlPcS₄ per mol MAb. Zelfs conjugaten met 16 AlPcS₄ moleculen waren volledig oplosbaar en lieten een vergelijkbare tumorselectiviteit zien als het ongeconjugeerde MAb in naakte muizen met darmkanker xenografts. De auteurs schreven dit toe aan de onveranderde hydrofiële eigenschappen van de MAbs na conjugatie. Zoals uit de volgende paragraaf zal blijken waren wij niet in staat om dergelijke ideale targeting resultaten met deze sensitizer te behalen. De effectiviteit van de conjugaten gemaakt door deze onderzoeksgroep bleek aanvankelijk echter erg tegen te vallen.

In **Hoofdstuk 4** werd het concept om internaliserende MAbs te gebruiken voor fotoimmunotherapie verder uitgediept met de therapeutisch idealere hydrofiële sensitizer AlPc(SO₃H)₄ ($\epsilon = 1.7 \times 10^5 \text{ M}^{-1}\text{cm}^{-1}$ bij 675 nm). De AlPcS₄-MAB conjugaten toonden enkele overeenkomsten met de *m*THPC-MAB conjugaten. Omdat AlPc(SO₃H)₄ ook geen functionele groep heeft die geschikt is voor directe conjugatie, werd de conjugatie uitgevoerd via het tetra-glycine derivaat. Bij molaire ratio's >4 nam de oplosbaarheid van de MAbs af, net zoals het geval was voor de eerder beschreven conjugaten. Tot slot waren de biodistributie resultaten in HNX-OE dragende naakte muizen vergelijkbaar met die van *m*THPC-MAB conjugaten: AlPcS₄-cMAB U36 hoopte selectief in de tumor op, hoewel in mindere mate dan het ongeconjugeerde MAb. Conjugaten met een hogere sensitizer:MAB ratio werden sneller geklaard uit het bloed dan het ongeconjugeerde MAb. Deze data vormen een interessant

contrast met die van Carcenac *et al.* (11). Een mogelijke verklaring voor de snellere klaring van onze conjugaten is dat de modificatie van alle 4 SO₃H groepen in AIPcS₄, leidend tot het tetra-glycine derivaat, de hydrofiliciteit dermate heeft verminderd dat daardoor de farmacokinetiek van het MAb beïnvloed wordt.

Preliminaire *in vitro* data suggereerden dat de AIPcS₄-MAb conjugaten fototoxischer waren dan de *m*THPC-MAb conjugaten. In hetzelfde model was het internalizerende AIPcS₄-MAb 425 conjugaat ongeveer 7500 keer toxischer voor A431 cellen (25 J/cm² bij 675 nm) dan de vrije verbinding (IC₅₀'s 0.12 versus 900 nM), en ongeveer 60 keer toxischer dan *m*THPC-MAb 425.

In Hoofdstuk 5 wordt een uitgebreide *in vitro* evaluatie van *m*THPC- en AIPcS₄-MAb conjugaten beschreven. De fototoxiciteit van beide typen conjugaten werd vergeleken met 5 plaveiselcelcarcinoom target-cellijnen en 3 MAbs (BIWA 4, E48 en 425) voor targeting (25 J/cm² bij 652 nm voor *m*THPC en 675 nm voor AIPcS₄). Aangaande de keuze van de MAbs, werden MAb-antigeen combinaties geselecteerd die realistisch zijn voor klinische toepassing in PDT van plaveiselcel-carcinoom. *m*THPC-MAb conjugaten waren in het algemeen nauwelijks effectief (in tegenstelling tot vrij *m*THPC), terwijl AIPcS₄-MAb conjugaten in hoge mate fototoxisch waren voor alle 5 cellijnen. Vooral AIPcS₄-BIWA 4 conjugaten, gericht tegen het tumor-geassocieerde antigeen CD44v6, waren effectief met IC₅₀ waarden tussen 0.06 en 5.4 nM.

De fototoxiciteit van de conjugaten werd gerelateerd aan hun celbindende en internaliserende eigenschappen. Een sterke correlatie werd gevonden tussen de fototoxiciteit van AIPcS₄-MAb conjugaten en de totale bindingscapaciteit (geïnternaliseerd en membraan-gebonden) van deze conjugaten. In tegenstelling tot onze voorgaande bevindingen lieten deze uitgebreidere studies zien dat de effectiviteit niet gecorreleerd was met de internaliserende capaciteit alleen.

Recent werden onze veelbelovende resultaten met AIPc(SO₃H)₄-MAb conjugaten bevestigd door Carcenac *et al.* (12). In een *in vitro* studie vonden ook zij een duidelijk voordeel van een internaliserend boven een niet-internaliserend sensitizer-MAb conjugaat.

Aan het slot van deze samenvatting kunnen enkele conclusies getrokken worden. De in dit proefschrift beschreven resultaten laten zien dat *m*THPC in vrije vorm veel fototoxischer is dan wanneer gekoppeld aan een MAb, en daarom is deze sensitizer niet optimaal voor gebruik in fotoimmunotherapie. In tegenstelling tot deze resultaten werden veelbelovende resultaten verkregen met AIPcS₄. *In vitro* bleek deze sensitizer een sterk anti-tumor effect te kunnen bewerkstelligen, vooral als deze gekoppeld werd aan het anti-

CD44v6-MAb BIWA 4. Echter, gezien de data van Carcenac (11), lijkt verdere verbetering van dit conjugaat voor *in vivo* toepassing mogelijk.

REFERENTIES

1. Pèlerin, A., Folli, S., Buchegger, F., Mach, J-P., Wagnières, G., and van den Bergh, H. Antibody-fluorescein conjugates for photoimmunodiagnosis of human colon carcinoma in nude mice. *Cancer*, 67: 2529-2537, 1991.
2. Ris, H.-B., Li, Q., Krueger, T., Lim, C. K., Reynolds, B., Althaus, U., and Altermatt, H. J. Photosensitizing effects of m-tetrahydroxyphenylchlorin on human tumor xenografts: correlation with sensitizer uptake, tumor doubling time and tumor histology. *Int. J. Cancer*, 76: 872-874, 1998.
3. Westermann, P., Glanzmann, T., Andrejevic, S., Braichotte, D. R., Forrer, M., Wagnières, G. A., Monnier, P., van den Bergh, H., Mach, J. P., and Folli, S. Long circulating half-life and high tumor selectivity of the photosensitizer *meta*-tetrahydroxyphenylchlorin conjugated to polyethylene glycol in nude mice grafted with a human colon carcinoma. *Int. J. Cancer*, 76: 842-850, 1998.
4. Reuther, T., Kübler, A. C., Zillmann, U., Flechtenmacher, C., and Sinn, H. Comparison of the *in vivo* efficiency of Photofrin II-, *m*THPC-, *m*THPC-PEG- and *m*THPCnPEG-mediated PDT in a human xenografted head and neck carcinoma. *Lasers Surg. Med.*, 29: 314-322, 2001.
5. Folli, S., Westermann, P., Braichotte, D., Pèlerin, A., Wagnières, G., van den Bergh, H., and Mach, J.P. Antibody-indocyanin conjugates for immunodetection of human squamous cell carcinoma in nude mice. *Cancer Res.*, 54: 2643-2649, 1994.
6. Boniface, G. R., Izard, M. E., Walker, K. Z., McKay, D. R., Soby, P. J., Turner, J. H., and Morris, J. G. Labeling of monoclonal antibodies with Samarium-153 for combined radioimmunoscintigraphy and radioimmunotherapy. *J. Nucl. Med.*, 30: 683-691, 1989.
7. Smith, A., Zangemeister-Wittke, U., Waibel, R., Schenker, T., Schubiger, P. A., and Stahel, R. A. A comparison of ⁶⁷Cu- and ¹³¹I-labeled forms of monoclonal antibodies SEN7 and SWA20 directed against small-cell lung cancer. *Int. J. Cancer*, 8: 43-48, 1994.
8. Van Gog, F. B., Visser, G. W. M., Klok, R., van der Schors, R., Snow, G. B., and van Dongen, G. A. M. S. Monoclonal antibodies labeled with Rhenium-186 using the MAG3 chelate: relationship between the number of chelated groups and biodistribution characteristics. *J. Nucl. Med.*, 37: 352-362, 1996.
9. Goff, B. A., Blake, J., Bamberg, M. P., and Hasan, T. Treatment of ovarian cancer with photodynamic therapy and immunoconjugates in a murine ovarian cancer model. *Br. J. Cancer*, 74: 1194-1198, 1996.
10. Hamblin, M. R., Del Governatore, M., Rizvi, I., and Hasan, T. Biodistribution of charged 17.1A photoimmunoconjugates in a murine model of hepatic metastasis of colorectal cancer. *Br. J. Cancer*, 83: 1544-1551, 2000.
11. Carcenac, M., Larroque, C., Langlois, R., van Lier, J. E., Artus, J.-C., and Pèlerin, A. Preparation, phototoxicity and biodistribution studies of anti-carcinoembryonic antigen monoclonal antibody-phthalocyanine conjugates. *Photochem. Photobiol.*, 70: 930-936, 1999.
12. Carcenac, M., Dorvillius, M., Garambois, V., Glaussel, F., Larroque, C., Langlois, R., Hynes, N. E., van Lier, J. E., and Pèlerin A. Internalisation enhances photo-induced cytotoxicity of monoclonal antibody-phthalocyanine conjugates. *Br. J. Cancer*, 85: 1787-1793, 2001.

LIST OF ABBREVIATIONS

ALA	δ -aminolaevulinic acid
AlPcS ₄	aluminium phthalocyanine tetrasulfonate
BCC	basal cell carcinoma
BCG	Bacillus Calmette-Guerin
BSA	bovine serum albumin
BTA	N,O-bis(trimethylsilyl)acetamide
CEA	carcinoembryonic antigen
CIS	carcinoma <i>in situ</i>
CR/PR	complete/partial response
DMEM	Dulbecco's modified Eagle's medium
DPPE	dipalmitoylphosphatidylcholine
EDC	1-ethyl-3-(3-dimethylaminopropyl)-carbodiimide
EGFR	epidermal growth factor receptor
FCS	foetal calf serum
HEPES	N-(2-hydroxyethyl)piperazine-N'-(2-ethanesulfonic acid)
¹ H-NMR	proton nuclear magnetic resonance
HNSCC	head and neck squamous cell carcinoma
HNX-OE	head and neck xenograft line OE
HpD	hematoporphyrin derivative
HPLC	high-performance liquid chromatography
IC ₅₀	concentration of drug needed to inhibit 50% of cell growth
%ID/g	percentage of injected dose per g of tissue
mMAb/cMAb	murine/chimeric monoclonal antibody
mTHPC	<i>meta</i> -tetrahydroxyphenylchlorin
MTT	3-[(4,5-dimethylthiazol-2-yl)-2,5-diphenyltetrazolium bromide]
PBS	phosphate-buffered saline
PEG	polyethylene glycol
PpIX	protoporphyrin IX
SDS-PAGE	sodium dodecyl sulfate-polyacrylamide gel electrophoresis
SRB	sulforhodamine B
TCC	transitional cell carcinoma
TFP	2,3,5,6-tetrafluorophenol
TrisMPyP- Φ CO ₂ H	5-[4-[5-(carboxyl)-1-butoxy]phenyl]-10,15,20-tris-(4-methylpyridiniumyl)porphyrin Iodide

DANKWOORD

Hoewel velen er de afgelopen tijd aan begonnen te twijfelen, is het er dan toch nog van gekomen: dit proefschrift nadert zijn afronding. Tot slot wil ik daarom hierbij graag diegenen bedanken, die bij de totstandkoming van dit proefschrift een belangrijke rol hebben gespeeld. Allereerst ben ik zeer veel dank verschuldigd aan mijn promotor prof. dr. G.A.M.S. van Dongen. Beste Guus, ik kan me bij alle lovende woorden van jouw eerdere promovendi aansluiten: door jouw enthousiaste, vriendelijke en behulpzame begeleiding heb ook ik onze samenwerking erg leuk gevonden. Mede door jouw grote kennis op vele gebieden, van basale biochemie tot klinische studies, was mijn periode op de VU zeer leerzaam.

Na enkele maanden kwam je al tot de conclusie: "Ieder onderzoek heeft één briljante vinding nodig, en hier is dat het cyanuurchloride." Dat 1,5 jaar later bleek dat alle met deze wonderverbinding verkregen resultaten de prullenbak in konden en we opnieuw konden beginnen, verminderde je interesse en stimulerende rol niet.

Mijn promotor prof. dr. G.B. Snow ben ik dank verschuldigd voor de gelegenheid die hij mij geboden heeft om het hier beschreven onderzoek te verrichten, en tevens omdat hij het mogelijk maakte het onderzoek als adjunct-onderzoeker af te ronden.

Op chemisch gebied was de bijdrage van mijn copromotor dr. G.W.M. Visser zeer belangrijk. Beste Gerard, jouw benadering, die zeer recht door zee is, heb ik altijd erg gewaardeerd. Jouw immer kritische kijk op experimenten en resultaten heeft het niveau van mijn werk zeker verhoogd. Ook de schaduwzijden van deze houding (de keer op keer afgekeurde NMR spectra, het eeuwige gebrek aan "kadans" in manuscripten) staan me nog helder voor de geest. Ook jouw talloze levenswijsheden, waaronder "Nooit terug komen op iets wat met bier in de hand gezegd is" komen nog wel eens van pas.

De leden van de promotiecommissie, prof. dr. P.E. Postmus, dr. W.M. Star, dr. F.A. Stewart, prof. dr. G. Storm, prof. dr. R.H.M. Verheijen en prof. dr. S.O. Warnaar wil ik hartelijk danken voor het kritisch doornemen van het manuscript en het zitting nemen in de promotiecommissie.

Mijn speciale dank gaat uit naar Marijke Stigter. Beste Marijke, jouw grote bijdrage aan alle *in vitro* experimenten en biodistributiestudies was onmisbaar. Ook was je vaak niet te beroerd je vrije vrijdag op te offeren voor de laserexperimenten. Ik heb onze samenwerking altijd erg gewaardeerd.

Van Frank van Gog heb ik de fijne kneepjes geleerd op het gebied van antilichaamconjugaten, maar ook wil ik hem bedanken voor de gezelligheid op het RNC,

waar wij, afgesloten van daglicht en collega's, enkele jaren op elkaar aangewezen waren. Ook de overige (ex)collega's van de afdeling Tumorbioïogie wil ik hierbij bedanken voor de prettige werksfeer. In dit opzicht wil ik met name Ruud Brakenhoff noemen. Samen met Guus hebben we al die tijd een kamer gedeeld, hopelijk ook tot jullie genoegen. Vaak werd ik 's ochtends met "Ook goedemiddag" begroet, op een tijdstip dat ik hier in het meer ontspannen Groningen één van de eersten ben. Ook David Colnot en Maarten Tabor mogen hier niet ontbreken. Ik ben bang dat ik jullie maar net voorgebleven ben.

Hugo Oppelaar, Marjan Ruevekamp en dr. F.A. Stewart van het Nederlands Kanker Instituut wil ik bedanken voor het beschikbaar stellen van de lasers en voor de technische hulp bij de *in vitro* belichtingen. Iedere keer werden we op het NKI met open armen ontvangen.

Ook gaat mijn dank uit naar prof. dr. F.P.J.T. Rutjes, voor zijn waardevolle adviezen over de organisch-chemische kant van de conjugaties beschreven in hoofdstuk 4.

De medewerkers van het Radionuclidencentrum, waar dit onderzoek bijna volledig is uitgevoerd, hebben mij steeds waar nodig geholpen. Graag wil ik met name Rob Klok bedanken voor de prettige samenwerking en de hulp bij de HPLC-analyses. Op praktisch gebied heb ik veel van je geleerd.

Lieve Cindy, door het uitlopen van dit onderzoek werd mijn vertrek naar Groningen, waar jij al woonde, keer op keer uitgesteld. Daarom bedankt voor alle geduld en vertrouwen in de goede afloop.

CURRICULUM VITAE

Maarten Vrouwenraets werd geboren op 3 april 1969 in Dieren. In 1981 ging hij naar het Stedelijk Lyceum in Zutphen waar hij in 1987 het diploma Ongedeeld V.W.O. behaalde. Vervolgens begon hij aan de studie Scheikunde aan de Universiteit van Amsterdam. In 1988 werd de propedeuse cum laude behaald, gevolgd door het doctoraalexamen in 1993. Zijn hoofdvakstage werd gevolgd bij de Sectie Bio-organische Chemie van prof. dr. U.K. Pandit, met als onderwerp de ontwikkeling van katalytische antilichamen.

In januari 1994 startte hij vervolgens zijn promotieonderzoek op de afdeling Keel-, Neus- en Oorheelkunde van de Vrije Universiteit in Amsterdam. Dit werd uitgevoerd onder begeleiding van prof. dr. G.A.M.S. van Dongen en prof. dr. G.B. Snow (afdeling Keel-, Neus- en Oorheelkunde) en dr. G.W.M. Visser (Radionuclidencentrum, Vrije Universiteit). In 1998 en 1999 werd dit onderzoek, waarvan de resultaten in dit proefschrift beschreven staan, als adjunct-onderzoeker vervolgd. Sinds 1 oktober 2000 is hij werkzaam als wetenschappelijk onderzoeker bij Biomade Technology Foundation in Groningen.